

Sara Raquel Gemelgo Pereira

**From scaffolds to endodontic sealers in dentistry:
an *in vitro* and *in vivo* approach**

October 2015



UNIVERSIDADE DE COIMBRA



FCTUC FACULDADE DE CIÊNCIAS
E TECNOLOGIA
UNIVERSIDADE DE COIMBRA

Sara Raquel Gemelgo Pereira

From scaffolds to endodontic sealers in dentistry: an *in vitro* and *in vivo* approach

*Dissertação apresentada à Universidade de Coimbra
para cumprimento dos requisitos necessários à
obtenção do grau de Mestre em Engenharia Biomédica*

Orientador(es):

Prof. Doutora Margarida Figueiredo (CIEPQPF, DEQ-FCTUC)

Prof. Doutora Ana Cristina Santos (IBILI-FMUC)

Coimbra, 2015

Este trabalho foi desenvolvido em colaboração com:

IBILI – Institute for Biomedical Imaging and Life Sciences



CIEPQPF - Chemical Process Engineering and Forest Products
Research Centre



Esta cópia da tese é fornecida na condição de que quem a consulta reconhece que os direitos de autor são pertença do autor da tese e que nenhuma citação ou informação obtida a partir dela pode ser publicada sem a referência apropriada.

This copy of the thesis has been supplied on condition that anyone who consults it is understood to recognize that its copyright rests with its author and that no quotation from the thesis and no information derived from it may be published without proper acknowledgement.

Acknowledgments

I would like to thank to *Prof^a. Doutora* Margarida Figueiredo and *Mestre* Patricia Coimbra from the Department of Chemical Engineering and *Prof^a. Doutora* Cristina Santos from to Biophysics Institute of the Faculty of Medicine of the University of Coimbra, for all the support and guidance during the development of this work. I also would like to thank them for the excellent experience I lived during the past year. I also want to thank to Henrique Cunha for all the support, friendship and also for the opportunity to develop a new project with him.

I also would like to acknowledge the Biophysics Institute for the resources provided and to the Hospital of the University of Coimbra for the sterilization. I also want to acknowledge Coltène Whaledent[®] for the availability of the root canal sealers, and to *Prof. Doutor* João Miguel Santos and *Mestre* Diana Sequeira, for allowing me to join their working team.

I also want to thank to *Prof^a. Doutora* Bárbara Oliveiros for helping me in the statistical analysis of the obtained results and to *Técnica Principal de Laboratório* Claudia Brites from to Faculty of Medicine of the University of Coimbra for helping me with the histological technique.

Beyond these direct actors in this work, others had a great importance in my university experience, not only during this last year, but also during the previous four. Namely I would like to thank to Fátima Machado and Rita Monteiro, and also to João Rodrigues and Paulo Sousa by all the coffee breaks. To Rita and Joana, my house mates during the last five years, I am extremely grateful to them for all the conversations, laughs and all the confidences. I also want to thank to João Sousa and Pedro Borlido, for their unconditional friendship, for all the “safariizadas”, for all the conversations and support, in short thanks for being part of the best five years of my life. I also am extremely grateful to Felipe for all the reliability, support, help and force, for being there when I need. Thanks for that and much more. Furthermore, I am also grateful to Fábio, Pontes, Costa, Remondes, and also to Catarina S. whom, despite the physical distance that separated us during this five years always remained present. I have to thank them not only all the confidences but also for all the hugs. To Patricia and Catarina for being always present. For all the “ladies night”, for all the conversations, simply for their big

friendships. To Filipe, Mauricio, Gui, Maria, and so many other people that are not here listed, for being part of the amazing five years that I spent in Coimbra.

At the last but not the least my deepest thanks go to my family, especially to my parents, for the unconditional support during all my life and for just “being there” when I most needed. Thanks for always believing in me.

Biocompatibility, described as the ability of a material to fulfil an appropriate response in a given application with the minimum of allergic, inflammatory or toxic reactions when in contact with tissues, is one of the most important characteristic of the materials used in tissue engineering and dentistry.

Tissue engineering is a scientific area in continuous expansion. The developments achieved in this area, have significantly contributed for many advances in the field of regenerative medicine. This interdisciplinary science combines the knowledge and experience of several different fields, from materials science to biology, in order to develop synthetic substitutes for human tissues. Aiming at this goal, the most common approach used nowadays involves the seeding of tridimensional porous structures (scaffolds), biocompatible/biodegradable, with donor cells to promote tissue regeneration. This process comprises at least three different stages: the production of the 3D structures, sterilization and cell seeding into scaffolds, and finally the cell culture of the set cell-scaffold.

On the other hand, dentistry has currently registered an increasing importance, namely in the endodontic field. Consequently, the development of biocompatible endodontic cements has become of high importance, since these materials can be in direct contact with different cell types, mainly if extrusion of the material to the periapical tissues occurs. There are a variety of commercial root canal cements available, based in different formulations, whose biocompatibility has been studied *in vitro* and *in vivo* over the years. However, all the endodontic cements commercially available show some degree of cytotoxicity. Thus, new endodontic cements are emerging, allowing the development of new approaches.

Throughout this work it was intended to evaluate the cytotoxicity of two different types of materials: scaffolds and endodontic cements, the latter also called filling cements. Thus, the first goal aimed to evaluate the *in vitro* cytotoxicity of pure PCL scaffolds and PCL-HA composite scaffolds. For this purpose, scaffolds were produced with different percentages of HA (10% and 25% per weight), and also with different types of HA: synthetic and natural HA (HA S and HA N, respectively). Scaffolds were produced by bioextrusion, a technique controlled by a computer, with different architectural characteristics (300 μm of filament

thickness, 300 and 600 μm of pore size and geometries of 0/90° e 0/45°). The second goal of this work aimed to assess the *in vitro* cytotoxicity regarding three different endodontic cements: an epoxy-resin, AH Plus JetTM, and two based-silicone cements, GuttaFlow^{®2} and an improved version of the latter material, that is not yet on the market, and thus it will be called “improved” Guttaflow[®] throughout this work. In order to evaluate the *in vitro* cytotoxicity of these materials, different volumes of material (0.01, 0.02 and 0.03 mL) and different incubation times (72 and 120 hours) were used. The *in vivo* cytotoxicity of these materials was also evaluated in a subcutaneous implantation model. Thus, the endodontic cements were placed inside tubes with 8 mm of length, obtained by section of 18 GA (1.3 mm \times 48 mm) abocats, which were implanted into three quadrants of the dorsum of Wistar rats. The possible reactions of the tissues were evaluated 8 and 30 days after implantation. As control, the reactions induced by abocat tubes without any material inside, were compared during the same time periods (first quadrant).

The cytotoxicity assay selected for this work, in order to reach both main goals, was the 3-(4,5-dimethylthiazol-2-yl)-2,5-diphenyltetrazolium bromide (MTT) assay, which is based upon the ability of the dehydrogenase enzyme (present in metabolically active cells), to cleave the tetrazolium ring of MTT and convert the yellow water-soluble tetrazolium salt into dark-blue/purple formazan crystals. In both cases (studies performed with scaffolds and endodontic cements), the MTT assay was done with macrophages, fibroblasts and co-culture of macrophages and fibroblasts.

Regarding the evaluated scaffolds, it was concluded that PCL-HA N composite scaffolds are the ones presenting better *in vitro* biologic behavior (less cytotoxic). The obtained results also indicate that the scaffolds’ architecture has a leading role in cell-scaffold interaction. Scaffolds with pores of 300 μm and geometry 0/45° show less cytotoxicity, which, in the present study, means that they promote a higher cellular adhesion and proliferation. In what concerns the endodontic cements, the performed *in vitro* studies allow to conclude that the “improved” GuttaFlow[®] is the least cytotoxic of the three tested materials, therefore it is the one presenting greater biocompatibility.

Key-words: Biocompatibility, cytotoxicity, tissue engineering, endodontics, scaffolds, endodontic cements.

A biocompatibilidade descrita como a capacidade de um material para desempenhar uma resposta apropriada numa determinada aplicação com o mínimo de reacções alérgicas, inflamatórias ou tóxicas quando em contacto com tecidos, é uma das características mais importantes dos materiais utilizados em Engenharia de Tecidos e em Medicina Dentária.

A Engenharia de Tecidos é uma área científica em contínua expansão. Os desenvolvimentos conseguidos por esta área têm contribuído significativamente para diversos avanços no campo da Medicina Regenerativa, ciência que combina conhecimentos de áreas tão distintas como a Engenharia de Materiais e a Biologia, com o objectivo de desenvolver substitutos sintéticos para os tecidos humanos. Para se atingir este objectivo, a metodologia mais utilizada actualmente envolve o uso de estruturas porosas tridimensionais (*scaffolds*), biocompatíveis e biodegradáveis, em conjugação com células, de forma a promover a regeneração de tecidos. Este processo compreende no mínimo três fases distintas: a produção das estruturas 3D, esterilização e deposição celular nos *scaffolds* e por último, cultura celular do conjunto *scaffolds*-células.

Por sua vez, a Medicina Dentária tem registado actualmente uma crescente importância, nomeadamente na área de endodontia. Consequentemente, o desenvolvimento de cimentos de obturação endodônticos biocompatíveis, tornou-se de extrema importância, uma vez que estes poderão contactar directamente com diversos tipos de células, principalmente se ocorrer extrusão do material para os tecidos periapicais. Estão disponíveis comercialmente inúmeros cimentos de obturação, com diferentes formulações, cuja biocompatibilidade tem sido estudada *in vitro* e *in vivo* ao longo dos últimos anos. Contudo, todos os cimentos endodônticos disponíveis comercialmente mostram algum nível de citotoxicidade. Por este motivo, têm surgido novos cimentos de obturação, os quais têm permitido desenvolver novas abordagens.

Neste sentido, ao longo deste trabalho pretendeu-se avaliar a citotoxicidade de dois tipos diferentes de materiais: *scaffolds* e cimentos endodônticos, estes últimos também designados de cimentos de obturação. Assim, o primeiro objectivo deste trabalho pretendia avaliar a citotoxicidade *in vitro* de *scaffolds* de PCL e *scaffolds* constituídos por PCL/HA. Para tal fabricaram-se *scaffolds* não só com diferentes teores de HA (10% e 25% de HA), mas também abrangendo diferentes tipos de HA: sintética e natural. Os *scaffolds* foram fabricados pela técnica de bioextrusão controlada por computador, com diferentes características arquitectónicas (300 µm de espessura do filamento, 300 e 600 µm de tamanho de poros e geometrias 0/90° e 0/45°). O

segundo objectivo deste projecto pretendia avaliar a citotoxicidade *in vitro* de três diferentes cimentos de obturação: uma resina *epoxy*, AH Plus JetTM, e dois cimentos tendo por base silicone, GuttaFlow[®]2 e uma versão melhorada deste último material, o qual por ainda não se encontrar no mercado, será ao longo do trabalho designado por “*improved*” GuttaFlow[®]. De modo a avaliar a citotoxicidade *in vitro* destes materiais, utilizaram-se diferentes volumes de material (0,01; 0,02 e 0,03 mL) e também diferentes tempos de incubação, 72 e 120 horas. Avaliou-se igualmente a citotoxicidade *in vivo* destes materiais em modelos de implantação subcutânea. Para tal, os cimentos de obturação foram colocados em tubos de 8 mm de comprimento, obtidos por secção de *abocats* 18 GA (1,3 mm × 48 mm), os quais foram implantados nos quatro quadrantes do dorso de ratos *Wistar*. Foram avaliadas as possíveis reacções dos tecidos aos 8 e 30 dias após a implantação e comparadas com as reacções induzidas com tubos de *abocat* sem material, nos mesmos períodos (grupos de controlo).

O teste de citotoxicidade efectuado *in vitro*, com vista a atingir ambos os objectivos referidos, foi o teste do brometo de 3-(4,5-dimetiltiazol2-il)-2,5-difeniltetrazólio (MTT), o qual se baseia na capacidade da enzima desidrogenase, presente em células metabolicamente activas, clivar os anéis tetrazólio do MTT e formar cristais formazano de cor violeta. Em ambos os casos (estudo efectuado com os *scaffolds* e estudo com os cimentos endodônticos), o teste de MTT foi realizado com macrófagos, fibroblastos e co-cultura de macrófagos e fibroblastos.

Nas condições deste estudo, relativamente aos *scaffolds* avaliados, concluiu-se que os *scaffolds* constituídos por PCL/HA natural são os que apresentam melhor comportamento biológico *in vitro* (menor citotoxicidade). Os resultados obtidos permitiram, ainda, verificar que a arquitectura dos *scaffolds* desempenha um papel preponderante na interacção entre as células e os *scaffolds*. *Scaffolds* com poros de 300 µm e geometria 0/45° mostraram ser menos citotóxicos, o que, no presente estudo, significa que promoveram uma maior adesão e proliferação celular. No que respeita aos cimentos endodônticos, os estudos efectuados *in vitro* permitiram concluir que o “*improved*” GuttaFlow[®] é o menos citotóxico dos três materiais avaliados, sendo portanto o que apresenta maior biocompatibilidade.

Palavras-chave: Biocompatibilidade. Citotoxicidade. Engenharia de Tecidos. Endodontia. *Scaffolds*. Cimentos de endodônticos.

Table of Contents

Acknowledgements	v
Abstract.....	vii
Resumo.....	ix
Table of Contents	xi
List of abbreviations	xv
List of Figures.....	xvii
List of Tables	xxi

Chapter 1: General Introduction

1.1 Introduction	1
1.2 Dissertation structure.....	3

Chapter 2: Literature review

2.1 Scaffolds for tissue engineering	5
2.1.1 Concepts of tissue engineering and its utility	5
2.1.2 Biomaterials for scaffolds production.....	9
2.1.2.1 Metals	10
2.1.2.2 Ceramics.....	10
2.1.2.3 Polymers.....	11
2.1.2.4 Composites	12
2.1.3 Technologies for scaffolds production	13

2.1.3.1 Conventional Fabrication Techniques.....	13
2.1.3.2 Non-Conventional Fabrication Techniques	16
2.2 Dental anatomy and root canal treatment.....	22
2.2.1 Root Canal Filling Materials	25
2.2.1.1 Gutta-percha	25
2.2.1.2 Sealers	26

Chapter 3: Materials and characterization techniques

3.1 Materials used for scaffolds fabrication and techniques for their production and characterization	29
3.1.1 Materials	29
3.1.2 Technology used for scaffolds production: BioExtruder	32
3.1.3 Scaffolds characterization	33
3.1.4 Scaffolds sterilization.....	36
3.2 Endodontic cements and study models used for its <i>in vivo</i> cytotoxicity evaluation	38
3.2.1 Endodontic cements used.....	38
3.2.2 <i>In vivo</i> cytotoxicity of endodontic cements and study models	40
3.3 <i>In vitro</i> cytotoxicity assay	45

Chapter 4: Experimental

4.1 Introduction	47
4.2 Cell lines and cell cultures	49
4.3 Tests with scaffolds	55
4.3.1 Preparation of PCL-HA mixtures	55
4.3.2 Scaffolds architectural design	57
4.3.3 Scaffolds characterizing techniques	57

4.4 Tests with endodontic materials	61
4.4.1 <i>In vitro</i> cytotoxicity studies	61
4.4.2 <i>In vivo</i> cytotoxicity studies	65
4.5 Statistical analysis	70
Chapter 5: Results and discussion	
5.1 <i>In vitro</i> studies with scaffolds	71
5.2 <i>In vitro</i> studies with endodontic cements	84
5.3 <i>In vivo</i> studies with endodontic cements – Histologic study	89
Chapter 6: Conclusions and future work	
6.1 Conclusions	93
6.1.1 Conclusions of the study with scaffolds for TE	93
6.1.2 Conclusions of the study with endodontic materials	95
6.2 Future work	96
References	97
Appendix.....	107

List of abbreviations

2D – Two-dimensional

3D – Three-dimensional

3DP – Three-dimensional printing

AM – Additive manufacturing techniques

ASTM – American Society for Testing and Materials

CAD – Computer Aided Design

CAM – Computer Aided Manufacturing

CaP – Calcium phosphate

DTG – Derivative Thermogravimetric curve

ECM – Extracellular matrix

FDA – Food and Drug Administration

FDM – Fused Deposition Model

HA – Hydroxyapatite

IPL – Instituto Politécnico de Leiria

LCD – Liquid crystal display

MIT – Massachusetts Institute of Technology

MTT - 3-(4,5-dimethylthiazol-2-yl)-2,5-diphenyltetrazolium bromide

PCL – Poly(ϵ -caprolactone)

PGA – Polyglycolic acid

PLGA – Poly(lactic-co-glycolic acid)

PLA - Polylactic acid

RP – Rapid Prototyping

SLS – Selective Laser Sintering

TE – Tissue engineering

T_g – Glass transition temperature

TG – Thermogravimetric curve

TGA – Thermogravimetric Analysis

T_m – Melting temperature

U.V. - Ultraviolet

List of Figures

Figure 1: Steps of RP/AM in tissue engineering in [3].	16
Figure 2: Stereolithography system in [3].	17
Figure 3: Writing methods in stereolithography processes. (a) Mask-based method. (b) Direct writing method in [3].	18
Figure 4: 3D printing process in [3].	19
Figure 5: Selective laser sintering process in [3].	19
Figure 6: Fused deposition modelling process in [3].	20
Figure 7: The BioExtruder device in [3].	21
Figure 8: The four tissues of the teeth.	23
Figure 9: Main steps of the root canal treatment adapted from [50].	24
Figure 10: Gutta-percha cones.	26
Figure 11: Synthesis of poly(ϵ -caprolactone) by ring-opening polymerization in [20].	30
Figure 12: (a) Multi-material extrusion system; (b) Single-material extrusion, in [3].	33
Figure 13: Example of a TG/DTG curve in [90].	34
Figure 14: Schematic diagram of a gas pycnometer in [95].	35
Figure 15: AH Plus Jet and Ah Plus in tubes, respectively.	39
Figure 16: Automaxic serynge of GuttaFlow [®] 2.	39
Figure 17: A schematic representation of the time course of the foreign body reaction to an implanted “biocompatible” material in [110].	42
Figure 18: Schematic MTT reduction to formazan. This reaction can only occur when the reducing enzymes are active. This conversion is, therefore, used to measure cell viability in [115].	45
Figure 19: Scaffolds of PCL produced in the BioExtruder with 300 μ m of pore size. The architectural orientation of the filaments 0/90 [°] is shown on the left side and the 0/45 [°] on the right side.	48
Figure 20: Injecting 20 mL of PBS (phosphate buffer saline) and harvesting macrophages (1 mL syringe with a 19G needle).	52
Figures 21 and 22: Microscopic image of macrophages and human fibroblasts, respectively	53
Figure 23 and 24: Neubauer cell chamber in an optical microscope and an example of an image seen in the microscope during cell counting.	56
Figure 25: Characteristics of tested scaffolds, where HA N and HA S corresponds to natural and synthetic HA, respectively.	53
Figure 26: Representation of one of the used 48-well microplates	59
Figure 27: Arrangement of the samples in a 96-well microplate, for the study performed with frozen and fresh macrophages for AH Plus Jet TM . The wells disposition for GuttaFlow [®] 2 and the “improved” Guttaflow [®] is the same.	62
Figure 28: Image of the 96-well microplates after MTT assay	65
Figure 29: Anatomical localization of materials implantation	67

Figure 30: Chirurgical removal of the implant.	68
Figure 31: Expellant with a wide margin of surrounding tissue	68
Figure 32: Representation of the fibroblasts response in function of the architecture of the scaffolds.	73
Figure 33: Representation of the macrophages response in function of the scaffolds architecture.	73
Figure 34: Representation of the co-culture response in function of the scaffolds architecture	74
Figures 35 and 36: Pareto Chart for the results obtained with macrophages and fibroblasts, respectively, where: A represents the type of HA, B the percentage of HA, C the size of the pores in μm and D the pore geometry (0/45 $^\circ$ or 0/90 $^\circ$).	77
Figure 37: Pareto Chart for the case of co-culture	77
Figure 38: Main effects that influence interactions between fibroblasts and scaffolds	78
Figure 39: Main effects that influence interactions between macrophages and scaffolds.	78
Figure 40: Main effects that influence cellular interactions with scaffolds for the co-culture.	79
Figures 41 and 42: Influence of the percentage of HA in function of the pore and type of HA for the geometry 0/45 $^\circ$ and 0/90 $^\circ$, respectively	80
Figures 43 and 44: Influence of the percentage of HA in function of the geometry and type of HA for the pores of 300 μm and 600 μm , respectively.	81
Figure 45 and 46: Pareto Chart for fibroblasts and macrophages, respectively, where A corresponds to the composition of the scaffolds, B to the Plasma treatment and C to the scaffolds geometry	82
Figure 47: Pareto Chart for the co-culture.	82
Figure 48 and 49: Representation of the interaction between factors with plasma treatment for fibroblasts and macrophages, respectively	83
Figure 50: Interactions between factors for co-culture.	83
Figure 51 and 52: Representation of the obtained results for fresh and frozen macrophages, with 0.02 mL of material (on the left) and with 0.03 mL of material, on the left	84
Figure 53: Representation of the obtained results for the control group with fresh and frozen macrophages	85
Figure 54: Representation of the behavior of the different materials for all the tested cell types, where GF2 corresponds to GuttaFlow 2, AH+ to AH Plus Jet, GF3 to the "improved" GuttaFlow, AH+&GP, to the set Ah Plus Jet plus small pieces of Gutta-percha cones and finally GP refers to Gutta-percha.	88
Figure 55: Microscopic image of the local where the control tube has been implanted, being A a blood capillary, B areolar cells, C the subcutaneous tissue where the control tube was implanted and D to adipose tissue cells.	89
Figure 56: Microscopic image of rat skin without tube/material implantation, where A corresponds to hair follicles, B to sebaceous glands, C to the hair erector muscle, D to collagenous fibers and E to the cellular subcutaneous tissue.	89
Figure 57: Microscopic image of the site where the tube with AH Plus Jet TM was implanted. In this image it is possible to observe collage fibers (A), areolar tissue (B), inflammatory infiltrate (C) and also sebaceous glandes (D).	90
Figure 58 Microscopic image of the site where the tube with AH Plus Jet TM was implanted. In this image it is possible to observe inflammatory infiltrate with medium degree of fibrous.	90

Figure 59: Microscopic image of the site where the tube with AH Plus Jet™ was implanted. In this image it is possible to see a fibrous capsule (A) around the tube with AH Plus Jet™.90

Figure 60: Microscopic image of the site where the tube with GuttaFlow® 2 was implanted. In this image the start of the fibrous organization, as well as some vascularization, can be seen.91

Figure 61: Microscopic image of the site where the tube with GuttaFlow® 2 was implanted. In this image the beginning of an inflammatory reaction can be seen.91

Figure 62: Microscopic image of the site where the tube with GuttaFlow® 2 was implanted. In this image also can be seen a fibrous capsule (A), well defined, around the local where the tube has been implanted.91

Figure 63: Microscopic image of the site where the tube with “improved” GuttaFlow® was implanted. In this image, some fibrous starts to appear, although it is not very evident.92

Figure 64: Microscopic image of the site where the tube with “improved” GuttaFlow® was implanted. In this image, some inflammatory infiltrate can be observed (A).92

List of Tables

Table 1: Relationship between scaffold characteristics and the corresponding biological effects based in [3,7].	9
Table 2: Currently applied 3D scaffold fabrication technologies in [17].	15
Table 3: Experimental groups for the in vitro study of cytotoxicity of the endodontic materials.	64
Table 4: Representation of the mean values obtained for the scaffolds porosity.	74
Table 5: Representation of the factors that were used for the DOE.	76
Table 6: Representation of the factors that were used for the DOE.	81
Table 7: Summary of the obtained “p” values for the comparison of the materials for each one of the used volumes.	85

Chapter 1

General Introduction

1.1 Introduction

In 1987, a biomaterial was defined as “a nonviable material used in a medical device, intended to interact with biological systems”. An important characteristic of a biomaterial is its biocompatibility that can be described as “the ability to perform with an appropriate host response in a specific application”. Thus, **biocompatibility** occurs when tissues come in contact with a particular material and do not show any toxic, irritating, inflammatory or allergic experience, or mutagenic or carcinogenic background. For a material to be biocompatible an appropriate host response is required, which means non-occurrence of adverse reactions of the organism face to the material. Therefore, biocompatibility is an essential requirement of biomaterials. Another important characteristic of biomaterials is non-cytotoxicity. Cytotoxicity is the quality of being toxic to cells. If materials are not biocompatible and if they show a cytotoxic effect, an adverse reaction of the organism and consequently the rejection of the material by the body can occur.

These properties are of utmost importance in many fields, namely in **Tissue Engineering** and **Dentistry**.

Tissue Engineering offers the possibility to help in the regeneration of tissues and, in some cases, to create new tissues and replace failing or malfunctioning organs. This is achieved through the use of degradable biomaterials to either induce surrounding tissue or cell ingrowth or to serve as temporary scaffold for transplanted cells to attach, grow and maintain differentiate functions.

Endodontics has recently assumed a crescent importance in the panorama of dentistry. The main goal of endodontic treatment is the complete tooth restoration, while trying to keep the natural tooth when possible.

Thus, the main objective of the present work is to study the cytotoxicity of two different materials: a 3D scaffold composed of poly(ϵ -caprolactone) (PCL) and hydroxyapatite (HA), that will be used in Tissue Engineering, and an endodontic sealer whose performance is to be compared with similar commercial products. Both, scaffolds and endodontic sealers tested in this work have, as final goal, an application in dentistry, specifically, scaffolds in bone tissue regeneration of the oral cavity (mandible and/or maxillary) and endodontic sealers in endodontic treatment.

In what concerns the tested scaffolds, it is intended to study the influence that the addition of hydroxyapatite (HA) to poly(ϵ -caprolactone) (PCL) has on their interaction with cells and consequently in their cytotoxicity behavior. Thus, in the present work, scaffolds of pure PCL and also composite scaffolds of PCL-HA were studied. Additionally, it is intended to test two different percentages and types of HA, natural and synthetic HA, and to compare their performance. Besides that, these scaffolds were fabricated with different architectures, namely pore size and geometry, in order to analyze its influence in scaffolds' cytotoxicity.

Regarding the endodontic materials, they should be non-toxic, biocompatible and able to seal completely the root canal system in three dimensions. Among the various types of sealers, the endodontic cements will be the ones subjected to investigation in the present work. A new cement (“improved” GuttaFlow[®]), not yet on the market, will be compared with two commercial products (AH Plus Jet[™] and GuttaFlow[®]2).

The biological performance of these two distinct materials (scaffolds and endodontic cements) will be investigated by *in vitro* cytotoxicity assays, specifically MTT assays, using macrophages, fibroblasts and their co-culture. Besides that, in order to prove the biocompatibility of AH Plus Jet[™], GuttaFlow[®]2 and of the “improved” GuttaFlow[®], the *in vivo* biocompatibility of these materials, through subcutaneous implants, will also be evaluated.

1.2 Dissertation structure

The present dissertation is divided in five chapters:

Chapter 1: General introduction

The present chapter presents a general framework of the work developed along this dissertation, as well as the summary of the main goals and organization of the dissertation.

Chapter 2: Literature review

This chapter intends to provide the theoretical framework necessary to understand the themes selected for this dissertation. This chapter is divided in two sub-chapters: in the first one the concepts of tissue engineering and the biological strategies that can be applied in tissue regeneration are described, as well as the biomaterials and technologies used for scaffolds' production. In the second sub-chapter the dental anatomy, the root canal treatment, and also the different types of endodontic materials (specifically cones of gutta-percha and different types of sealers) that can be used in endodontic treatment are addressed.

Chapter 3: Materials and used characterization techniques

In this chapter, as the name denotes, the main materials and techniques used in this work are described. For this purpose, the chapter is divided in three sub-chapters. In the first one, the materials used for scaffolds' production (PCL and HA) are described, as well as the techniques used for their production (bioextrusion) and characterization (Thermogravimetric analysis, Helium pycnometry and low-pressure plasma treatment). In the second sub-chapter the composition and main characteristics of the different endodontic cements, used in this work, are described. Finally, in the last sub-chapter of this chapter, the cytotoxicity assay that was used for the study of the biologic behavior of the scaffolds and of the endodontic cements is referred.

Chapter 4: Experimental design

This chapter begins with an introduction where the main goals of this work are described in detail. Afterwards, the cell lines used in the *in vitro* studies (macrophages and fibroblasts) to achieve the main goals of this work are addressed, as well as cell cultures and the importance of the *in vitro* studies. Then, the procedures adopted for the cytotoxicity studies with scaffolds, which were done in order to study the influence of HA addition to PCL and also of pore architecture in cell-scaffold interaction, are described. The *in vivo* and *in vitro* studies that were done to study the cytotoxicity and inflammatory reaction, respectively, of the endodontic cements used in this work, are also described in this chapter. Finally, the statistical analysis that was done in order to analyze the obtained results for both studies (studies with scaffolds and with endodontic cements) is referred.

Chapter 5: Results and discussion

This chapter summarizes the most significant aspects of the present study. For this purpose, this chapter is divided in two sub-chapters. In the first one, the results obtained for the *in vitro* cytotoxicity studies with scaffolds are described and analyzed. Then, the results obtained with the *in vitro* studies with AH Plus JetTM, GuttaFlow[®]2 and with the “improved” GuttaFlow[®] are analyzed.

Chapter 6: Conclusion and future work

This chapter summarizes the most significant features of the present study and perspectives some future work.

Chapter 2

Literature review

Since in this work two different materials with different applications will be studied, several themes will be addressed in order to facilitate the understanding of the work, in the present chapter.

Initially, a literature review on tissue regeneration (TE) based upon the use of scaffolds will be done. Special attention will be devoted to scaffolds' requirements, biomaterials and production, as well as characterization technologies.

Afterwards, to address the second material in study, an endodontic cement, which is used in root canal treatment, a literature review on dental anatomy and root canal treatment is presented. At this point, emphasis will be put on different types of commercially available endodontic materials.

2.1 Scaffolds for tissue engineering

2.1.1 Concepts of tissue engineering and its utility

The failure of organs and tissues as a result of injury is currently one of the major health problems. Treatments encompass, in most cases, transplants, surgical repair, placement of artificial prosthesis and mechanical devices. However, these procedures often involve the risk of immune rejection and require invasive therapies, causing discomfort to the patient, increasing time of convalescence and decreasing his quality of life.

In the last decades, there has been a significant development of some areas of tissue engineering (TE), aimed to produce biological substitutes able to repair, replace or regenerate organs and tissues more effectively than conventional therapies [1-2].

TE comprises three main groups of approach strategies for tissue regeneration [2-5]:

- the use of isolated cells or cell substitutes. This strategy comprises the direct *in vivo* implantation of isolated cells or cell substitutes. It avoids possible complications associated

with surgery. However, there is a possibility of immunological rejection or loss of cell function after implantation;

- the use of growth factors. The success of this strategy, as the denomination indicates, depends on the behavior of growth factors and controlled released systems. Growth factors are signaling molecules regulating several cellular functions, such as proliferation, differentiation, migration, adhesion and gene expression;

- the use of scaffolds. This strategy is based on a temporary scaffold which provides both a substrate for the implanted cells and a physic support for the formation of new tissue. The transplanted cells will adhere to the scaffold, proliferate, secrete their own extracellular matrices and stimulate new tissue formation. During this process the scaffold will be degrading until it is eliminated by the body.

The last strategy is the most used in TE since it allows the experimental manipulation at three different levels: cells, materials and technologies for scaffolds' production. The cells used in this strategy are harvested from living tissues removed from the own patient (autogenic) or from another person (allogenic), deposited in 3D scaffolds and cultured *in vitro* in order to obtain a biological implant for transplantation. This strategy can be applied with several variations that rely on the origin of the cells, on scaffold's biomaterial, the conditions and duration of cell culture, and also on the type and properties of the tissue to regenerate.

Scaffolds

Scaffolds are 3D matrix structures, with high degree of porosity, which act as temporary supports for the cells, enabling regeneration of target tissues [1]. They act as a reservoir of ions, water, nutrients, cytokines and growth factors. Therefore, a scaffold can be considered an artificial substitute of natural extracellular matrix (ECM), as well as of the mineralized phase, promoting activity, which leads to bone growth, until its regeneration is complete [4,6-7]. They also support the vascularization of the newly formed tissue. They can actively participate in the regenerative process through the release of growth and/or differentiation factors, present in their tridimensional structure [4,6]. Thus, it can be assumed that a scaffold with the appropriated properties is an essential component for TE strategies, since its

properties affect not only cell survival, signaling, growth, propagation and reorganization, but also their gene expression and the preservation (or not) of their phenotype.

The criteria that defines a good scaffold for TE include having the adequate materials with suitable internal architecture, surface properties and sufficient mechanical properties that match the host tissue, including elastic modulus, compressive strength and fatigue resistance [1]. The bone biomechanical system is very complex, thus there is not yet a consensus on how to produce an ideal scaffold. However, the following properties have been defined as being essential:

- biocompatibility: one of the primary requirements of any scaffold. The biocompatibility of a scaffold is described as its capacity to support normal cellular activity, including molecular signaling without inducing systematic toxic effects to the host tissue and immunological reactions [5, 8-9]. The implantation of a scaffold can initiate a series of events in the organism being an answer to the presence of a foreign body. The typical initial inflammation can, in some cases, lead to a chronic inflammation, which may promote the development of a fibrous capsule and consequent failure of the implant [10]. The degree of biocompatibility of a material can be measured by the level of deviation from a normal process of tissue regeneration [11];

- osteointductivity: an ideal scaffold should be osteoconductive, allowing adhesion, cell proliferation and differentiation in the host tissue [6, 8-9]. The scaffold should induce bone formation through biomolecular signaling and stem cells recruitment. Moreover, an ideal scaffold need to let form blood vessels around or inside the implant in just a few weeks of implantation, aiming to help the supply of nutrients, oxygen and removal of waste products [9];

- biodegradability: the scaffold material should degrade into biodegradable metabolites and be excreted, or reused in tissue remodeling process. The scaffold degradation rate should be inversely proportional to the rate of tissue regeneration, in such a way that by the time the injury site is totally regenerated the scaffold is totally degraded [3,6,8,12];

- appropriate surface chemistry for cell attachment, proliferation and differentiation: since adhesion is a pre-requisite for future cellular functions, the different types of cells require the presence of a suitable substrate to retain their ability to proliferate and perform

differentiated functions [12]. Therefore, the surface characteristics of materials, (such as their topography, chemistry, surface energy and wettability) play a key role in cell adhesion to biomaterials [14]. Nevertheless, it is very rare that a material with good bulk properties also possesses the required surface characteristics. This is why surface modification is essential for most of the scaffolds used for medical applications [15];

- porosity and pore size: porosity is defined as the percentage of empty spaces within a solid body and it is independent of the material [16]. It is necessary for *in vivo* bone tissue growth to allow migration and proliferation of osteoblasts and mesenchymal cells, as well as matrix deposition. Generally, the required porosity is around 90% with a pore size between 20 and 250 μm . Pore size of 20 μm has been reported for fibroblast ingrowth, from 20 to 125 μm for regeneration of adult skin and 100-250 μm for bone regeneration [3]. Recent studies indicate that a high number of pores, combining micro and macroporous structures, allows the improvement of vascularization, comparatively with macroporous scaffolds, since an interconnected pore network structure enhances the diffusion rates to and from the center of the scaffold and facilitates vascularization thus improving oxygen and nutrient supply and waste removal [13]. However, porosity decreases with the mechanical properties, such as compressive strength, increasing the difficulty of scaffolds manufacturing. Small diameter pores are preferable to provide a high surface-volume rate;

- mechanical and physical properties: scaffolds should have sufficient mechanical strength to withstand hydrostatic pressure and tensions in host tissue, enabling a good coupling between the scaffold and the host tissue, and allowing cell adhesion and cell proliferation. The chemical and topographic properties of the surface, can affect cell adhesion and proliferation. The chemical properties are related with the ability of cells to adhere to the material, and also with the interaction between proteins and the material. The topographic properties are of particular interest regarding the osteoconductive activity (process through which osteogenic cells migrate to the surface of the scaffold after the implantation of the material) [6]. The mechanical properties of bone vary from cancellous to cortical bone. Young's modulus of cortical bone is between 15 and 20 GPa, whereas for cancellous bone is between 0.1 and 2 GPa. Compressive strength varies between 100 and 200 MPa for cortical bone and between 2 and 20 MPa for cancellous bone [9].

The wide variation in mechanical properties and pore geometry makes it difficult to design an ideal bone scaffold.

Table 1 shows the relationship between some scaffold characteristics and their corresponding biological effects.

Table1: Relationship between scaffold characteristics and the corresponding biological effects based in [3,7].

Scaffold characteristic	Biological effect
<i>Biocompatibility</i>	cell viability and tissue response
<i>Biodegradability</i>	helps tissue remodelling
<i>Porosity</i>	cell migration inside the scaffold transport of soluble signaling molecules, nitrogen, oxygen and metabolic waste removal vascularization
<i>Chemical properties of the material</i>	helps in cell attachment and signaling in cell environment allows release of bioactive substance
<i>Mechanical properties</i>	affects cell growth and proliferation response <i>in vivo</i> load bearing capacity

TE strategies based on scaffolds are very dependent on the selected material and of the technological process used for its production. Nowadays, four different classes of materials have been used in TE area: polymeric materials of natural origin (e.g. collagen), polymeric materials of synthetic origin (e.g. polyglycolic acid (PGA), polylactide acid (PLA) and poly(ϵ -caprolactone) (PCL)), metals (e.g. Magnesium) and ceramic materials (e.g. hydroxyapatite (HA)).

2.1.2 Biomaterials for scaffolds production

The design and fabrication of a porous 3D scaffold represent one of the most important steps of TE. In general, the scaffold should be made from a highly biocompatible material

which does not have the potential to initiate an immunological or clinically detectable foreign bone reaction [17].

Over the last century, there has been a great increase in the use of biomaterials such as biocompatible metals, ceramics and polymers for surgical purposes. Metals and ceramics are mainly used in orthopedics. However, these materials are not biodegradable and their processability is very limited. Thus, polymer materials have received special attention and have been widely used in tissue engineering, due to an easy control over biodegradability and processability [18].

2.1.2.1 Metals

Metals, such as stainless steel and titanium, are biocompatible, exhibit high compressive strengths, are easy to shape and relatively inexpensive. However, they show some disadvantages: they are not biodegradable, they are stiff and there is the possibility of metal ions release [8-9]. Moreover, they have a high Young's modulus, which induces stress shielding that can protect the native bone tissue from mechanical stimulation. Mechanical stimulation is an important initiator of differentiation and activation of osteoblasts. Therefore, metallic materials are used for scaffolds production in a limited number of situations, for example in spine surgery and also to coat the surface of prosthetic implants to promote bone ingrowth and secondary implant stability [19].

In the last years, a biodegradable scaffold material made from magnesium alloys has been developed. This material allows an increasing of the rate of bone formation and a suitable degradation rate. The osteoinductive properties of this material are based on the corrosion product magnesium hydroxide, which can temporarily enhance osteoblast activity and decrease the number of osteoclasts [8].

2.1.2.2 Ceramics

A ceramic is a material made from an inorganic, non-metallic material with a crystalline structure [19]. Ceramic materials have been widely used in biomedical engineering and in bone regeneration/substitution, mainly due to the ability of being osteoconductive and osteoinductive. They are mono or poly-crystalline biocompatible materials that show

strong chemical bonds among constitutive atoms, correlated with a high hardness and high melting temperature.

The major disadvantages of these materials are brittleness and low mechanical stability [4,6], which prevent their use in situations of regeneration of large bone defects. Moreover, they are usually difficult to process into porous structures with complex shapes [4]. Furthermore, due to *in vivo* features, like osteoclastic activity, their degradation/ dissolution rates are difficult to predict. This could be a problem, since a fast degradation will compromise the mechanical stability of the system, which is low by itself [6].

The most common ceramic material used to build scaffolds is calcium phosphate (CaP). CaP is an ideal candidate to produce matrices as it mimics the inorganic component of bone - calcium hydroxyapatite [19]. However, a too fast degradation of scaffolds made from CaP would lead to an increase of the extracellular concentration of Ca and P, which can cause cellular death [6]. Their physical properties including stability, their degradation rate and processability can be modified in a particular range by using different compositions. These materials are known to have an excellent biocompatibility and are bioactive, as they connect to bone, allowing an increase of bone tissue formation [8].

2.1.2.3 Polymers

Polymeric materials, for TE applications, should be biocompatible, biodegradable and easy to process. *In vivo*, polymers degrade mainly due to chemical reactions like hydrolysis. However, some polymers, especially natural polymers and their derivatives, are also susceptible to enzymatic degradation. The degradation rate of these materials can be modified based upon copolymerization and changes in its hydrophobicity and crystalline structure. Degradation reactions are not limited to the material surface, but can also occur for some polymers in the whole volume of the scaffold (BULK-degradation), due to the fast diffusion of water into the material [8].

The ideal polymer for TE applications should have the following properties [20-21]:

- should not induce an inflammatory response;
- must be metabolized in the body after finishing its purpose without a trace;
- should be easily processed into the final product form and easily sterilized.

These materials can be divided in two different types: **natural biodegradable polymers** and **synthetic biodegradable polymers**. Natural polymers are usually biocompatible, whereas synthetic polymers can contain a residue of initiators and other impurities that do not allow cell adhesion and growth. On the other hand synthetic polymers have better mechanical properties and thermal stability than several natural polymers [22].

Some examples of natural polymers are alginate, collagen and chitosan which promote a higher cell growth since they have a similar structure to the extracellular matrix of the tissue to regenerate. However, their regeneration rate cannot be controlled hindering their use.

Among synthetic polymers the most frequently used are polyglycolic acid (PGA), polylactic acid (PLA), and their copolymer PLGA, which obtained approval from the US Food and Drug Administration (FDA) for clinical use in sutures and some implantable devices. The natural polymers are obtained, as their name implies, from natural animal and vegetal sources, and have as their main advantage a low immunogenic potential, the ability to interact with the host tissues and a high chemical versatility. Besides, their use in TE is especially attractive due to their ability to be remodelled *in vivo* [8,18].

2.1.2.4 Composites

To overcome the limitations associated to individual biomaterials, the combination of materials with different characteristics has been studied in order to produce scaffolds. By selecting the right combination of materials, this strategy allows the adjustment of the mechanical properties, degradation and absorption rates and biocompatibility of the produced scaffolds. The degradation rates of the composites can be optimized by adjusting the composition and molecular weights of the polymers, in such a way that the degradation rate is complementary to the new bone formation rate [23].

For bone tissue regeneration, the combination of organic and inorganic materials is particularly interesting, since bone is *per se* a composite material made up of an organic phase (mainly collagen) and a mineral phase (hydroxyapatite).

In this work, a composite material based upon the aliphatic polyester PCL and the ceramic hydroxyapatite has been used to produce the scaffolds.

2.1.3 Technologies for scaffolds production

The mechanical, chemical and biological behaviour of scaffolds depend, in a first instance, on the intrinsically properties of the biomaterials used for their production.

In recent years, a number of fabrication technologies has been applied to process biodegradable and bioresorbable materials into 3D polymeric scaffolds. Nowadays, there are several techniques to produce scaffolds with different gradients, which can be categorized as conventional fabrication techniques or as advanced processing methods (non-conventional fabrication techniques).

2.1.3.1 Conventional Fabrication Techniques

Conventional technologies represent the oldest group of techniques used for scaffolds fabrication. They have been used in a large scale at a global level, with relative success. These methods include [3,6,17,20,24-26]:

- particulate leaching: involves the mix of solid impurities into a polymer solvent solution and casting the dispersion to produce a membrane of polymer and salt particles. The salt particles are then leached out with water, in order to obtain a porous membrane;
- phase separation: involves dissolving a polymer in a suitable solvent. Then it is necessary to place it in a mould, and to cool the mould until the solvent is frozen. The micro and macro structure can be controlled varying the quenching temperature, solvents and polymer concentration and material;
- supercritical fluid-gassing process: involves the use of polymers highly amorphous. The polymer granules are plasticized due to the employment of a gas, such as nitrogen at high pressure. The diffusion and dissolution of the gas into the polymer matrix results in a reduction of viscosity;
- electrospinning: is a technique to produce nano-fibrous scaffolds. Polymers are dissolved into a proper solvent or melted before being submitted to a very high voltage to overcome the surface tension and viscoelastic forces, as well as to form different fiber diameter (50 nm - 3 μm). They feature a morphologic similarity to the extracellular matrix of natural tissue with effective mechanical properties.

These processes are easy to implement and allow shape and pore size variations by changing the parameters of these techniques. However, the resulting organization of the pores is random, which can lead to pore pathways that are only partially connected. This could impair the supply of nutrients and the ingrowth of tissue and vessels into the scaffold. Furthermore, the existence of a substantial number of closed pores makes the resulting structures of these scaffolds fabrication processes as effective as films, allowing the proliferation in a 2D environment. Nevertheless, they are not suitable to obtain 3D tissues.

Beyond these limitations, conventional techniques often involve the use of organic solvents that may be toxic to the cells. Moreover, these techniques usually involve long fabrication times on top of being labour-intensive processes with increased costs [3].

The following table (Table 2) summarizes some of the key characteristics and parameters of these and other conventional techniques currently used.

Table 2: Currently applied 3D scaffold fabrication technologies in [17].

Fabrication technology	Processing	Material properties required for processing	Achievable pore size (μm)	Porosity (%)	Architecture
Solvent casting in combination with particular leaching	Casting	Soluble	30-300	20-50	Spherical pores, salt particles remain in matrix
Melt moulding	Moulding	Thermoplastic	50-500	< 80	
Emulsion freeze drying	Casting	Soluble	< 200	< 97	High volume of inter-connected microporous structure
Supercritical-fluid technology	Casting	Amorphous	< 100	10-30	High volume of non-interconnected microporous structure
Supercritical-fluid technology in combination with particle leaching	Casting	Amorphous	Micropores < 50 Macropores < 400	< 97	Low volume of non-interconnected microporous structure combined with interconnected
Fused deposition modelling	Solid free form fabrication	Thermoplastic	>150	< 80	100% of interconnected macroporous structure design and fabrication layer by layer.

2.1.3.2 Non-Conventional Fabrication Techniques

Lately, the scaffolds production with high geometrical precision has been done using automatic fabrication technologies [27-28]. The classification of these technologies has undergone many changes over time. Initially, they have been classified as technologies of Rapid Prototyping (RP), but more recently, according to the standards of the American Society for Testing and Materials (ASTM), they became classified as technologies of additive manufacturing techniques (AM).

The basic concept of AM technologies focus on physical reproduction of 3D objects, layer-by-layer, from bidimensional data (2D), achieved by the slicing of 3D models created with systems of CAD/CAM (CAM – Computer Aided Manufacturing) [30].

Figure 1 provides a general overview of the necessary steps to produce RP/AM scaffolds for tissue engineering.

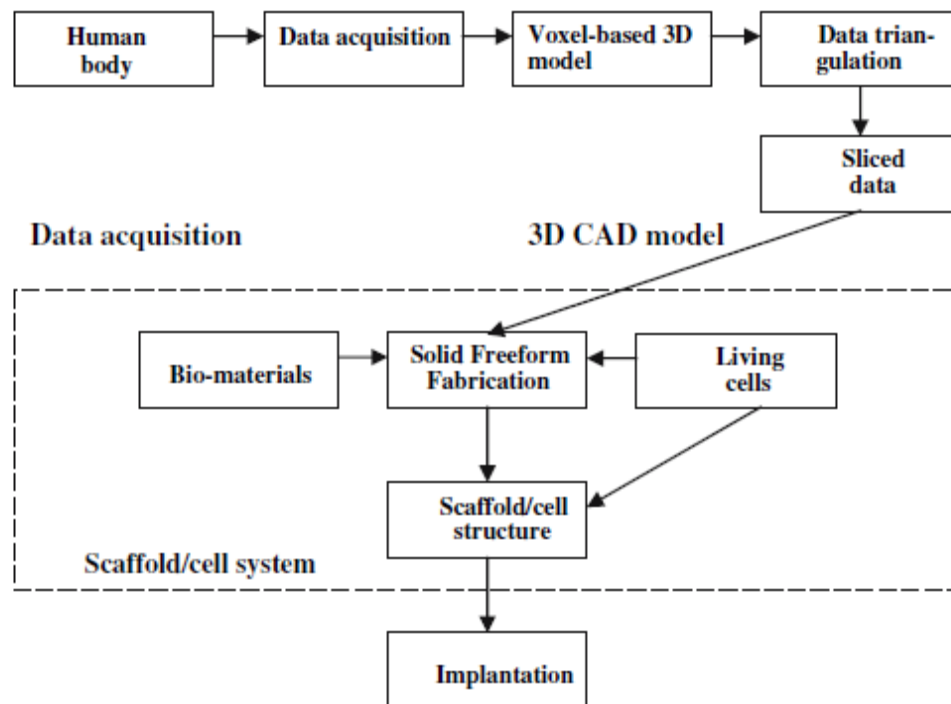


Figure 1: Steps of RP/AM in tissue engineering in [3].

The main advantages of AM technologies are the ability to rapidly produce very complex 3D models and to use different materials. These techniques also offer the assurance of reproducibility, and, due to the additive nature of the process, this also ensure a minimum wasting of biomaterials, being less expensive. Moreover, when combined with imaging data, these fabrication techniques can be used to produce custom implants with an adequate internal and external geometry, allowing a good coupling between the implant and the native tissue in the implantation site [4].

These techniques include stereolithographic processes, laser sintering, melt extrusion and three dimensional printing.

Stereolithographic processes

Stereolithography (Figure 2) is one of the most important AM technologies currently available. With this process 3D solid objects enables the production in a multi-layer procedure through the selective photo-initiated cure reaction of a liquid photosensitive polymer [3,30-31]. These processes usually uses two distinct methods of irradiation: **mask-based method** and **direct writing process** (see Figure 3).

In the mask-based method an image is transferred to a liquid polymer by irradiating through a mask with transparent areas, corresponding to the model section to manufacture. The irradiated part of the liquid polymer is then solidified [3]. The second method, a direct writing process, uses a focused UV beam to produce the polymer structure.

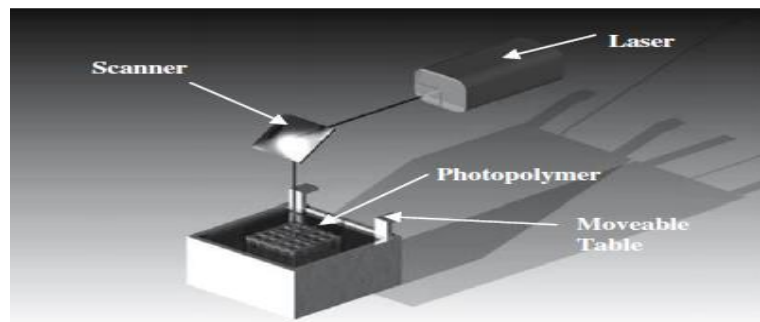


Figure 2: Stereolithography system in [3].

The direct writing system consists in a vat containing a photosensitive polymer, a moveable platform where the model is built, a laser to irradiate the polymer with UV radiation, and a dynamic mirror system to direct the laser beam over the polymer surface. After construction of each layer, the platform dips into the polymer vat containing the polymer, promoting the production of a non-crosslinked polymeric film from which the next layer will be formed [3,31]. The next layer is drawn after a wait period to recoat the surface of the previous layer [31].

The mask-based method builds models by shining a flood lamp through a mask, which lets light pass through it [3,30-31]. The exposure energy will start the curing process on the exposure area, forming each cross-section of the 3D physical object [26]. These systems often require the generation of a lot of masks, with precise mask alignments. One solution for this problem is the use of a liquid crystal display (LCD) or a digital projection system as a flexible mask.

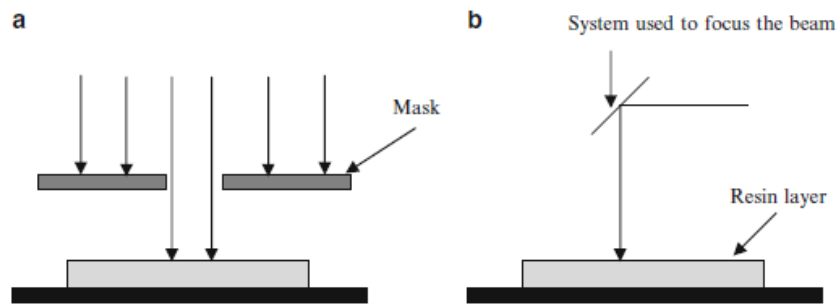


Figure 3: Writing methods in stereolithography processes. (a) Mask-based method. (b) Direct writing method in [3].

Three-dimensional printing

Three-dimensional printing (3DP) has been developed at the Massachusetts Institute of Technology (MIT) by Sanchs *et al.* (1989) [29,32]. This process consists in a homogeneous distribution of a powder material layer over the work platform, followed by selective deposition of an adhesive material in building zones. After the formation of each layer, a piston lowers the construction platform, according to the layer thickness, and a new layer of powder can be spread over the surface of the previous layer and then selectively joined to it. These steps are repeated until the 3D object is completely formed. After finishing the whole process,

a small airflow is used to remove unbound powder that remained in the internal structure of the piece [3,29-30,33].

Figure 4 represent the 3D printing system.

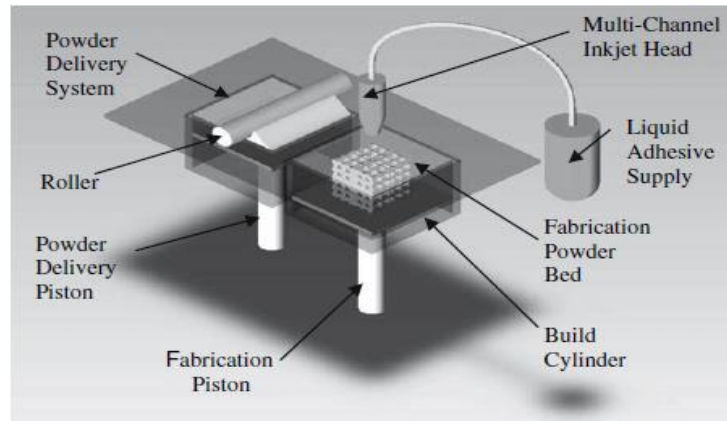


Figure 4: 3D printing process, in [3].

Laser Sintering

The process of Selective Laser Sintering (SLS), initially proposed by Deckard, uses a laser emitting infrared radiation, to selectively heat powder material until reaching a temperature near its melting point, Figure 5 [3,30].

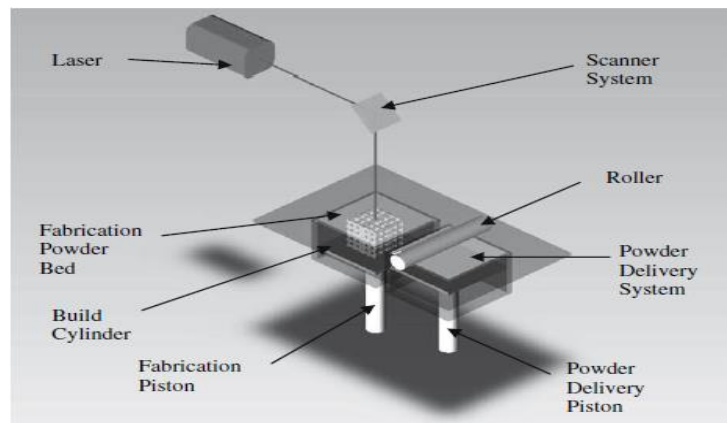


Figure 5: Selective laser sintering process in [3].

SLS constructs scaffolds from 3D digital data by sequentially fusing regions on a powder bed, layer-by-layer, via a computer controlled scanning laser beam [50]. The laser supplies energy

that fuses neighbouring powder particles, and also bonds each new layer to those previously sintered. After the formation and solidification of each layer, the piston over the model retracts to a new position and a new layer is supplied using a mechanical roller. The powder that remains unaffected by the laser acts as a natural support for the model, remaining in place until the model is complete [3-4,30].

SLS allows the construction of scaffolds with complex internal and external geometries. Virtually any powdered biomaterial that will fuse but not decompose under a laser beam can be used to produce scaffolds by this technique [34-35].

Extrusion- based processes

The extrusion-based rapid prototyping technique, proposed by Crump, is also known as Fused Deposition Modelling (FDM), Figure 6. Through this process, thin thermoplastic filaments are melted and deposited, layer-by-layer, by a robotic device controlled by a computer, to form the intended 3D object. A coil containing material in a wire form feeds the robotic device. The melted material leaves the extruder in a liquid form and is deposited in a construction platform where it hardens immediately [3-4,30,36]. The previously formed layer acts as substrate for the next layer, and must be maintained at a slightly lower temperature than the solidification temperature of the thermoplastic material. This will promote the proper deposition of the next layer and enables a good inter-layer adhesion [3,37].

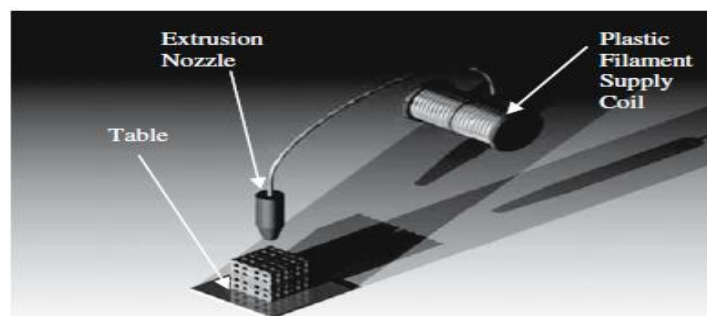


Figure 6: Fused deposition modelling process in [3].

The major limitations of FDM are due to the use of filament-based materials and the high heat effect on raw material [37]. Moreover, the phase change phenomena and the processing

conditions, considered for each application, may induce chemical and physical transformations of the material. As a consequence, the biocompatibility of the initial material can be altered during its fabrication process [38]. In order to solve some of these problems, some alternative processes have been proposed, such as the requirement of precursor filaments or high processing temperatures.

The IPL (Instituto Politécnico de Leiria) has developed a variant of the FDM process called BioExtruder (Figure 7). The scaffolds used in this work were produced by this equipment [3].

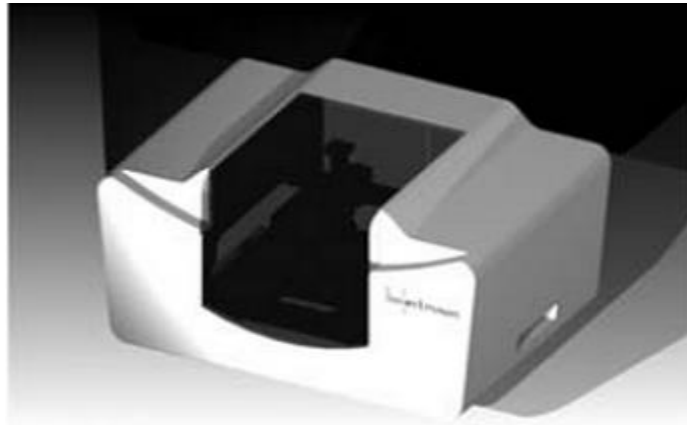


Figure 7: The BioExtruder device in [3].

2.2 Dental anatomy and root canal treatment

Dental anatomy can be defined as the study of the development, morphology, function and identity of each of the teeth in the human dentition, as well as the way in which the teeth are related in shape, form, structure, colour and function to the other teeth in the opposite arch [39].

In the human dentition, two sets of teeth erupt during the human lifetime. The first set of teeth is the primary dentition, which consists of 10 maxillary and 10 mandibular teeth. It normally begins to form 14 weeks after conception and usually it is completed around 3 years of age. The second set is the permanent dentition which consists of 16 maxillary and 16 mandibular teeth [39-40]. Scientifically, the permanent human dentition can be expressed by the following formula:

$$I \frac{2}{2} C \frac{1}{1} P \frac{2}{2} M \frac{3}{3} = 16$$

in which the denomination of each tooth is represented by the initial letter of its name (e.g., I for incisor, C for canine, P for premolar, M for molar), followed by a horizontal line with the number of that kind of teeth in the upper jaw written above the line, and the number in the lower jaw written below the line [39,41].

Each tooth is divided into two major parts: the **crown** and the **root**. The crown of the tooth is the visible part outside of the gums, projecting from the tissues to which the root is fixed. The root of the tooth is the portion which normally is not visible in the oral cavity, and is anchored within the bone. Within each tooth there are four different tissues (Figure 8): enamel, dentine, cementum (the hardest tissues of a tooth) and pulp, the soft tissue [39-42].

Enamel forms the outer surface of the crown of the tooth and it is the hardest tissue in the body, which allows the tooth to be able to withstand a great amount of stress, pressure and temperature changes [39-40,43]. It is formed by ameloblasts [44]. Chemically, enamel is a highly mineralized crystalline structure with approximately 95% to 98% of inorganic matter by

weight. The largest mineral present in enamel is hydroxyapatite (HA), which is present in 90% to 92% by volume. The remaining constituents of the enamel are an organic content of about 1% to 2% and a water content of about 4% by weight [40]. When enamel is formed it does not have the ability to grow or repair [43,45]. Structurally, enamel is very brittle, and has a high elastic modulus and low tensile strength.

Dentin is formed by odontoblasts, which are considered not only part of the dentin but also of the pulp. Hence, many authors consider dentin and pulp as a single specialized connective tissue [41]. Chemically, human dentin consists approximately of 75% of inorganic material, which is composed mainly by HA, 20% of organic material (mainly collagen), and 5% of water and other remaining materials. It is softer than enamel, but harder than cementum and bone.

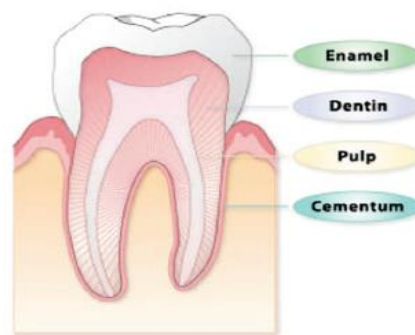


Figure 8: The four tissues of the teeth.

Cementum is the hardest dental tissue of the teeth covering the roots and is formed by cementoblasts. Chemically, cementum is composed of approximately 55% of organic material and 45% of inorganic material, mainly calcium salts. The organic portion is primarily composed of collagen, protein and polysaccharides. Cementum is avascular [40].

Dental pulp is a connective tissue located in the core of the tooth, and is surrounded by dentin. It is composed by arteries, nerves, veins, lymph vessels, intercellular substances, macrophages and odontoblasts, which are able to produce dentin [39-40,43]. The pulp can be divided into two areas: the pulp chamber, located in the crown of the tooth; and the pulp canal(s), located in the root(s) of the tooth [43]. Beyond the formation of dentin, pulp also has other functions: provides

the sensation to the tooth and responds to irritation by forming a secondary dentin or by becoming inflamed [46].

When pulp becomes inflamed or infected a **root canal treatment**, also known as endodontic treatment, is necessary. During this kind of treatment, the inflamed or infected pulp is removed and the inside of the root canals are carefully cleaned and disinfected. After cleaning of the pulp chamber and root canals, the latter are filled with a biocompatible material, with adequate physical, chemical and biological properties, to prevent any further infection (Figure 9) [47-49]. The filling has three different primary functions: sealing against the penetration of bacteria from the oral cavity, isolation of the remaining microorganisms, and prevention of infiltration of fluids, that can act as nutrients for bacteria.

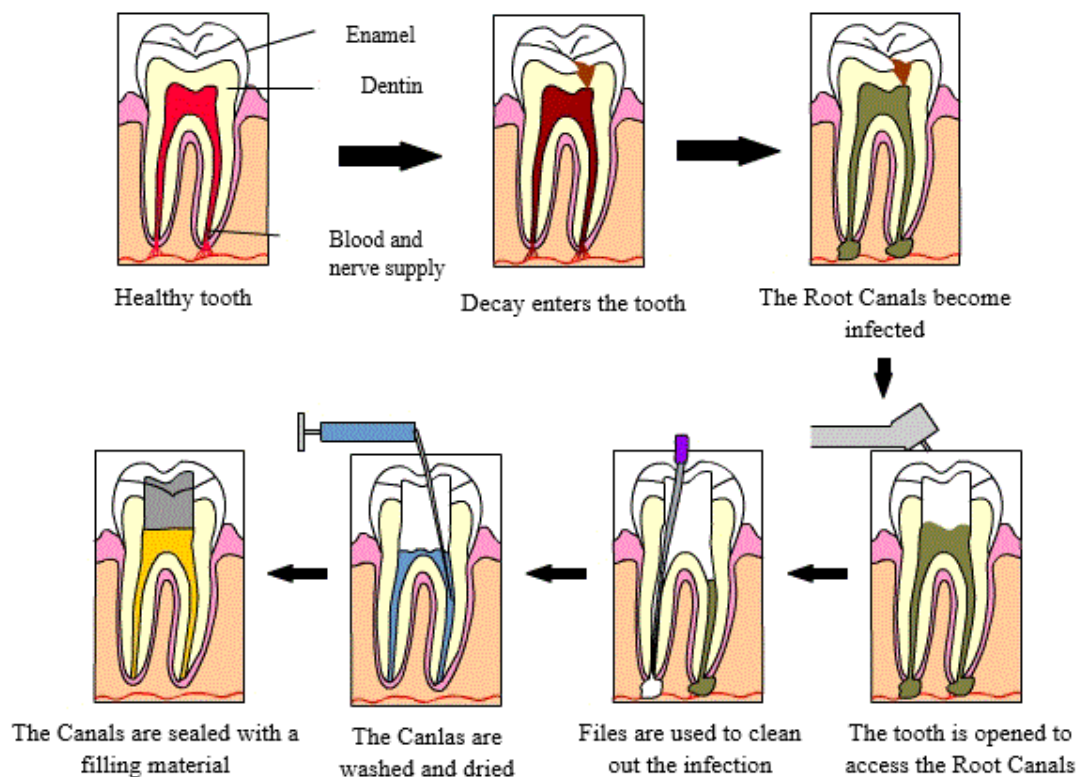


Figure 9: Main steps of the Root Canal treatment adapted from [50].

It is possible to say that the success of root canal treatment depends on proper diagnosis, adequate cleaning and shaping and three-dimensional filling of the root canals to prevent microorganisms from re-entering in the root canal system and cause re-infection [47,51-52].

This procedure allows saving the natural tooth, which implies several advantages: it maintains natural appearance, protects other teeth from excessive wear or strain, maintains a normal biting force and sensation and also an efficient chewing.

2.2.1 Root Canal Filling Materials

An ideal root canal filling material should be biocompatible, seal the root canal system in three dimensions, should not be affected by tissue fluids and should be insoluble in an oral environment [51,53-54]. It also must be nontoxic, radiopaque and easily removed from the canal if necessary (to enable re-treatment). Furthermore, it should be easily manipulated, have ample working time, should not corrode [51,53-54] and must possess ability to allow or induce bone repair [49,54]. Some of these materials also have the ability to flow adequately into the canal irregularities and ramifications of the root canal system, which, together with their antimicrobial efficacy, aid to eliminate microorganisms from the canal [47].

The classic filling technique associates a sealer with a solid core material. The core material acts as a nucleus for the sealer, and this sealer should fill in the blanks and adhere to the walls of the dentin. Root canal filling materials can be divided in two different categories: solid core materials (usually gutta-percha cones) and cements/sealers.

2.2.1.1 Gutta-percha

Gutta-percha is the dried resin of the trees of the family *Sapotaceae* [55] and has been universally accepted by professionals as the best filling material due to its dimensional stability and sealing ability. Nowadays, gutta-percha is available in the market in the form of cones (Figure 10) of a polymer of an organic matrix (latex) or combined with waxes and resins, zinc oxide, calcium carbonate, barium sulphate, strontium sulphate and other components, namely dyes. In fact, gutta-percha cones contain only approximately 20% of gutta-percha [56]. While pure gutta-percha does not show cytotoxicity effects, cones of gutta-percha show some

cytotoxicity, which has been attributed to the zinc oxide component, which is released over time [57].



Figure 10: Gutta-percha cones.

At room temperature gutta-percha is rigid, becoming pliable at temperatures between 25 and 30 °C, and melting at 100°C, with partial decomposition [58].

Gutta-percha shows good characteristics such as radiopacity, biocompatibility and dimensional stability. However, when it is used alone, the cones of gutta-percha do not ensure the complete seal of the canals and they also do not adhere to the dentin walls [59], reasons why there is

the need to add a sealer.

2.2.1.2 Sealers

Endodontic cements, also called sealers, have been demonstrated to be the essential components in the formation of a seal during canal filling [60]. They are designed to be used only within the root canal system. However during endodontic treatments, sealers sometimes become in contact with periapical tissues. Thus, biocompatibility of the sealers is of great importance to clinical success of endodontic treatment [61].

The ability of a sealer to flow, during canal filling procedures, reflects its capacity to penetrate into small irregularities and ramifications of the root canal system [47]. It is universally accepted that sealers should be able to fill imperfections and increase adaptation of the root canal filling [60-63]. Moreover, sealers act as a lubricant during insertion of the gutta-percha cones into the radicular system, and allow the filling of spaces where gutta-percha was not able to adapt [60].

Nowadays, there are many types of endodontic sealers commercially available. To date, they can be divided into five different groups: zinc-oxide-eugenol-based cements, calcium hydroxide cements, glass-ionomers, epoxy resins and silicone-based cements [55,62].

In the experimental study performed in this work, the cytotoxicity of three different endodontic materials has been studied: one epoxy resin (AH Plus Jet™) and two silicone-based sealers (GuttaFlow® 2 and an “improved” GuttaFlow®).

Zinc-oxide-eugenol-based cements

Zinc oxide-eugenol has been used by dentists for many decades as a temporary filling and also as a cement for endodontic treatments. Eugenol is correlated with phenol, a weak acid, and both have shown anaesthetic effects and germicidal activity [97] although biological effects of eugenol vary with concentration. At lower concentrations eugenol may have a beneficial effect, but higher concentrations may be cytotoxic (can cause cell death and/or inhibit cell division and respiration) [59,64].

When eugenol is mixed with zinc oxide, a chelation reaction occurs between the eugenol and the zinc ion of the zinc oxide, and a zinc eugenolate is formed [64-65]. This reaction can also occur between the eugenol and the zinc oxide phase of gutta-percha, which may explain the increase in volume of gutta-percha in contact with eugenol. Thus, increasing the proportion of eugenol into the zinc-oxide-eugenol-based cement enhances the volume expansion of the gutta-percha [65], which can result in a better sealing ability, but increase the risk of undesirable effects of eugenol.

Calcium hydroxide cements

The first clinical use of calcium hydroxide as a root filling material occurred in 1940, by Rhoner. Initially, these sealers were popular for pulp covering and for apexification techniques, although today the two main reasons for its use in endodontic treatment are stimulation of the periapical tissues in order to promote regeneration and its anti-microbial effects [66].

The therapeutic effect of calcium hydroxide in endodontic treatment is due to its dissolution when in contact with tissue and tissue fluids in the root canals, which leads to a continuous dissociation of calcium hydroxide in its ions (Ca^+ and OH^-) [67].

Glass-ionomers

Glass ionomer cements are a group of materials based on acid/base reaction between poly(alkenoic) acid and an ion-leachable silicate glass. These materials show a release of fluoride ions over an extended period of time [68].

Initially, its use in dentistry was limited by its slow setting time and its lack of strength, although some alterations in the formulations of these materials result in new materials with properties that are clinically useful in dentistry. Its biocompatibility with bone and osteoconductive behaviour are two of those properties. Besides, it exhibits modified working and setting times, no shrinkage upon setting and high adaptation to the canal walls and radiopacity [69].

Epoxy resins

Epoxy resin are commonly used as root canal filling materials due to their favourable properties regarding leakage prevention and biological responses [70]. Within this group of resins AH Plus is the most successful of the sealers.

Silicone-based cements

Silicone has been used in medicine as implant material due to its desirable properties like biocompatibility and inertness [71]. Silicone-based materials have been developed as root canal sealers, showing laboratory and clinical promising data [72]. Silicones show little leakage, and are virtually non-toxic [73].

The most used silicone-based cement is GuttaFlow[®], which was replaced by GuttaFlow[®] 2. GuttaFlow[®] 2 is the result of some modifications in the composition of GuttaFlow[®] in order to improve it, since the presence of silicone in GuttaFlow[®] induces poor wetting on the root dentin surface. This condition produces high surface tension forces, making the spreading of these materials more difficult. Another disadvantage of GuttaFlow[®] is that it does not adhere chemically to the dentin [73].

Chapter 3

Materials and characterization techniques

In this chapter the main materials and techniques used in this work will be described. This chapter is divided into three main sections. In the first, the materials used for scaffolds fabrication, specifically PCL and HA, and the techniques used for their production and characterization will be described. In the second section, the compositions of the endodontic cements tested in this work will be referred, as well as their main characteristics. Finally, in the third section, the assay used for cytotoxicity evaluation of both scaffolds and endodontic sealers will be described.

3.1 Materials used for scaffolds fabrication and techniques for their production and characterization

3.1.1 Materials

As previously referred, the production of scaffolds with adequate biomechanical properties for TE depends on several factors: materials used, pore geometry and structure interconnectivity. Over the past few years several studies have been reported based on the use of ceramic and polymeric materials. For example, biphasic composite materials (organic-inorganic) have the ability to combine the good mechanical strength of polymers with the high compressive strength of ceramics. Thus, based in the literature, for this work, composite scaffolds of PCL and HA were used. HA can be from natural or synthetic origin. Different pore sizes and geometries, have been selected in order to analyse their influence in cell adhesion, differentiation and proliferation.

Poly (ϵ -caprolactone)

Poly(ϵ -caprolactone), an US Food and Drug Administration (FDA)-approved material [17] is one of the most widely diffused biodegradable and non-cytotoxic polymer used as biomaterial for the production of scaffolds for TE [1-2]. It is an aliphatic polyester, semi-crystalline, biocompatible, with a melting temperature (T_m) between 55 and 60 °C and a glass transition temperature (T_g) of ≈ -60 °C [28,74]. The molecular structural unit of PCL is composed by five non-polar methylene groups and one relatively polar ester group. This structure gives PCL some unique properties, such as high processability and high thermal stability (its degradation temperature is near to 350°C).

PCL can be prepared either by ring-opening polymerization of ϵ -caprolactone (using anionic, cationic and co-ordination catalysts) or via free radical ring-opening polymerization of 2-methylene-1-3-dioxepane, Figure 11 [28]. Ring-opening polymerization can be applied to produce high molecular weight polymers, under mild reaction conditions and in shorter time, opposing to polycondensation, which requires higher temperature and longer reaction times [75].

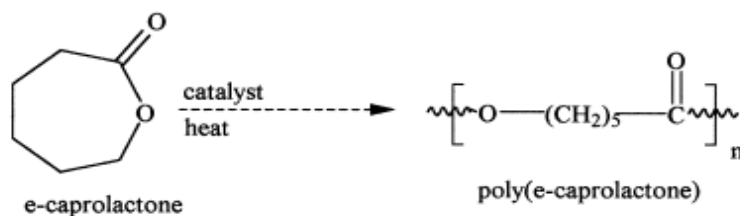


Figure 11: Synthesis of poly(ϵ -caprolactone) by ring-opening polymerization in [20].

PCL can be degraded by micro-organisms or by a hydrolytic mechanism under physiological conditions. In some specific situations, cross-linked PCL also can be degraded enzymatically by surface erosion [2]. Its degradation rate can be modified by the co-polymerization with other lactones or mix with other polymers [2]. Moreover, PCL has good dissolution in common organic solvents and its mechanical properties, added to its rate of bioresorption, contributes for PCL being one of the most used biomaterials in bone scaffold's applications [1,8].

Even though it has a good bioresorption for bone tissue engineering, as well as suitable mechanical properties [1], PCL shows a lack of bioactivity. Thus, when used in bone TE, the new bone tissue cannot bind tightly to the polymer surface [3]. This impairs its use as a scaffold for hard tissue regeneration, unless mechanical reinforcement is provided [74].

Hydroxyapatite (HA)

Hydroxyapatite is one of the most attractive materials for hard tissue implants due to its close resemblance to bones and teeth [75-78]. It is a class of calcium phosphate based bioceramic, with high biocompatibility and osteoconductivity [76-79]. HA is not only a biocompatible and osteoconductive, non-toxic, non-inflammatory and non-immunogenic agent, but also bioactive, i.e. it has got the ability to form a direct chemical bond with living tissues [76-78,80]. Additionally, the chemical similarity with bones and teeth is determinant in apatite deposition process (*in vitro* and *in vivo*), protein adsorption and subsequent bone regeneration. Its high biocompatibility with hard tissues, skin and muscle contributes to increase its acceptance as an implant [76,81]. Moreover, HA ceramics have the ability to induce mesenchymal cells to differentiate into osteoblasts. Therefore, HA is considered a good scaffold material for tissue engineering [82].

However, despite its inherent bioactivity and its excellent biocompatibility, HA is very brittle, difficult to shape and has poor tensile properties [77,79].

HA can be derived from natural or synthetic sources. The ceramic form of synthetic HA ($\text{Ca}_{10}(\text{PO}_4)_6(\text{OH})_2$), polycrystalline and densely sintered, is considered non-resorbable [83] or very little resorbable (1-2% per year) [84]. It has low bioactivity and acts mainly as a bioactive implant. The natural HA is non-stoichiometric (exhibits a Ca/P ratio higher than 1.67) and contains carbonate groups $(\text{CO}_3)^{2-}$ instead of groups $(\text{PO}_4)^{3-}$ and magnesium and sodium ions (Mg^{2+} , Na^{2+}) in place of calcium ions (Ca^{2+}) [85-86]. The presence of carbonate groups tends to decrease the crystallinity and to augment the solubility of HA, enhancing its biodegradation rate. Thus, the main difference between the synthetic and natural HA is the carbonate content which is smaller in synthetic HA [87].

The natural HA materials have the advantage to maintain the chemical composition and structure of the raw materials, from which they were manufactured, such as the pore structure [85]. Nevertheless, the use of natural HA in TE as substitute can induce the risk of disease transmission [44]. One way to reduce this risk is to do a heat treatment, usually at high temperatures. However, this can result in a change of composition, particularly by carbonate loss. This treatment can also induce a modification of the structure due to sintering of crystals, with consequent decrease of porosity, which reduces the effectiveness of the material [87].

3.1.2 Technology used for scaffolds production: BioExtruder

As referred in Chapter 2, the scaffolds used in this work were developed at IPL (Instituto Politécnico de Leiria) using a variant of FDM (fusion deposition modelling) called BioExtruder

BioExtruder is a low cost and high reproducible system enabling the fabrication of multi-material scaffolds, as well as a controlled definition of pores into the scaffold, to modulate mechanical strength and molecular diffusion [4,37-38].

The BioExtruder comprises two different deposition systems: one rotational system for multi-material deposition and another one for a unimaterial deposition that uses a screw to assist the deposition process [Figure 12 (a) and (b)] [38]. The multimaterial deposition system is composed by a rotational structure with four reservoirs, two of which with temperature control system, that are motioned by a pneumatic mechanism. The unimaterial extrusion system is endowed with a screw that assists in the material deposition. The BioExtruder allows the utilization of extrusion nozzles with diameters between 0.1 and 1 mm. The deposition code developed in Matlab (The Math-Works, Inc.) is based on the programming language ISO, usually used in CNC machines (Computer Numerical Control).

The information flow chart to produce scaffolds through the unimaterial extrusion system, which will be used in this work involves three main steps: (1) generation of a virtual 3D solid model directly by CAD software, or using data obtained by the imaging techniques (Magnetic Resonance Imaging or Computer Tomography); (2) conversion of the 3D model to a STL file (Stereolithographic file), which is the standard file for faceted models (common language for

all rapid prototyping equipment); (3) mathematical slicing of the STL file into thin layers or slices (sliced model); (4) each layer or slice is then physically reproduced by the BioExtruder [3].

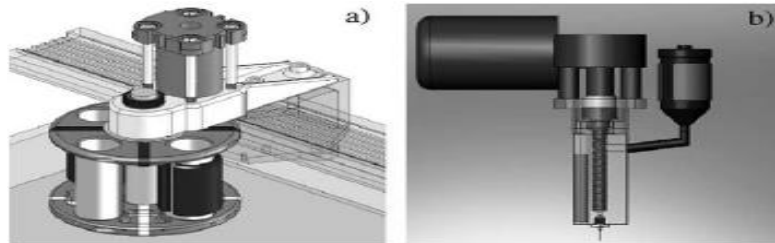


Figure 12: (a) Multi-material extrusion system; (b) Single-material extrusion in [3].

3.1.3 Scaffolds characterization

Thermogravimetry

Thermogravimetric analysis or thermal gravimetric analysis (TGA) is used as a method to investigate the thermal decomposition of polymers and to assess their relative thermal stabilities [88]. TGA uses heat to force reactions and physical changes on materials. The sample is placed in a micro-weighting machine, which is within an oven, to induce the heating conditions. TGA allows that changes in physical and chemical properties of materials are measured as a function of temperature increase (with a constant heating rate) or as function of time (with constant temperature or constant mass loss) [89].

The obtained results can be shown as a thermogravimetric curve (TG), in which it is reported the mass variation (in percentage) of the sample in function of temperature/time or in the form of a derivative termogravimetric curve (DTG), where the first curve TG is shown as function of temperature/time, Figure 13.

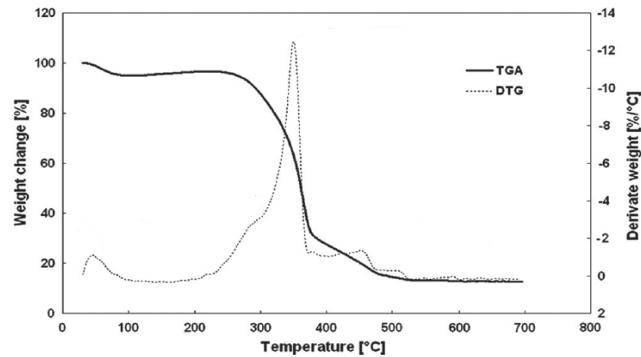


Figure 13: Example of a TG/DTG curve in [90].

Characteristic thermogravimetric curves are given for specific materials and chemical compounds due to a unique sequence from physicochemical reactions occurring over specific temperature ranges and heating rates. This characteristics are related to the molecular structure of the sample.

The weight and the preparation settings of the sample can influence the results obtained. Thus, samples with reduced mass and dimensions should be used, to avoid linearity deviation during heating [91].

Helium pycnometer

Helium pycnometer (Figure 14) is a laboratory device used for measuring the density and volume of a wide variety of materials in a simple and accurate manner [92]. The test for pycnometric density of solids is intended to determine the volume occupied by a known mass of powder. This is achieved by measuring the volume of gas displaced under defined conditions, similarly to the Archimedes method (the volume of liquid displaced by an object completely immersed in it, is equal to the volume of the object) [93-94].

The basic technique relies on measuring the material volume within the scaffold from a change in helium pressure, due to the presence of the scaffold in a known volume of gas. Helium is able to fully penetrate the porous structure of the scaffold without any problem due to surface tension, since it behaves as an ideal gas and has small atomic dimensions.



Figure 14: Schematic diagram of a gas pycnometer in [95].

Low-pressure plasma treatment

Plasma is a simple concept which refers to the fourth chemical state of matter (i.e., in the presence of sufficient energy, a solid can be melted to a liquid, a liquid vaporized into a gas, and a gas ionized into plasma). Plasma is a partially ionized gas containing ions, electrons, atoms and neutral species [96].

Plasma surface modification involves the interaction of the plasma-generated excited species with a solid interface [97]. When the plasma comes in contact with the material surface it transfers additional energy from the plasma to allow subsequent reactions to take place on the material surface. The plasma process results in a physical and/or chemical modification of the first few molecular layers of the surface, while maintaining the bulk properties.

Low-pressure plasma technology is an environmentally friendly and cost-efficient way to modify material surfaces, at microscopic level, without manual operations or the use of chemical products [96]. The process is carried out under vacuum conditions, to enable the gas to be ionized in a controlled manner. Plasma systems generally comprises five main components: the vacuum vessel, a pumping group, a gas-introduction and gas-control system, a high-frequency generator and a microprocessor-based system controller [96].

The surface modification processes can be divided into four categories: contamination removal, surface activation, etch and crosslinking. The surface activation was the used technique in this work. Plasma surface modification employs gases such as oxygen and nitrogen, which, when exposed to the plasma, will dissociate and react with the surface, creating different chemical

functional groups on the surface of the material. The new functional groups have strong chemical bonds with the bulk material and have the ability to further bond with adhesives to promote better adhesion. The functional groups also increase the surf adhesive strength [97-98]. A specially developed plasma activation process can be used to make a substrate surface more hydrophilic. Gas selection and surface type determine the functional group that will be substituted on the surface.

3.1.4 Scaffolds sterilization

Sterilization is defined as a process that intends to remove or destroy all viable forms of microbial life, including bacterial spores, in order to achieve an acceptable level of sterilization. Thus sterilization implies the inactivation and removal of all forms of life [99]. The efficacy of any sterilization process will depend on the nature of the product, the extent and type of contamination and conditions under which the final product has been prepared. It is expected that the sterilization method should not damage or modify the surface/structure of the material.

Biomedical devices prepared from biodegradable polyesters are usually sterilized by ethylene oxide, since other sterilization procedures, such as irradiation and heat, can cause extensive deformation of the devices and accelerated polymer degradation.

Ethylene oxide sterilization

Ethylene oxide (EO) sterilization is a commonly used method for the sterilization of heat-sensitive materials, such as medical equipment and pharmaceutical products that cannot endure conventional high temperature steam sterilization, due to the extreme penetrability of EO molecule and its compatibility with a wide range of materials [100-101].

EO sterilization has stood the test of time as a very effective sterilant, being good at killing a wide range of pathogens and sterilizing the most complex shapes [102]. It was developed in 1940 as a sterilizing agent by the US military, and its use as a medical sterilant dates to the late 50's. The sterilizing efficiency of EO depends on a series of factors such as the concentration of the gas, humidity, time of exposure, temperature and the nature of the load [103].

Sterilization via EO exposure begins with the adequate packaging of the scaffolds and their placement into a pressurized sterilization chamber. The humidity within the chamber is controlled by the introduction of moisture (40-90% humidity) and the temperature is maintained between 40 and 50°C. The EO is then introduced into the chamber at concentrations ranging 600 to 1200 mg.L⁻¹ for sufficient time (between 2-48 h) to achieve the desired SAL (sterility assurance level). After the sterilization, room air is used to flush the vessel to remove residual EO and its toxic byproducts but increases the overall sterilization time.

Chemically, EO reacts with nucleic acids, which contributes to kill microorganisms. Moreover, EO is an exceptional sterilizing agent due to its bactericidal, sporicidal, and virucidal activity. The greatest disadvantage of EO sterilization is the toxicity and carcinogenicity of the residual byproducts: ETO, ETC (ethylene chlorohydrin) and ETG (ethylene glycol) [99].

3.2 Endodontic cements and study models used for its *in vivo* cytotoxicity evaluation

3.2.1 Endodontic cements used

In this work, as referred in Chapter 1, three different sealers will be tested: AH Plus Jet™, which is an epoxy-resin composed of amines, and two silicone-based cements GuttaFlow®2 and the “improved” GuttaFlow®, that combines gutta-percha in a powder form with a sealer (polydimethylsiloxane). These sealers are available in self mixing syringes for direct application. In this work AH Plus™, GuttaFlow®2 and the “improved” GuttaFlow® were evaluated in order to determine which of these three endodontic cements show lower cytotoxicity and better biocompatibility.

The composition and characteristics of the “improved” GuttaFlow® will not be described, since it is not yet on the market, being still in study (under non-disclosure/confidentiality).

AH Plus™

AH Plus™ is an epoxy-resin whose first formulation was developed more than 50 years ago in Switzerland [55]. It has been shown to have low solubility and outstanding flow characteristics. AH Plus™ also shows low disintegration, good adhesion and excellent radiopacity [104]. It is usually used in combination with gutta-percha. However, although it has adequate long-term dimensional stability, it does not bond to gutta-percha, which is why its ability remains controversial [105].

Nowadays, AH Plus™ is commercially available into two different forms (Figure 15):

- AH Plus™ in tubes, pastes A and B, for manual mixing;
- AH Plus Jet™ in self-mixing syringes for direct intra-oral application, for a more appropriated application (easier, quicker and precise).

The pastes A and B of AH Plus™ have different compositions. Paste A is an epoxy paste and is composed by bisphenol-A epoxy resin, bisphenol-F epoxy resin, calcium tungsten,

zirconium oxide, silica and iron oxide particles. While paste B is an amine paste composed by three different types of amines, calcium tungsten, zirconium oxide, silicone oils and silica. The calcium tungsten, present in the AH Plus Jet™ composition, is much used to increase the radiopacity of the filling materials.

The form used in this work was the AH Plus Jet™.



Figure 15: AH Plus Jet™ and Ah Plus™ in tubes, respectively.

GuttaFlow® 2

GuttaFlow® 2 (Coltène/Whaledent, Langenau, Germany) is a novel silicone-based material for root canal filling that combines gutta-percha in a powder form with a particle size of less than 30 µm and a sealer (polydimethylsiloxane), into an auto-mix syringe (see Figure 16) [106-107].



Figure 16: Automaxic serynge of GuttaFlow®2.

It is the first sealer/gutta-percha combination sealer, flowable at room temperature that can be used not only as a sealer, but also as an obturating paste without a solid master cone. This

combination has as main goal to solve the problems resulting from the formation of interfaces between sealer - gutta-percha cones and sealer – and internal tooth structure which on setting causes shrinkage of sealer and, thus, voids are created resulting in the absence of complete seal.

The micro-silver in GuttaFlow[®] 2 is a metallic silver that is uniformly distributed on the surface of the filling [106] and which constitutes the antibacterial component, providing an optimum protection against re-infection of the root canal. It does not cause corrosion or colour changes in the GuttaFlow[®] [75].

It has some characteristics that makes it almost an ideal root filling material, such as good homogeneity and adaptation to the root canal walls [81], excellent physical and biological properties [107], good biocompatibility [106] and excellent flow properties, which ensure optimum distribution throughout the root canal. GuttaFlow[®] 2 also shows virtually no solubility, resulting in a dimensionally stable and impervious root canal filling with great adhesion to the dentine wall [73].

Despite all these advantages, a study done by Rana M. *et al.* [52] compared the results obtained using GuttaFlow[®] 2 with and without the solid support (gutta-percha cones). The results showed that, although GuttaFlow[®] 2 without the solid support has good adherence to the dental walls and also good physical properties, when combined with a solid support it shows better results [52]. In this context, Coltène developed a new material in order to improve the physical and mechanical properties of GuttaFlow[®] 2. The study of the cytotoxicity of this new material (which will be designed by “improved” GuttaFlow[®] in this dissertation) is one of the main goals of this work.

3.2.2 *In vivo* cytotoxicity of endodontic cements and study models

The implantation of endodontic cements in tissues of small size animal models has as its goal to test the local toxic effect [108].

Bone and connective tissues have been widely used to test the *in vivo* cytotoxicity and consequent biocompatibility of endodontic cements. The materials are introduced in the above mentioned tissues, using mainly small size animals, such as rabbits and rats. The interface

material/tissue can be direct or indirect, by inclusion in tubes/supports of different compositions [108-109].

For bone implantation, the materials are placed in cavities that are prepared for this purpose in the mandible, tibia or skull of the animal. For connective tissue implantation, the materials are injected or implanted in *locas* created by surgical dissection in the cellular subcutaneous tissue or in oral mucosa. Many authors have chosen to use cellular subcutaneous tissue of rats as a model to evaluate the histological response to the implantation of endodontic cements, which can be contained in tubes made of several materials or in direct contact with tissues [108].

Subcutaneous implantation

In the present work, the histological response of the subcutaneous tissue of the rat to the presence of AH Plus Jet™, GuttaFlow®2 and of the “improved” GuttaFlow® is studied. For this purpose, the tested materials were inserted in 8 mm tubes (Chapter 4), which latter were implanted in *locas* done by surgical dissection in the cellular subcutaneous tissue.

The materials that are implanted adsorb a layer of proteins, which results in a surface modification of the implant by them. The aggression that is caused in a vascularized tissue, due to the placing of the material, triggers an inflammatory response with immediate release of active biological substances that induce the migration of blood cells (e.g. neutrophils) to the reaction site [110]. Toxic materials cause necrosis of the surrounding tissues. Biocompatible materials are not susceptible to phagocytosis by neutrophils. The macrophages, whose migration is slower, are the ones that engulf and digest the implant as a foreign body. Macrophages are unsuccessful, and in order to increase their effectiveness in the engulfment process, they will fuse to form giant cells. However, these cell are incapable of engulfing the implant. Thus, the giant cells send chemical signals in order to bring fibroblasts to the implant site. This process is often called frustrated phagocytosis. Fibroblasts encapsulate the implant in a thin, avascular collagenous bursa to isolate it from the body [109-110]. This process is illustrated in Figure 17.

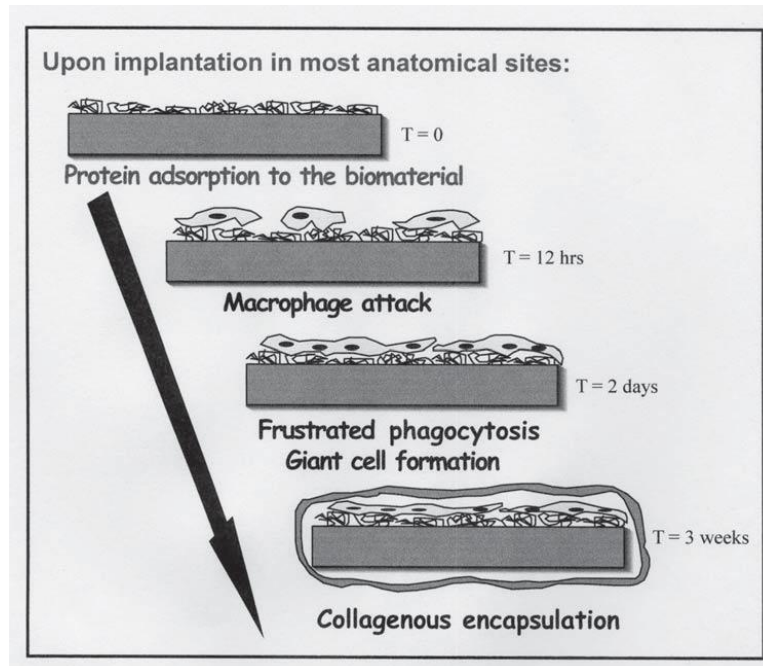


Figure 17: A schematic representation of the time course of the foreign body reaction to an implanted “biocompatible” material in [110].

Histologic technique

Histology is the study of cellular organization of body tissues and organs. The histologic technique is the operation set that has as its main goal to transform cells and tissues into preparations for light microscopy. The required steps occur in successive phases according with the fundamental principles of the histologic technique. These steps include **fixation**, **dehydration**, **embedding** in a suitable medium, **sectioning** into thin slices to enable the observation by transillumination, and **staining** [108-110].

Fixation refers to treatment of the tissue with chemical agents that retard the alterations of tissue subsequent to death (or after removal from the body) and maintain its normal architecture. [110]. This process can be divided into two different phases: (1) the coagulation or precipitation of several components of the tissue and cells; (2) their preservation in a state as nearly as possible like the living condition by forming stable chemical compounds [111]. An ideal fixative must penetrate quickly, render all parts of all cells permanent and allow the use of all kinds of stains. However, since the cell is a highly complex mixture of proteins, carbohydrates and lipids, and an ideal fixative would not only have to form stable compounds

with all of these, but also render them insoluble both in lipic solvents and in water, it has not been possible to find an ideal fixative. Some fixatives not only fail to preserve certain parts of the cell but actually dissolve or destroy them. For example, acetic acid destroys mitochondria. Moreover, some fixatives change the shape and relationship of parts of a tissue by shrinkage. Nowadays, the most common fixative agent used in light microscopy is neutral buffered formaldehyde. It penetrates rapidly, causes little distortion, does not destroy any of the cellular constituents and can be followed by almost all staining methods. However, it hardens the tissues very slowly, and does not protect them from the shrinking agents employed in embedding and sectioning. For this reason it is often combined with other fixing agents [109,111-112].

Dehydration is done due the fact that a large fraction of the tissues is composed of water, and water and paraffin (the usual embedding medium for light microscopy) do not mix. Thus, this phase consists in transferring the sample of tissue through a series of alcohol-water solutions beginning with 50% or 75% alcohol and progressing in graded steps to 100% alcohol, in order to remove the water (dehydration). Then, the tissue is treated with xylene. This last process is known as clearing, since the tissue becomes transparent in xylene [109,111].

In order to distinguish the overlapping cells in a tissue and the extracellular matrix, the tissues must be embedded in a proper medium (e.g. paraffin/paraplast) and then sliced into thin sections. **Embedding** takes place when the paraffin-infiltrated tissue is placed in fresh paraffin and the latter allowed to cool. After the blocks of paraffin are trimmed of excess embedding material, they are mounted for sectioning. **Sectioning** is accomplished by using a cutting apparatus called a microtome. The microtome will drive a knife across the surface of the paraffin cube and produce a series of thin sections of very precise thickness. The objective is to produce a continuous "ribbon" of sections adhering to one another by their leading and trailing edges. The thickness of the sections can be preset, and a thickness between 5 - 10 μm is optimal for observation with a light microscope [109-111]. The sections can then be mounted on glass slides and then stained by water-soluble stains that enable differentiation of the different cellular components [109,113].

Staining of histological sections allows observation of features otherwise not distinguishable. For routine histological work, it is common to use two dyes, one that stains certain components a bright color and the other, called the counterstain, which stains other cellular structures, a contrasting color. The most commonly used stains in histology are hematoxylin and eosin (H&E). Hematoxylin is a base that preferentially colors the acidic components of the cell a bluish tint. Since the most acidic components are deoxyribonucleic acid (DNA) and ribonucleic acid (RNA), the nucleus and regions of the cytoplasm rich in ribosomes stain dark blue; these components are referred to as basophilic. Eosin is an acid that dyes the basic components of the cell in a pinkish color. As many cytoplasmic constituents have a basic pH, regions of the cytoplasm stain pink; these elements are said to be acidophilic [109-110].

3.3 *In vitro* cytotoxicity assay

Measurement of cell viability and proliferation are the basis for several *in vitro* assays of a cell population's response to external factors. The reduction of tetrazolium salts is now widely accepted as a reliable way to examine cell proliferation and, consequently, the cytotoxicity of the materials in study.

The MTT (3-(4,5-dimethylthiazol-2-yl)-2,5-diphenyltetrazolium bromide) assay is based on the ability of the dehydrogenase enzyme, present in metabolically active cells, to cleave the tetrazolium ring of MTT and consequently convert the yellow water-soluble tetrazolium salt into dark-blue/purple formazan crystals insoluble in aqueous solution [10-12]. This reduction process (Figure 18) is associated with the function of dehydrogenases, but may also be due to the action of molecules such as NADH and NADPH (reducing equivalents). The amount of formazan crystals formed is directly proportional to the mitochondrial enzyme activity, i.e. to the number of viable cells present [114-116]. After an adequate period of incubation of cells in the presence of the MTT solution, the MTT formazan reaction product is only partially soluble in the medium, thus an alcohol is used to dissolve the formazan and produce a homogenous solution, suitable for measurement of optical density [10]. Therefore, by ELISA spectrophotometry, it is possible to quantify the amount of formed crystals, which is a measure of metabolic activity.

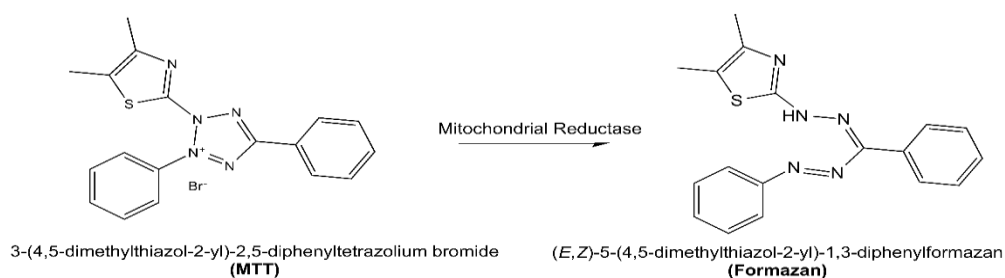


Figure 18: Schematic MTT reduction to formazan. This reaction can only occur when the reducing enzymes are active. This conversion is, therefore, used to measure cell viability in [115].

Chapter 4

Experimental

4.1 Introduction

In this chapter the procedures used to test the biological performance of the biomaterials, namely their cytotoxicity character, will be described in detail.

Regarding the biofabricated scaffolds, different aspects have been explored. As mentioned before, these scaffolds were produced by an additive biofabrication process, controlled by a computer (bioextrusion) using a mixture of poly(ϵ -caprolactone) and hydroxyapatite. Scaffolds with different composition and architectural features have been produced, being one of the aims of this work to study the effects of these properties on the cytotoxicity/cellular interaction.

The following points have been studied:

- **pore size and geometry:** porous matrices can be produced with different structural parameters by varying pore size and the deposition angle of the filament of the material during the layers formation. In the present work samples with two different pore sizes and angles were used: pore size of 300 and 600 μm and geometries of 0/45° and 0/90° (Figure 19). In fact, nowadays it is recognized that the microstructure of the scaffolds, more specifically the pore dimension and geometry, plays an essential role in cell adhesion, proliferation and differentiation, as well as in the vascularization process and tissue growth [6, 44];
- **matrix composition:** the scaffolds have been produced of pure PCL and of mixtures of PCL and hydroxyapatite (HA) in different percentages (10% and 25% of HA by weight). The idea behind the addition of HA is to improve osteoconduction, bioactivity, hydrophilicity and mechanical properties of the scaffolds, based on literature data [117]. In this work two different types of HA were used, synthetic and natural: HA S and HA N, respectively. As previously referred HA N differs from HA S since HA N is a poor

crystalline apatite and calcium deficient, resulting in alterations of its physical properties, which in turn highly affects the development of the cells;

- **surface properties:** due to the hydrophobic character of PCL, it was decided to modify the surface of the scaffolds using plasma technology, in order to improve the scaffolds hydrophilicity and thus promote a greater interaction between cells and scaffolds. The samples with a modified surface by plasma treatment tested in this work were composed of pure PCL and of PCL with 10% of HA S by weight.

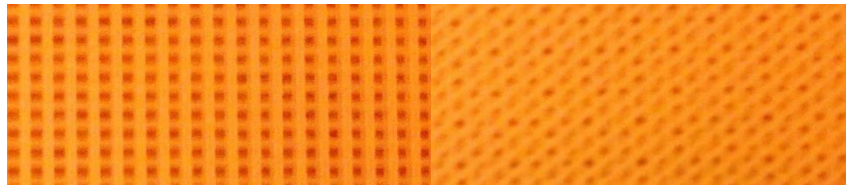


Figure 29: Scaffolds of PCL produced in the BioExtruder with 300 μm of pore size. The architectural orientation of the filaments 0/90° is shown on the left side and the 0/45° on the right side.

Concerning the endodontic materials, three different samples were tested: an epoxy-resin and two different silicone-based sealers, one of them not yet on the market as referred in Chapter 3. For these samples, besides *in vitro* cytotoxicity assays, *in vivo* studies were performed, in order to evaluate the inflammatory response to these materials.

Thus, this chapter is divided in four main parts. In the first one, the cells used in this work will be addressed, as well as the justification for their selection. In the second part the procedures adopted for the study of the influence of HA and of the scaffolds architecture in cell adhesion and proliferation will be described. Then, the *in vitro* and *in vivo* studies performed with endodontic materials/cements will be described. Finally, in the last part of this chapter, the statistical analysis done in order to analyze the obtained results will be referred.

4.2 Cell lines and cell cultures

The toxicity of materials is usually tested using cell cultures, at least in early stages, in order to decrease the number of *in vivo* studies. Indeed, tests on cell cultures are simple, fast and economical, and allow to test a wide variety of cells and co-culture under the same conditions. Additionally, these tests are reproducible and easy to perform. Moreover, *in vitro* tests have the advantage of using a culture medium with standard composition, defined incubation environment and sterile working conditions, enabling precise quantitative and qualitative assessments. However, the *in vitro* obtained results cannot be directly extrapolated to clinical situations. The importance of conducting *in vitro* studies is due to the fact that they are a first approach to analyze the effects of the tested materials and provide preliminary information to plan with the experimental process. They are intended to determine the biological mechanisms of action, without interference of other variables to influence results. This is one of the main reasons why the *in vitro* design has a fundamental role in the development of such studies, allowing to decrease the number of the performed *in vivo* studies (according to the 3R's principle)¹.

Since one of the possible applications of the materials tested in this study is the *in vivo* maxilla-mandible-facial implantation, they will be in direct contact with the cells of the connective

¹ The 3 R's principle was launched in the early 1960s by two English biologists, Russel and Burch in their book "The Principle of Humane Experimental Technique". The 3 Rs stand for Replacement, Reduction and Refinement.

Replacement: refer to the substitution of conscious living higher animals for insentient material. There are a number of alternative methods that can be used to replace the use of living animals in either all or part of a project. Replacement may be relative, when animals are still required to provide cells or tissue, but experiments are conducted *in vitro*: tissue culture, perfused organs, tissue slices, cellular and subcellular fractions [118].

Reduction alternatives: refer to any strategy that will result in fewer animals being used to obtain sufficient data to answer the research question, or in maximizing the information obtained per animal and thus potentially limiting or avoiding the subsequent use of additional animals, without compromising animal welfare [119].

Refinement alternatives: refer to the modification of husbandry or experimental procedures to minimize pain and distress, and to enhance the welfare of an animal used in science from the time it is born until its death [119].

tissue of the gum. Regarding the endodontic cements, in case of root canal perforation, they will be in direct contact with the periapical tissues. In this context it was decided to perform *in vitro* studies with **human fibroblasts**, since they are the major cell constituent of connective tissue and are found in all areas of the body. Fibroblasts are responsible for the synthesis of most components of connective tissue, including collagen, elastic fibers and proteoglycans [120-122]. They are adherent cells with a flat and elongated shape. Their main function is to produce extracellular matrix components (ECM), which consist of glycosaminoglycans, proteoglycans and fibrous structural proteins such as laminin, fibronectin, elastin and collagens that make up the extracellular matrix and maintain tissue architecture. The matrix proteins are also involved in wound healing and epithelial repair. Thus, they are used in culture studies as a support layer for cell proliferation.

The fibroblasts used in the development of this work are human fibroblasts isolated and cultured from the dental pulp. These fibroblasts were provided by the Area of Endodontics, Department of Dentistry of Coimbra University².

Besides human fibroblasts, macrophages were also used in the *in vitro* studies, since **macrophages** (and their precursors, monocytes) are the “big eaters/cleaners” of the immune system. They have highly variable morphological characteristics that will depend on their state of functional activity, and on the tissue where they were found. Macrophages are frequently used in *in vitro* studies since they are large, specialized cells that recognize, engulf and destroy target cells/particles/materials. They can change their functional phenotype depending on the environmental cues they receive [123]. Through their ability to clear pathogens and instruct other immune cells, macrophages have a central role in protecting the host but also contribute to the pathogenesis of inflammatory and degenerative diseases [124-125].

The harvest of human macrophages maintaining the desirable characteristics is very difficult to achieve and can be a source of possible biological contamination for the user. Rat or mouse peritoneal macrophages have the same characteristics as human macrophages [126]. Since naive macrophages do not divide *in vitro* by themselves, the Cell Line Companies must modify the

² I want to acknowledge Master Diana Sequeira and Professor João Miguel Santos for providing us the human fibroblasts used in this work.

harvested macrophages from either of these three species. This can be achieved with long periods of time of cell culture with exogenous growth factors [*Rattus norvegicus* alveolar macrophages, ATCC[®] CRL-2192[™]] or transformation using virus (e.g. SV40³ or murine leukemia virus) [*Mus musculus* peritoneal macrophages, ATCC[®] TIB-186[™] or ATCC[®] TIB71[™]] or, if obtained from mononuclear peripheral human blood, they grow as single cells in suspension [ATCC[®] CRL-9855[™]]. Neither of these hypotheses was viable for this work purposes or budget.

In this context, at IBILI, peritoneal macrophages of rats are currently used for *in vitro* studies to study the inflammatory response of living tissues, since they play a key role on innate acquired immune defense. The peritoneal macrophages used in this work were harvested by the team from Wistar rats raised at IBILI.

To harvest these macrophages, each animal was sacrificed by cervical dislocation (according to Annex II of the Portuguese Law Decree n° 113/2013). Then the procedure was done in another room with a flow laminar chamber (Holten, HB 2448, verified by IPAC), where UV light was previously on during approximately 30 minutes. After this time the UV is switched off and the flow laminar chamber was cleaned with alcohol at 75%. All the necessary procedures were done inside the flow laminar chamber using gloves and sterile material. All the enclosed sterile materials entering the flow chamber (syringes, needles and falcons) had been previously disinfected with alcohol at 75%.

Rats were disinfected with alcohol and put inside the chamber in a disinfected container. Then, 20 mL of a *Phosphate Buffer Saline* (PBS) [137 mM of NaCl (Sigma, S7653), 2.7 mM of KCl (Sigma, P9333), 10 mM of NaH₂PO₄ (Panreac, 1319651211), 1.8 mM of KH₂PO₄ (Merck, 6580), ultrapure water; pH 7.4] were injected in the peritoneum using a 25G × 1'', 0.5 × 25 mm, needle (T Terumos[®] Neolus, NN-2525R) and, after an abdominal massage, the liquid was harvested with a 1 mL syringe (T Terumos[®], SS+01T1) coupled to a 19G × 1'', 1.1 × 25 mm, needle (T Terumos[®] Neolus, NN-1925R) (Figure 20). Sterile 15 mL falcon tubes (Corning[®], 430052) with the recovered cell suspension were kept cooled in crushed ice.

³ Simian vacuolating virus 40, a poliomavírus.

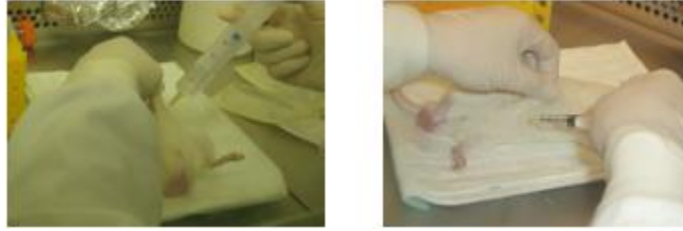


Figure 20: Injecting 20 mL of PBS (phosphate buffer saline) and harvesting macrophages (1 mL syringe with a 19G needle).

Afterwards, in a certified cell culture laboratory, the cell suspension previously collected was centrifuged during 10 minutes at 1100 rpm and 4°C in a *Heracus multifuge* centrifuge (1 L-R, certified by Certilab). The following procedures were done in a dedicated laminar flow chamber in sterile conditions. The supernatant was discarded and the pellet was re-suspended adding the complete culture medium RPMI-1640 [*Roswell Park Memorial Institute Medium* (Sigma, R8758), 10% of FBS (*Fetal Bovine Serum* (FBS, Sigma, F7524), 1% L-Glutamine (Sigma, G7513), 1% antibiotic Penicillin/Streptomycin (Pen/Strep, Sigma, A5955)].

As it has been mentioned, all the procedures described in this chapter were carried out in a cell culture room, in sterile conditions in a laminar flow chamber.

In fact, the main goal of cell cultures, the cultivation and propagation of disperse cells, requires the establishment of strict aseptic and sterile conditions.

Both cell lines, peritoneal macrophages and human fibroblasts, are adherent cell lines and both are maintained at 37°C in a humidified atmosphere of 5% CO₂ in a *Binder* incubator (06-10960 verified by Certilab).

The peritoneal macrophages were cultured in RPMI-1640 medium and human fibroblasts were propagated in *Dulbecco's Modified Eagle's Medium*, DMEM (Sigma, D5648) supplemented with 15% of FBS; 1% of antibiotic (Pen/Strep) and 1% L-Glutamine.

The peritoneal macrophages were placed in culture, at first, in 6-well flat bottom microplates (Costar®, Corning Incorporation, 3516) with approximately 1 mL of complete RPMI-1640. This was done to separate macrophages (adherent cells) from other blood cells harvested simultaneously, which are non-adherent. After 24 hours, if there were no experiments to

perform, macrophages should be frozen in a -80°C chamber (ThermoScientific, Herafreeze, HFU TSeries), since they do not divide *in vitro*. An image of the macrophages and the human fibroblasts used in this work is represented in Figures 21 and 22, respectively.



Figures 21 and 22: Microscopic image of macrophages and human fibroblasts, respectively.

To detach macrophages from the wells the supernatant was discarded. Then, with gentle circular motions the bottom of each well was scraped with a sterile scraper and macrophages were collected using approximately 1 mL of complete RPMI-1640 added to the well. After that, the suspension was collected with a Gilson pipette, using always sterile tips and inside the laminar flow chamber, to a sterile falcon and centrifuged (1100 rpm, 4°C). Inside the laminar flow chamber, the supernatant was discarded and a new volume (usually 1 mL) of complete culture medium was added to re-suspend the pellet. An aliquot of 10 mL of the cell suspension was taken to a sterile eppendorf. In order to count the number of viable cells 10 μL of Trypan Blue at 4% (Sigma, T8154) were added and the mixture was observed, in a Neubauer chamber (Marienfeld, 0610030), with an contrast phase optical microscope (Nikon Eclipse, TS100) coupled to a photo camera (Nikon Coolpix, S400), see Figures 23 and 24. The number of cells was recorded on the label of the cryopreservation tubes (Sarstedt, 72380992). These cryopreservation tubes can take up to 1.6 mL.

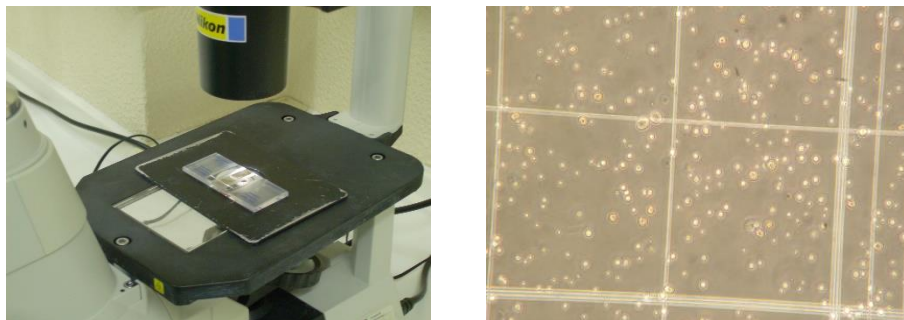


Figure 23 and 24: Neubauer cell chamber in an optical microscope and an example of an image seen in the microscope during cell counting.

In order to increase the number of viable cells during cryopreservation, 10% of the volume of the suspension placed in each tube of *Dimethyl Sulfoxide* (DMSO) (Sigma, D2650) was added. Finally the identified tubes were kept in a dedicated freezer at -80°C. Macrophages were kept in these conditions until a maximum of 2-3 weeks, and afterwards transferred to a liquid nitrogen chamber (-190°C) (ThermoNorma, Cryoplus 1).

Human fibroblasts used in these *in vitro* studies were cultured in 75 cm² flasks (Corning®, 4314640) with complete DMEM 5% (DMEM, 5% of FBS, 1% L-Glutamine, 1% antibiotic Pen/Strep). They had to be transferred from the flasks of 75 cm², when they reached confluence into new flasks by an enzymatic method. Fibroblasts were incubated at 37°C with 3-4 mL of a trypsin 0.25 % solution (BioWest, L0930-100), during the necessary time to become detached from the bottom of the flask. About 1 mL of culture medium was added to the flask in order to inactivate the enzymatic reaction. The cellular suspension was collected to a sterile 15 mL falcon tubes and centrifuged as previously referred. Human fibroblasts can also be frozen with a similar protocol, but they need to be kept sooner at -190°C in a liquid nitrogen chamber.

4.3 Tests with scaffolds

These studies, as previously referred, intend to evaluate the influence of the addition of HA to pure PCL regarding the interaction between cells and scaffolds, and also to evaluate the influence of different types and percentages of HA. Additionally, these studies also intended to assess the effect of pore size and geometry on the biological properties of the analyzed scaffolds. Finally, scaffolds whose surface was modified by plasma treatment were also tested. All the scaffolds used in this work were produced at IPL (Instituto Politécnico de Leiria) by qualified people.

4.3.1 Preparation of PCL-HA mixtures

For the development of a scaffold for TE some aspects must be considered, namely the easiness and flexibility of production, and characteristics like biocompatibility, bioactivity and osteoconductivity. As discussed before, HA satisfies these requirements. Despite these favorable characteristics, the mechanical strength of HA (which is very brittle) and the difficulty to manufacture complex structures are some of the main drawbacks of this material. On the other hand PCL, being equally biocompatible, fully meet these processing requests. Thus, composite scaffolds of PCL and HA lead, in principle, to an improvement of both biological and mechanical properties of the scaffolds. Additionally, it is expected that the mixture of HA to PCL, besides modulating the hydrophobicity/hydrophilicity of the composite, also improve the adsorption of specific proteins that help to regulate cellular adhesion and proliferation [127]. Studies involving polymers reinforced with hydroxyapatite showed that the incorporation of HA in different amounts allows the modulation of the composite elasticity.

As also pointed out earlier, the present work aims to compare the biologic performance of scaffolds produced with two types of HA (synthetic and natural), in the same conditions. For the production of composite scaffolds four different PCL-based mixtures were initially prepared using different types and percentages of HA (synthetic and natural HA with 10% or 25% of HA by weight).

In Figure 25 the different scaffolds compositions and the four architectures tested for each one of the compositions, are summarized.

These mixtures were prepared by melt blending, dispersing the HA particles in a PCL solution.

The solution preparation consists of the addition of PCL to a solvent mixture of chloroform and methanol (3:1) with 1% (w/v) of oleic acid, to promote the dispersion. Small portions of HA were added to this solution, which was heated and in constant agitation through a hot plate/magnetic stirrer. When the mixture was complete and uniform, it was placed in a plate for solvent evaporation during approximately 24 hours. Then, the mixture was placed in vacuum to eliminate any solvent residue. The solid mixture was fragmented into pellets to enable its placing into the deposit compartment on the BioExtruder.

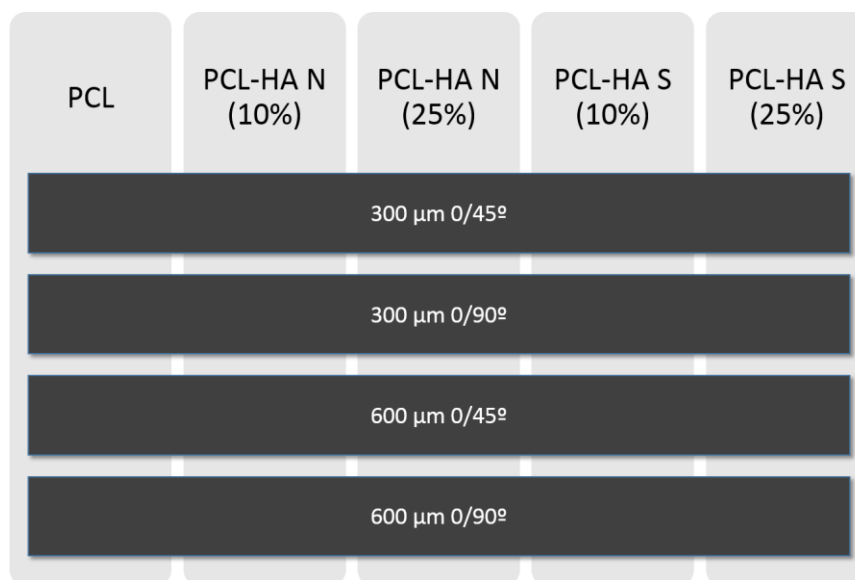


Figure 25: Characteristics of tested scaffolds, where HA N and HA S corresponds to natural and synthetic HA, respectively.

The used PCL [CAPA 6500 from Perstorp (UK)] has a molecular mass of 50 000 g/mol. Synthetic hydroxyapatite with an average particle size of 4 μm was purchase from Altakitin (Aveiro, Portugal), while natural hydroxyapatite was obtained thought the calcination of bovine bones at 600°C. Both natural and synthetic hydroxyapatite had identical average particle sizes.

4.3.2 Scaffolds architectural design

Besides studying the possible influence that different types and percentages of HA can have in cell adhesion and proliferation, the present study also intended to evaluate the influence of the size and geometry of the pores. Structures with different architectures were prepared to achieve this goal: two different pore sizes, 300 and 600 μm , and two different geometries (deposition angles), 0/45° and 0/90° were used.

4.3.3 Scaffolds characterizing techniques

The produced scaffolds were previously characterized to evaluate their thermal behavior and porosity as described below.

Thermogravimetric analysis (TGA)⁴

The thermal behavior of the matrices tested was assessed by TGA using a *TA Instrument SDT Q600*. From these results it is possible to determine the effective weight percentage of PCL in the composite scaffolds, as well the degradation temperature of the polymer. The mass loss of the samples as a function of temperature was observed between room temperature and 600°C, for each composition. Samples were analysed in triplicate.

Porosity⁵

The porosity of each scaffold was evaluated using the following methodology:

- the weight of the scaffold was measured;
- the dimensions of the scaffold (with the geometry of a square prism and the stander dimensions of 2×2×0.1 cm) were rigorously measured with the help of a ruler (length and width) and a micrometer (height) and its volume was calculated;
- the apparent density of the scaffold, ρ^* , was calculated according to the following equation:

^{4,5} These techniques were done by Doutora Patricia Coimbra at the Chemical Engineering Department of Coimbra University.

$$\rho^* = \frac{m}{V},$$

where m represents the mass of the scaffold in grams and V corresponds to the volume of the scaffold (cm³).

Finally, the porosity was calculated applying the following mathematical equation:

$$Porosity (\%) = \left(1 - \frac{\rho^*}{\rho}\right) \times 100,$$

where ρ (g/cm³) is the density of PLC or of the PCL/HA mixture, determined experimentally in a helium pycnometer (AccuPyc Pyknometer 1330, micromeritics).

Low pressure plasma treatment

Although PCL has good biocompatibility and structural stability, it demonstrates low surface energy, which together with the absence of bioactive functional groups on PCL surface create an interference with cells affinity and subsequent cellular interaction [128].

To enhance bioactive properties of pure PCL scaffolds, surface modification techniques can be used. Plasma surface modification is one of these techniques and has the advantage of altering surface properties without changing the bulk behavior of the scaffolds and is free of residual solvents over the scaffold surface [128], as referred in Chapter 3. For plasma treatments, the exact control of the process conditions, such as working gas, time of reaction and pressure in the plasma chamber, allows high surface homogeneity [129].

For the plasma surface modification experiments, a laboratory and small-scale production plasma system FEMTO (low pressure plasma) was used. This equipment was manufactured by Diener Electronics (Germany), with a stainless steel plasma chamber of 100 mm of diameter and 270 mm of length [127,129]. The scaffolds were placed in the plasma chamber at \approx 80 mm from the electrode and oxygen (O₂) was purged into the chamber. The chamber was kept at 400 mTorr through vacuum pump, during 3 minutes. The plasma generated modified the 3D scaffolds surface.

Cytotoxicity assays

For this study a cell suspension with $\approx 5 \times 10^4$ cells/mL in culture medium for peritoneal macrophages and a cell suspension with $\approx 1.3 \times 10^4$ cells/mL for human fibroblasts were necessary. The scaffolds used for these assays were cut into circular blocks, with 1 mm of height and a diameter of 11 mm, to be inserted in 48-well microplates (Costar®, Corning Incorporation, 3548). The scaffolds were sterilized by ethylene oxide.

Inside the laminar flow chamber, in sterile conditions, the prepared suspensions were distributed by the 48-well microplates according to the pre-selected disposition of the scaffolds disks, with a final volume of 300 μ L per well. The suspensions were directly deposited on the scaffolds in the following way (see Figure 26):

- 150 μ L of the suspension of peritoneal macrophages plus 150 μ L of complete RPMI 10%;
- 150 μ L of the suspension of human fibroblasts plus 150 μ L of complete DMEM 15%;
- 150 μ L of the suspension of peritoneal macrophages plus 150 μ L of the suspension of human fibroblasts;
- wells containing only cells and culture medium, without scaffolds, were used as control groups.

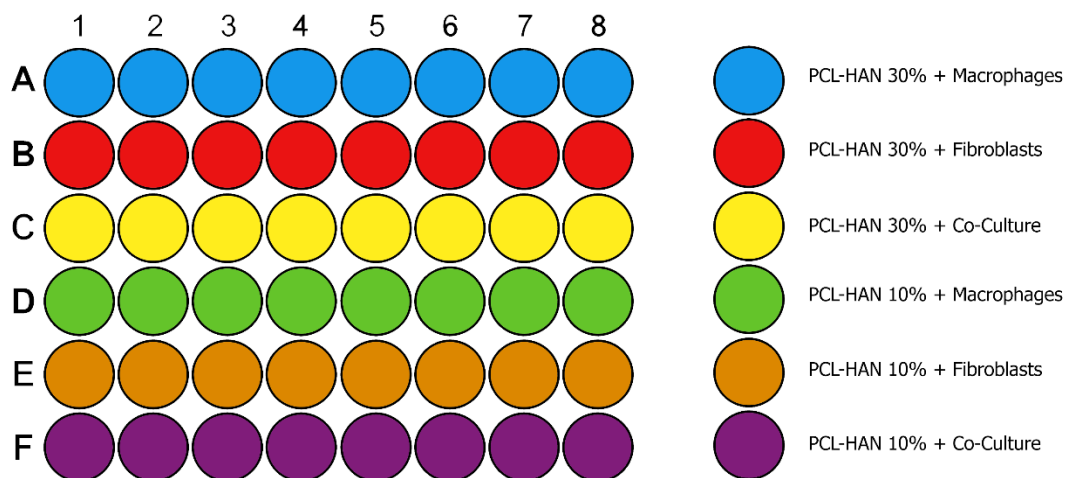


Figure 36: Representation of one of the used 48-well microplates.

For the case of co-culture, the same suspension of peritoneal macrophages and fibroblasts were used, leading to a proportion of ≈ 1 fibroblast per 5 peritoneal macrophages. This proportion was used since, as previously mentioned, macrophages do not divide *in vitro* contrarily to what happens with fibroblasts.

Cell proliferation and cytotoxicity were evaluated at 72 hours, for all scaffolds compositions, in the same conditions, through the MTT assay (Chapter 3).

To assess cell proliferation, always in sterile conditions, the culture medium was discarded and 270 μL of culture medium and 30 μL of MTT (0.5 mg/mL; Sigma, M2128) were added to each well of the assay. After four hours of incubation in the dark, at 37°C, with 5% CO_2 and at 95% relative humidity, the MTT was aspirated and the blue crystals were solubilized in 300 μL per well of a 0.04M solution of hydrochloric acid (HCl) (Sigma-Aldrich[®], H1758) in isopropanol (Sigma-Aldrich[®], 278475). After 15 minutes, the absorbance was measured with an ELISA spectrophotometer, using a wavelength of 570 nm and a reference length of 620 nm [130].

4.4 Tests with endodontic materials

As previously mentioned, the tests with these materials comprise both *in vitro* and *in vivo* tests.

4.4.1 *In vitro* cytotoxicity studies

These studies have as main goal to determine which of the three tested materials is less cytotoxic hence more biocompatible. For this purpose, it was decided to study the influence that different volumes of the tested materials might have in the cytotoxicity and to compare the biologic behavior of the different materials for two lengths of time: 72 and 120 hours.

These studies have been done with macrophages, fibroblasts and co-culture of macrophages and fibroblasts.

Initially, it was decided to compare the results obtained with fresh and with frozen macrophages in order to confirm if the chosen freezing protocol did not modify the biologic behavior (cell-material interaction) of the macrophages.

Two different volumes (0.02 mL and 0.03 mL) of AH Plus Jet™, GuttaFlow® 2 and of the “improved” GuttaFlow® were used (see Figure 27). The volume of materials were primarily placed in the wells of a 96-well microplate, with the help of a 1 mL syringe with a 21G × 1½”, 0.8 × 40 mm, needle (T Terumos® Neolus, NN-2138R), and only then the cells suspensions were added to the wells. A cell suspension of 6×10^4 fresh macrophages/mL and another of 6×10^4 frozen macrophages/mL were used.

To thaw the frozen macrophages, the containing cryopreservation tubes were heated during 1 to 2 minutes in a water bath at 37°C (Gesellschaft für, 10485789d). Afterwards, inside the flow laminar chamber in sterile conditions, cell suspension was transferred to a sterile falcon, adding approximately 2 mL of complete culture medium, RPMI-1640. This falcon was centrifuged during 10 minutes, at 4°C and 1,100 rpm. The supernatant was then removed and the pellet resulting of the centrifugation was re-suspended in 1 mL of new complete culture medium. Macrophages harvested and isolated on the day prior to the experiment and cultured during 24 hours are catalogued as fresh macrophages.

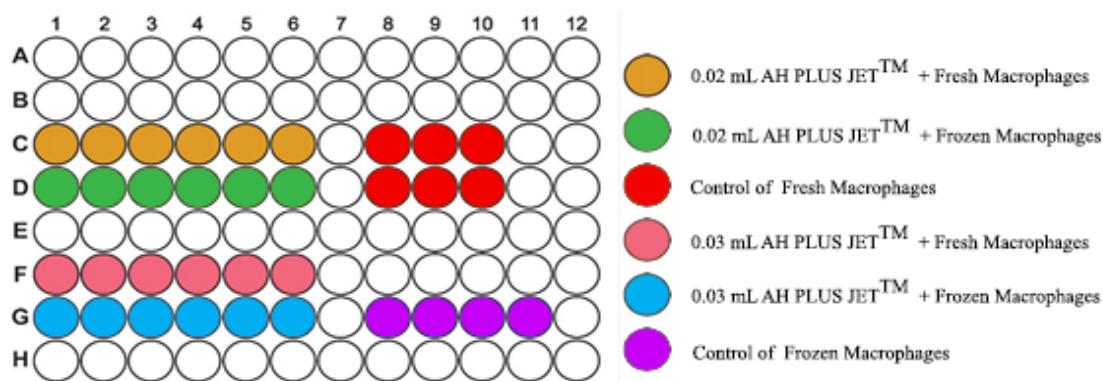


Figure 27: Arrangement of the samples in a 96-well microplate, for the study performed with frozen and fresh macrophages for AH Plus Jet™. The wells disposition for GuttaFlow® 2 and the “improved” Guttaflow® is the same.

The results obtained in this part of the study demonstrate that the biologic behavior of frozen macrophages is similar to the one of the fresh macrophages, as observed in Chapter 5. In this context the following assays were only done with frozen macrophages. Furthermore, the results of this study also demonstrate that there are not significant differences between the results obtained with 0.02 and with 0.03 mL of each one of the materials.

Thus, later studies were carried out as previously referred with frozen macrophages, fibroblasts and co-culture of fibroblasts and frozen macrophages. For the case of co-culture, the proportion of cells used was ≈ 1 fibroblast per 10 frozen macrophages (1:10). A cell suspension of 6×10^3 fibroblasts/mL and a cell suspension of 6×10^4 frozen macrophages/mL was used. The concentration of each cell suspension used in co-culture was the same as that used for each type of cell per itself.

In order to study the influence of the volume of material in the interaction between the referred cell lines and endodontic materials, two different volumes (0.01 mL and 0.02 mL) of AH Plus Jet™, GuttaFlow® 2 and the “improved” GuttaFlow® were used. These volumes of each one of the materials were placed in different wells of a 96-well microplate (Costar®, Corning Incorporation, 3596), according to a pre-selected disposition. Then 150 μ L of each one of the three prepared cell suspensions were placed in the different wells of the microplates, being directly deposited on materials, as pre-selected. These volumes of material (0.01 and 0.02 mL) were chosen trying to mimic the volumes used for the endodontic procedures. These volumes

are also chosen because they are the smallest volumes that are possible to measure with a syringe with a certain confidence degree, due to the fluidity of the endodontic materials.

Since GuttaFlow[®] 2 and the “improved” GuttaFlow[®] have Gutta-percha in their composition, and AH Plus Jet[™] is always used in combination with a solid support in clinic, it was also decided to perform tests with 0.01 and 0.02 mL of AH Plus Jet[™] in combination with small pieces of Gutta-percha cones, in the presence of frozen macrophages, fibroblasts and their co-culture.

In all the tests that were performed, wells containing only cells and culture medium, without endodontic materials, were used as control groups. When it was intended to study the behavior of AH Plus Jet[™] in combination with small pieces of Gutta-percha cones, wells containing cells, small pieces of Gutta-percha cones and culture medium were also used as control groups.

In Table 3 the different groups that were established during the development of this study are summarized.

The cytotoxicity of the three endodontic sealers tested was evaluated at 72 and 120 hours of incubation. These times were chosen because, as previously referred, macrophages do not divide *in vitro*, several toxic products are accumulated in the culture medium and cells start to die after 120 hours of incubation.

To assess cell proliferation, the culture medium was discarded and 135 μ L of culture medium and 15 μ L of MTT (0.5 mg/mL) were added to all wells of the assay. After four hours of incubation in the dark, at 37°C, in an atmosphere containing 5% CO₂ at 95% relative humidity, the MTT was removed and the purple bluish crystals were solubilized in 150 μ L per well of a 0.04 M solution of hydrochloric acid (HCl) in isopropanol. After 15 minutes, the absorbance was measured with an ELISA spectrophotometer, using a wavelength of 570 nm and a reference standard of 620 nm [130].

Table 3: Experimental groups for the *in vitro* study of cytotoxicity of the endodontic materials.

Experimental groups	
<p>Control incubated with the adequate culture medium (complete RPMI 1640 at 10% for macrophages and complete DMEM at 15% for fibroblasts)</p>	<ul style="list-style-type: none"> • fresh macrophages; • frozen macrophages • fibroblasts • co-culture of frozen macrophages and fibroblasts; • frozen macrophages with small pieces of Gutta-percha; • fibroblasts with small pieces of Gutta-percha; • co-culture of fibroblasts and frozen macrophages with small pieces of Gutta-percha;
<p>Fresh macrophages incubated with complete RPMI 1640 at 10% during 72h</p>	<ul style="list-style-type: none"> • with 0.02 and 0.03 mL of AH Plus JetTM; • with 0.02 and 0.03 mL of GuttaFlow^{®2}; • with 0.02 and 0.03 mL of the “improved” GuttaFlow[®];
<p>Frozen macrophages incubated with complete RPMI 1640 at 10% during 72h</p>	<ul style="list-style-type: none"> • with 0.01, 0.02 and 0.03 mL of AH Plus JetTM; • with 0.01, 0.02 and 0.03 mL of GuttaFlow^{®2}; • with 0.01, 0.02 and 0.03 mL of the “improved” GuttaFlow[®]; • with small pieces of Gutta-percha;
<p>Frozen macrophages incubated with complete RPMI 1640 at 10% during 120h</p>	<ul style="list-style-type: none"> • with 0.01 and 0.02 mL of AH Plus JetTM; • with 0.01 and 0.02 mL of GuttaFlow^{®2}; • with 0.01 and 0.02 mL of the “improved” GuttaFlow[®];
<p>Fibroblasts incubated with complete DMEM 15% during 72h</p>	<ul style="list-style-type: none"> • with 0.01 and 0.02 mL of AH Plus JetTM; • with 0.01 and 0.02 mL of GuttaFlow^{®2}; • with 0.01 and 0.02 mL of the “improved” GuttaFlow[®]; • with small pieces of Gutta-percha;
<p>Co-culture of frozen macrophages and fibroblasts incubated with complete DMEM at 15% during 72h</p>	<ul style="list-style-type: none"> • with 0.01 and 0.02 mL of AH Plus JetTM; • with 0.01 and 0.02 mL of GuttaFlow^{®2}; • with 0.01 and 0.02 mL of the “improved” GuttaFlow[®]; • with small pieces of Gutta-percha;

In Figure 28 it is possible to see an image of a 96-well microplates, used in this study. The purple color is due to the reduction of the tetrazolium salts of MTT by the dehydrogenase enzyme (see Chapter 3).

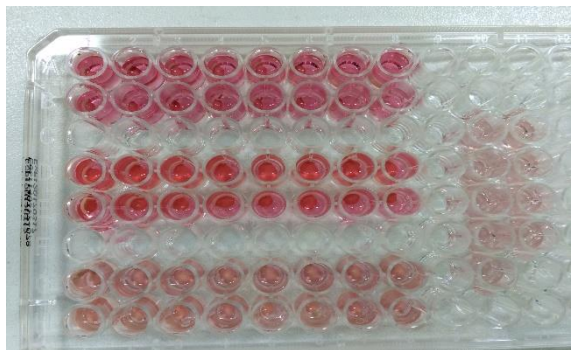


Figure 28: Image of the 96-well microplates after MTT assay.

As in the study with scaffolds, all these procedures were undertaken in a cell culture room, in sterile conditions inside a laminar flow chamber, using sterile material, and the gloves and all enclosure being previously disinfected with alcohol at 75%.

4.4.2 *In vivo* cytotoxicity studies

Although cell culture studies are relevant, when the final goal is the *in vivo* implantation, the obtained *in vitro* results cannot be directly extrapolated to the clinic, being necessary to resort to animal models, since *in vitro* assays cannot reproduce the *in vivo* anatomy and physiology. Wistar rats are the most used animals in laboratory research worldwide, since they are mammals and their body temperature ($\approx 37^{\circ}\text{C}$), physiology, anesthesia/drug administration is similar to humans.

Additionally, they are homoeothermic and regulate their body temperature by generating heat through metabolic processes and heat loss control. Heat loss is reduced by a thick fur cover and a layer of subcutaneous fat. In addition they are cost “effective” and easy to house, feed, breed and manipulate.

During these studies, some humanitarian critical limits have been taken into account as, for example, discomfort signs or severe pain, weight loss higher than 15% of the initial weight, respiratory difficulties and posture and motor activity changes [131].

Experimental protocol

For the *in vivo* assays 20 Wistar rats, adult females, were used with weights ranging between 120 and 260 grams.

The study comprised two different time periods, 8 and 30 days. The inflammatory response of the following materials was studied: AH Plus Jet™, GuttaFlow® 2 and the “improved” GuttaFlow®. The ultimate goal is to compare the behavior of the latter, not yet marketed, with the first two already available.

The evaluation was assessed by routine histological study, using optical microscopy. All the materials were implanted in all the animals, in distinct points of subcutaneous cellular tissue as described later (page 67).

Anesthesia

A combination of Ketamine 50 mg (Ketalar®, Cetamina Pfizer, 8276907) and chlorpromazine 5mg/mL (Largactil®, Laboratórios Vitória, 9977827) (3:10) i.m. was used. This combination was administrated in the thigh, via intramuscular (i.m.), with a dosage of 0.3 mL per 100 g of body weight.

Preparation of the chirurgic site and materials implantation

Trichotomy of the involved areas in the intervention was done, in 4 dorsum quadrants, at level of right and left scapular and right and left pelvic regions (Figure 29). The animal was positioned in ventral *decubitus*. Then, the disinfection of the trichotomized areas was carried out with a dermal solution of iodine polyvidone (Egrema, Paracelsia, 0670). The surgical procedure was performed inside a laminar flow chamber, and all surgical equipment (scalpel+blade 11, scissors, tweezers, needle holder, sutures) was sterile. The skin incisions (4 per animal) were done in a selected point of each quadrant, and a *loca* was created by blunt dissection of the subcutaneous cellular tissue. The studied materials were placed inside 18 GA, 1.3 mm × 48 mm, abocath tubes (BD Insyte™, 381247) with 8 mm long just prior to

implantation. This procedure was done in sterile conditions in another flow laminar chamber, using gloves and sterile material.

The materials were implanted in all the animals as represented in Figure 29:

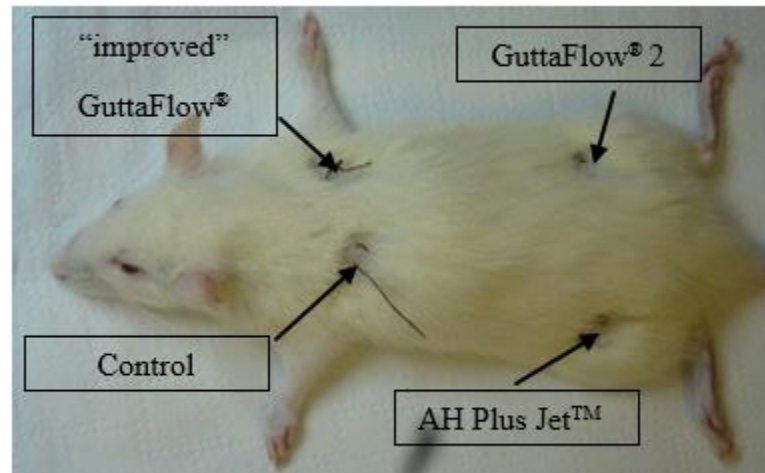


Figure 29: Anatomical localization of the implantation of the studied materials.

The interventions were finalized with closure of operatory wounds, using non-resorbable suture material, silk 4/0. All enclosures of used materials were previously disinfected with alcohol at 75% before going inside the laminar flow chamber.

Post-operative and control along time

At the end of surgery the animal was harmed up and monitored until awaking. Animals were kept in cages (an animal per cage), inside a temperature, light and in & out air flow controlled cabinet (Tecniplast, 9ARMI/4120). Animals were provided with proper food and water *ad libitum*, and bedding was changed once or twice a week, as needed. Animals were checked daily and weighted (Seca, model 734, serie 1/1) once a week.

Euthanasia

At the end of each period (8 and 30 days), animals were sacrificed by cervical dislocation according to the procedure described in Annex II of the Portuguese Law Decree n° 113/2013, August, 7th.

Necropsy and harvests

The weight of the animals was registered every 8 days. They were placed in ventral *decubitus* over an absorbent material. The location of the implants was searched by tactile sensitivity and trichotomy of the areas was re-done. Then the chirurgic removal of the implants was done (see Figure 30), with a wide safety margin of surrounding tissue.



Figure 30: Chirurgic removal of the implant.

The collected materials were photographed and immediately fixed in pre-identified laboratory cassettes (see Figure 31) for Anatomical Pathology routine processing by immersion in buffered formaldehyde at 10% (Sigma, 252549) (usually a volume 40 times larger than the samples). Containers were placed at 4°C for at least 48 hours. Routine processing was performed [109] for inclusion in paraplast (Sigma, P3568) and further histologic studies.

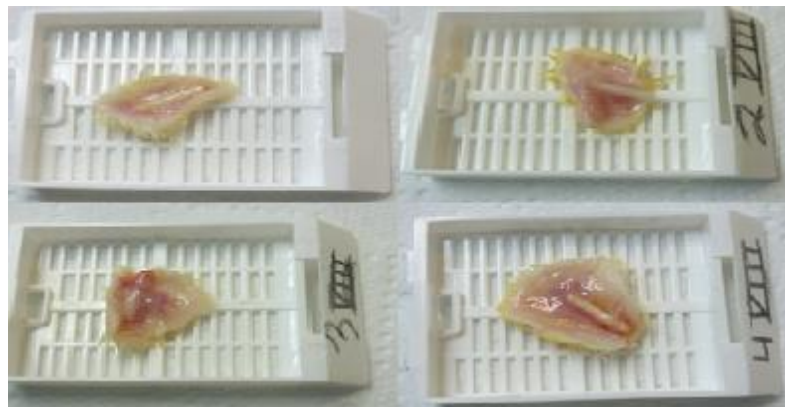


Figure 41: Explant with a wide margin of surrounding tissue.

Histology

Samples were prepared for the histological study at the Laboratory of Experimental Pathology of the Dentistry Department of the Medicine Faculty of the University of Coimbra.

In what concerns the histological preparation of the implants with surrounding tissue, they were fixed by immersion in neutral buffered formaldehyde at 10% (as referred in the previously topic). Following fixation, each tissue sample has been placed in an alcohol water solution, beginning with 60% alcohol and progressing in graded steps to 100% alcohol, in order to remove the water content. Then, the alcohol was replaced by xylene (Sigma-Aldrich, 534056), and in a next step xylene was replaced by paraplast (Sigma, P3568) (overnight at 56°C). The samples were included in paraplast to make blocks, using a dedicated equipment. Finally, the tissue blocks were cut into thin sections (5 µm of thickness), using a microtome (Leica RM 2155, Leica, Portugal) with disposable knives. The sections were, then, mounted on individual microscope slides (previously coated with a liquid adhesive and dried), using a black background water bath at 37°C. Afterwards, the microscope slides were placed in a store tray, in order to dry in incubator at 37°C.

The hematoxylin and eosin routine histologic coloring technique has been done in order to enable optical microscopy observation. Since the dyes are aqueous, the paraplast was removed with several steps of xylene, followed by a grading sequence of alcohols (from absolute ethanol to 60%). The sections were washed with tap water and were finally stained with Aldrich hematoxylin (Sigma-Aldrich, MHS1). Dye excess was removed with tap water and counterstaining was done with eosin (Sigma-Aldrich, HT110280) [109]. In order to obtain long lasting preparations, the sections have to be protected with a glass coverslip. The mounting media are not water soluble, hence the removal of water with an upgrading sequence of alcohol baths and xylene. After drying over night at room temperature or in the incubator at 37°C for a short period of time, sections were ready to be observed with an optical microscope and to obtain digital photos using a dedicated computer program.

4.5 Statistical analysis

In order to study the scaffolds, Kruskal-Wallis test was applied with adjusted pairwise comparisons to evaluate possible differences in MTT values due to different types and percentages of HA and different architectures (pore geometry and size). All the “*p* values” were obtained using the software IBM[®] SPSS[®] Statistic, version 22 (IBM Corporation, Armonk, New York, EUA).

In order to analyze the influence of the different parameters under study two different softwares were used. Initially MiniTab, (version 18), was used, however, as this software is normally only adequate when there are a large volume of data, the software Statistic *Data Mining*, version 10.0 (Dell Software) was used to try to confirm the previously obtained results with MiniTab.

Regarding the analysis of the cytotoxicity data of endodontic sealers, all the analysis were done with SPSS, applying the Kruskal-Wallis test and Mann-Whitney test.

Chapter 5

Results and discussion

As referred in Chapter 4, this work has two main objectives:

- i) assessing the biological performance/cytotoxicity of scaffolds for tissue regeneration;
- ii) assessing the cytotoxicity of three different endodontic cements in order to study the behavior of a new endodontic material in comparison with two other materials already on the market.

Both studies have been done using macrophages, fibroblasts and their co-culture.

In what concerns the first objective, the results analysis is done in order to evaluate the influence that scaffolds' architecture and composition have in cell adhesion and proliferation. It is important to note that the higher the cell adhesion and proliferation the smaller the cytotoxicity of the scaffolds is.

The aim of the analysis of the results of the second goal consists on assessing the *in vitro* cytotoxic effect of the three endodontic materials tested in this work (AH Plus Jet™, GuttaFlow® 2 and an “improved” GuttaFlow®), in order to evaluate the cytotoxic behavior of the new endodontic cement, the “improved” GuttaFlow®.

5.1 *In vitro* studies with scaffolds

In the literature, there are several references to the use of some biodegradable synthetic polymers in the field of biomedical engineering as they are ease to process, and due their mechanical and physical properties, low toxicity, low immunogenicity and low risk of infections.

The most widely used synthetic polymer is PCL (polycaprolactone), which is a linear aliphatic polyester, hydrophobic, biocompatible and biodegradable, with a melting temperature of $\approx 60^{\circ}\text{C}$. It also has high processability and high thermal stability. However, despite all these

advantages, the use of PCL in scaffolds' fabrication is limited due to its hydrophobic character. Thus, in this field, PCL has been used in the preparation of composites based on ceramic materials, in order to improve the mechanical strength, osteocompatibility/osteoconductivity and implant degradation rate.

Since the requirement of scaffolds can vary according to the cell type, it is necessary to ensure that the design and the production of porous structures are sufficiently flexible to accommodate and promote the growth of specific cell lines. Besides, the cell colonization process of scaffolds is highly dependent on the ability that cells have to build bridges between the pores and to migrate into the interior of scaffolds. It is known that a scaffold with an interconnected pore structure with appropriate pore size and distribution should facilitate the attachment and the proliferation of cells necessary for a complete tissue regeneration.

In order to evaluate all these factors, it was programmed to study the influence that different percentages (10 and 25%) and different types of HA - natural HA (HA N) and synthetic HA (HA S) - have in cell adhesion and proliferation within scaffolds. Two different cell lines, macrophages and fibroblasts, and their co-culture have been selected. Furthermore, the scaffolds that were used also had different architectures trying to evaluate the influence that the pore size and geometry might have in the interaction between cells and scaffolds (Figures 32-34).

In Figures 32-34 the obtained results for each one of the studied cells are represented.

Through the analysis of the results in these figures it is possible to see a clear influence of the pore architecture in the obtained results. The higher the intensity in the microplate reader, which is shown in the y-axis of the graphs, the higher is the number of living cells within the scaffolds. The obtained results suggest an increased number of metabolically active cells for pores of 300 μm and a geometry of 0/45° compared to the 0/90° one. Only for two of the analyzed compositions (HA S 25% 600 μm and HA N 10% 300 μm) better results were obtained with a geometry of 0/90°.

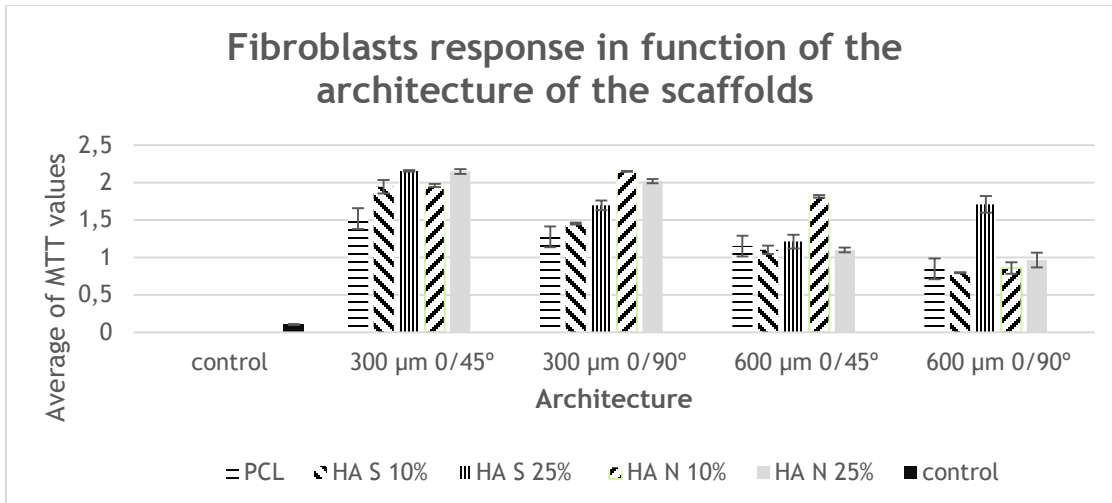


Figure 32: Representation of the fibroblasts response in function of the architecture of the scaffolds.

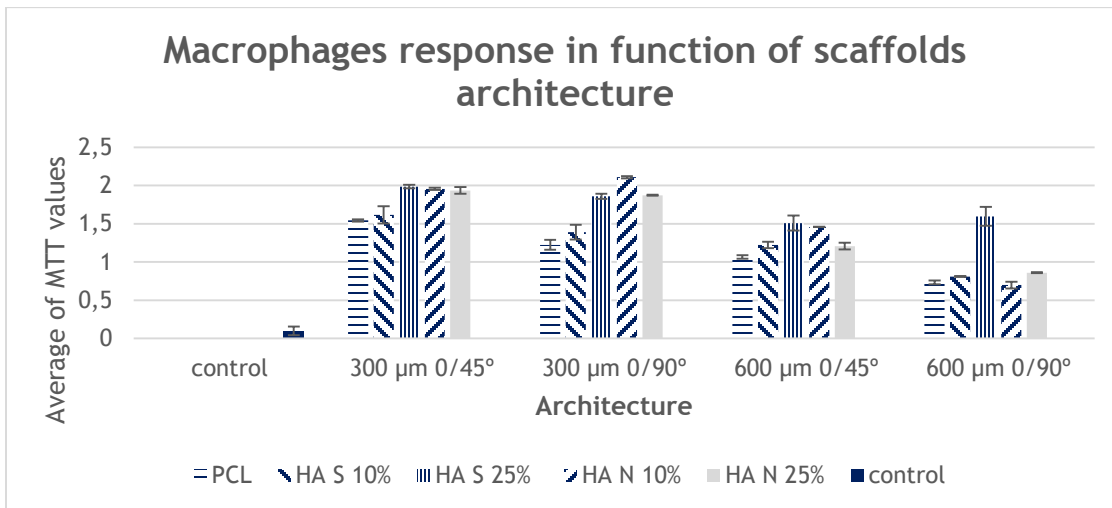


Figure 33: Representation of the macrophages response in function of the scaffolds architecture.

Using **SPSS** (IBM, version 2.2) it was possible to confirm these conclusions, since the obtained results show statistically significant differences ($p < 0.01$) for the pore size (300 vs 600 μm) and also for the geometry (0/45° vs 0/90°). The fact that cells prefer pores of 300 μm can be correlated with a better reproduction of what happens *in vivo*. The effective distance between cells and blood vessels *in vivo* are of the order of the 200-250 μm . In the literature a pore size around of 150-500 μm has been reported to facilitate vascularization and enable a good penetration of cells to promote the growth of new tissue [3,13]

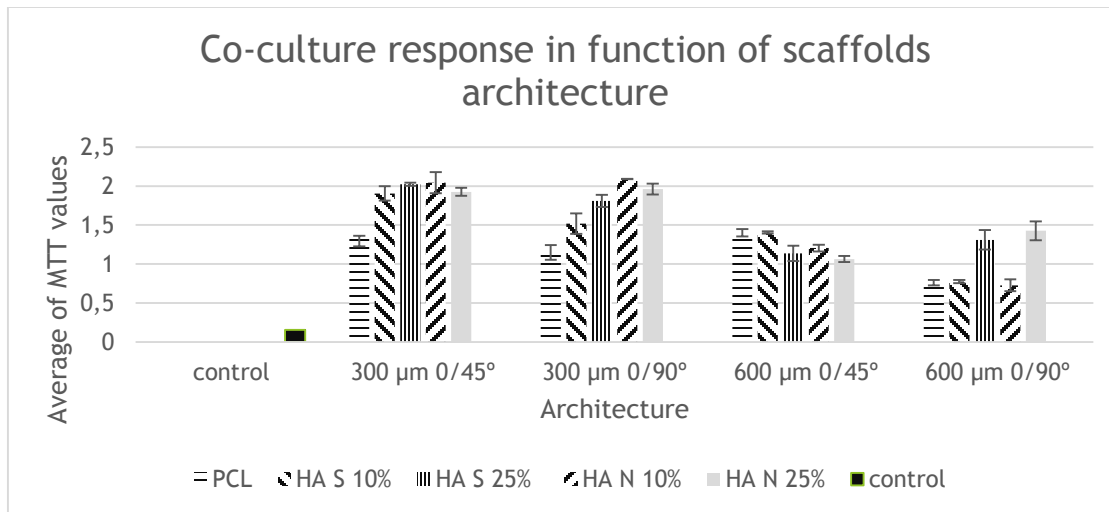


Figure 34: Representation of the co-culture response in function of the scaffolds architecture.

Observing the results in Table 4, regarding the scaffolds' porosity, based on gravimetric measurements, the architecture 300 μm 0/45° is the one presenting the lowest porosity values. However, these results do not clarify if cells migrate to the interior of the scaffolds or if they mainly adhere to the surface. Such a conclusion could be achieved after viewing the respective scaffolds using SEM (*Scanning Electron Microscope*) technology which has not been possible to do until the moment.

Table 4: Representation of the mean values obtained for the scaffolds porosity.

	Pure PCL	PCL-HA N 10%	PCL-HA N 25%	PCL-HA S 10%	PCL-HA S 25%
600 μm; 0/45°	59	44	52	50	50
600 μm; 0/90°	62	45	55	48	50
300 μm; 0/45°	42	19	34	33	29
300 μm; 0/90°	42	19	33	33	29

Observing Figures 32-34 it is also possible to see that independently of the architecture of the scaffolds, the results of the MTT assay show that the number of metabolic active cells for PCL/HA scaffolds was higher than for pure PCL scaffolds. This confirms the need to add a bioactive ceramic to the PCL. Although PCL is a biocompatible, biodegradable and easily

processable material, it has low ability to promote cell adhesion, proliferation and differentiation, mainly due to its hydrophobic characteristics. Moreover, PCL has low bioactivity, which limits the ability of the structures to recruit cells from surrounding tissues (when implanted *in vivo*), as well as the ability to promote cell adhesion, proliferation and differentiation *in vitro*. The superior biocompatibility of the PCL/HA scaffolds may result from the gradual dissolution of the incorporated HA particles into calcium and phosphate ions, which can help to regulate the behavior of the nearby cells.

Comparing the results obtained for each one of the cell types for each composition and architecture of the scaffolds, it can be observed that in most cases the higher values of MTT were obtained for fibroblasts. A possible justification could be the fact that fibroblasts are cells larger than macrophages, therefore occupying a larger surface area than the latter. In the case of co-culture, the presence of fibroblasts can difficult the adhesion of macrophages, even though care has been taken to seed macrophages immediately prior to fibroblasts. Furthermore, in contrast to fibroblasts, macrophages do not divide *in vitro*. This last factor was, however, taken into consideration during the experimental assay, having been used (as mentioned in page 60) a proportion of 1 fibroblast per 5 macrophages.

In order to investigate the impact and the magnitude of each factor in cellular response (MTT value) and the interaction between these factors, the experiments using scaffolds with HA were carried out following a design of experiments (DOE) of factorial type. DOE is a test, or series of tests, where intentional changes are made to the variables of a process in order to measure the responses of the process. The main goal of the DOE encompasses determining which variables have more influence on the response of the process. There are several types of DOE's, the one chosen for this analysis was the 2^4 design with four replicas per point. This means that there are four independent variables (factors) – pore, geometry, percentage of HA (HA %) and type of HA – studied at two levels, designated by low and high, and each point of the design has four replicas.

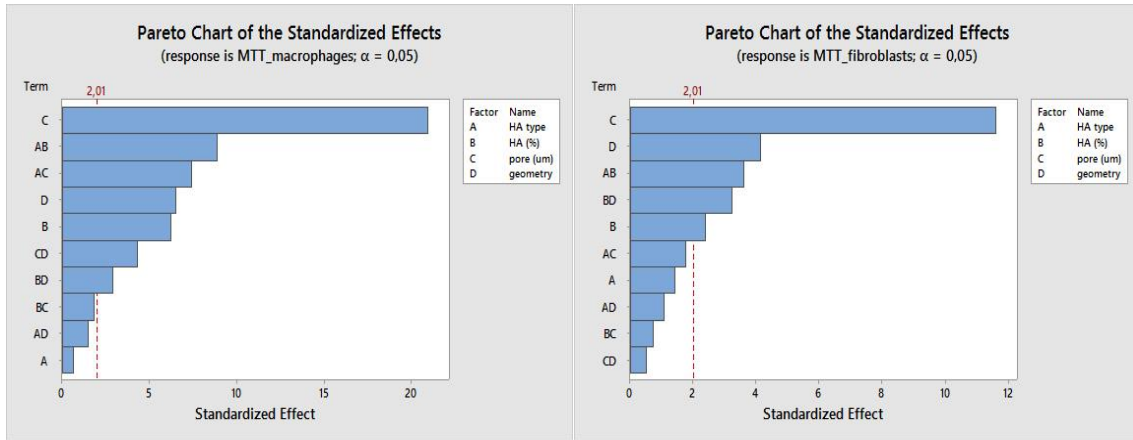
Table 5 shows the parameters used in DOE. The design layout, generated by the software miniTab is presented in appendix 1.

Table 5: Representation of the factors that were used for the DOE.

Factor	Name	Type	Levels	
			Low (-1)	High (+1)
A	HA Type	categorical	S	N
B	HA (%)	numerical	10	25
C	Pore (μm)	numerical	300	600
D	Geometry	categorical	0/45°	0/90°

Based on the DOE it was possible to adjust the results to a linear model (appendix 1) and to generate several graphs including **Pareto Charts**, Figures 35 to 37. In these graphs all the effects that exceed the line corresponding to a 2.01 value, are statistically significant. Thus, it can be seen that, regardless of the cell type used in this assay, the C factor (pore size) is the factor that most influences the obtained MTT values. The effect of C is about 5 to 10 times higher than the effect of the other factors. Although the MTT values for the percentage of HA and pore geometry are also significant, they had lower effects comparatively to the pore size factor. In this assay, the C factor (pore size) is the factor that most influences the obtained MTT values. Between the factors B and D, the most significant is factor D. Regarding the A factor (type of HA), it seems that it is the least significant of the four analyzed factors, being negligible for macrophages. The Pareto Charts obtained for each one of the studied cells types are represented in Figures 35 to 37.

Based on these results, it is possible to conclude that the scaffolds architecture, C and D factors, has more influence than the others analyzed factors, on the interaction between cells and scaffolds, which can be seen in the following three figures (Figures 35 to 37). This is in accordance with what was concluded based on previous results, and with what is reported in the literature, since the scaffolds colonization process is highly dependent on the ability of cells to build bridges between the pores. If the pore size is not adequate (too big or too small) cells will not have the ability to migrate and colonize the scaffolds in a homogeneous way.



Figures 35 and 36: Pareto Chart for the results obtained with macrophages and fibroblasts, respectively, where: A represents the type of HA, B the percentage of HA, C the size of the pores in μm and D the pore geometry ($0/45^\circ$ or $0/90^\circ$).

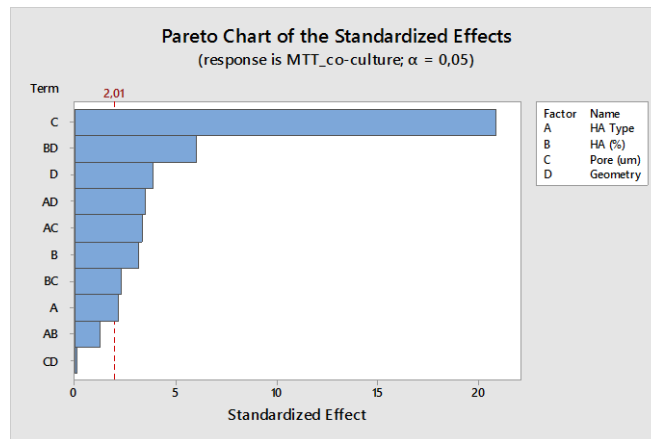


Figure 37: Pareto Chart for the case of co-culture.

As previously seen, the addition of HA to PCL significantly improves the MTT values, but this analysis also reveals that, being present, the type (synthetic HA or natural HA) and the percentage in which it is present (10% or 25%) have little influence on the results. However, this does not mean that the HA type is not important to the interaction of the scaffolds with other cells like osteoblasts, as well as for *in vivo* studies. Perhaps in these cases the effects of this factor will be statistically significant, but relying on the performed studies no conclusions can be drawn. The same can be concluded about the percentage of HA in the scaffolds, which surely will have a great influence on the mechanical properties and in the rate of *in vivo* degradation.

The effect of the interactions between factors are also significant, though their influence when compared with the effect of factor C is also small.

The analysis using SPSS and miniTab led to the same conclusions.

Figures 38 to 40 represent the main effects in the MTT values and their degree of influence. These figures confirm what was previously said about the influence of the factors. Observing the Figures 38-40 it is clear that the factors C and D (pore and geometry, respectively) are the factors that most influence the obtained results. By the slope of the line it is possible to see the influence that the different variables have in the MTT values. For example, the slope of the first graph on the Figures 38-40 is very small and positive, which indicates that HA N provides a slightly better interaction between cells and scaffolds (better MTT results), compared with HA S, but this difference is very small. In fact, the Pareto Charts indicate that this difference is not statistically significant both for fibroblasts and macrophages.

Concerning the percentage of HA, the increase from 10% to 25% results in a small increase of the MTT values. The results obtained regarding the pore and geometry are in accordance with the previous conclusions.

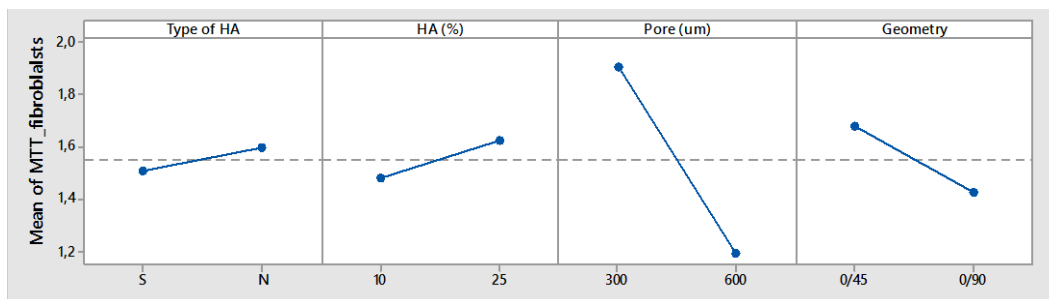


Figure 38: Main effects that influence interactions between fibroblasts and scaffolds.

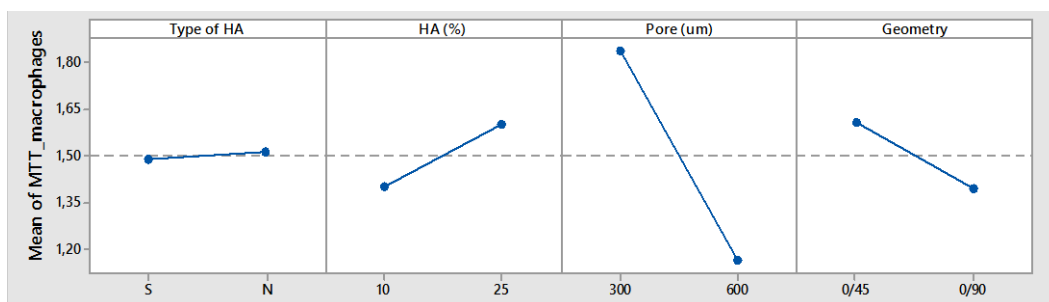


Figure 39: Main effects that influence interactions between macrophages and scaffolds.

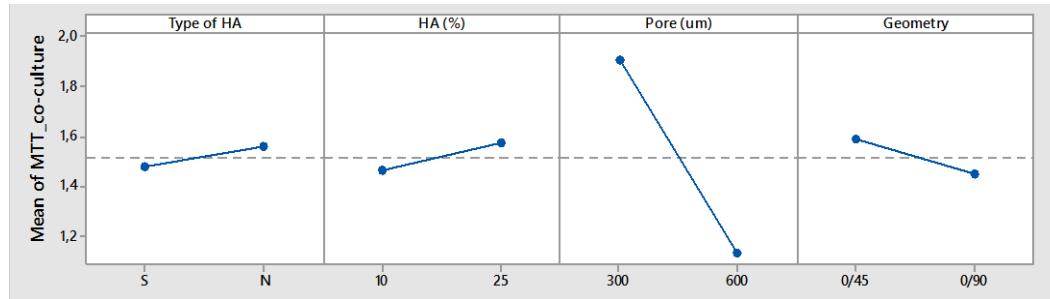


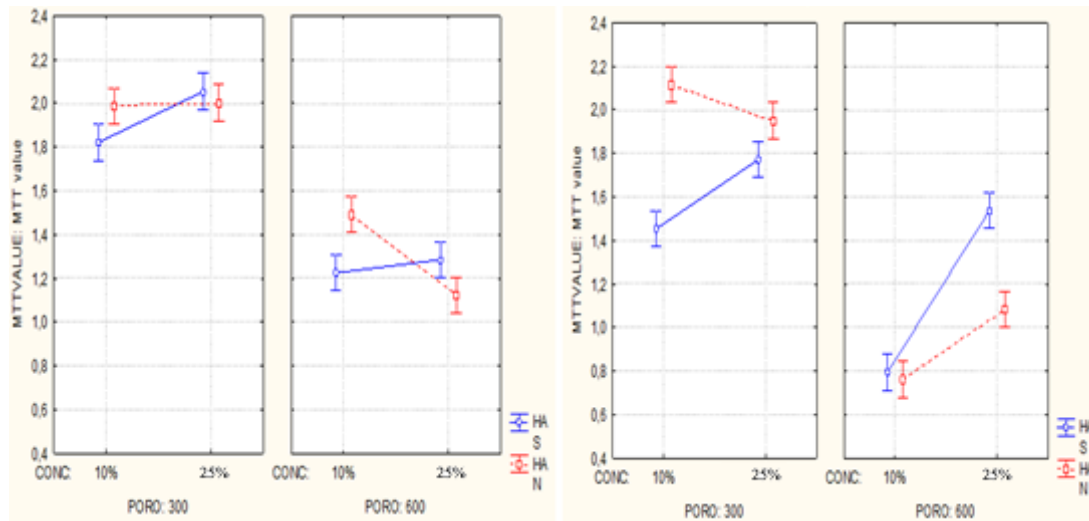
Figure 40: Main effects that influence cellular interactions with scaffolds for the co-culture.

As it is possible to see in the Pareto Charts in Figures 35 to 37, the interaction between factors also has significant effects in the results, although their influence is less significant than the one of C factor. Figures 38 to 40 represent the influence of each one of the interactions that occurred during the experiments. For example, observing the graph relative to the interaction between factors A and B (type and percentage of HA) - (first graph of Figures 38 to 40), and considering the combined results for macrophages, fibroblasts and their co-culture, it can be observed that the percentage of HA has a positive effect in the MTT values, being more significant (therefore having a greater effect) for HA S than for HA N. Analyzing the graphs of the Figures 35 to 37, it can be seen that only the interaction BD (interaction between the percentage of HA and the geometry) is always statistically significant, and that the effect of the geometry is more significant for the percentage of 10% of HA than for 25%.

In order to try to understand the interactions, the software **Statistic** (version 10.0) was used, allowing to evaluate the interaction between the four factors in study.

As it can be seen in the graphs of Figures 41 and 42, the percentage of HA for the geometry of 0/45° has a statistically significant effect but the same effect is not as significant for the geometry 0/90°.

Likewise, the results are always better for pores of 300 μm as previously concluded. This can be correlated to the fact that scaffolds with a geometry of 0/45° and 300 μm provide a larger surface area than pores of 600 μm and 0/90°.



Figures 41 and 42: Influence of the percentage of HA in function of the pore and type of HA for the geometry 0/45° and 0/90°, respectively.

Observing Figures 43 and 44, it seems that the four cases have significant differences in their results, although the major differences occur for the geometry of 0/45° and a pore of 300 µm, which is in accordance with Figures 41 and 42.

In appendix 2, 3 and 4 the graphs relatives to normal probability for macrophages, fibroblasts and co-culture response are represented.

In order to improve cell attachment, proliferation and differentiation within scaffolds, two different types of scaffolds were submitted to an **oxygen-based plasma modification**. These two types of scaffolds were chosen based on the previous results. Thus, the architecture that provides better results (300 µm, 0/45°) was first chosen. The chosen scaffolds' compositions were pure PCL and PCL-HA S with 10% of HA S by weight. The main goal of this experiment was to try to evaluate if a plasma treatment would improve the scaffolds' surface bioactivity. Furthermore, based on the obtained results, it was also possible to compare the effect of the composition and the geometry on MTT results after the plasma treatment.

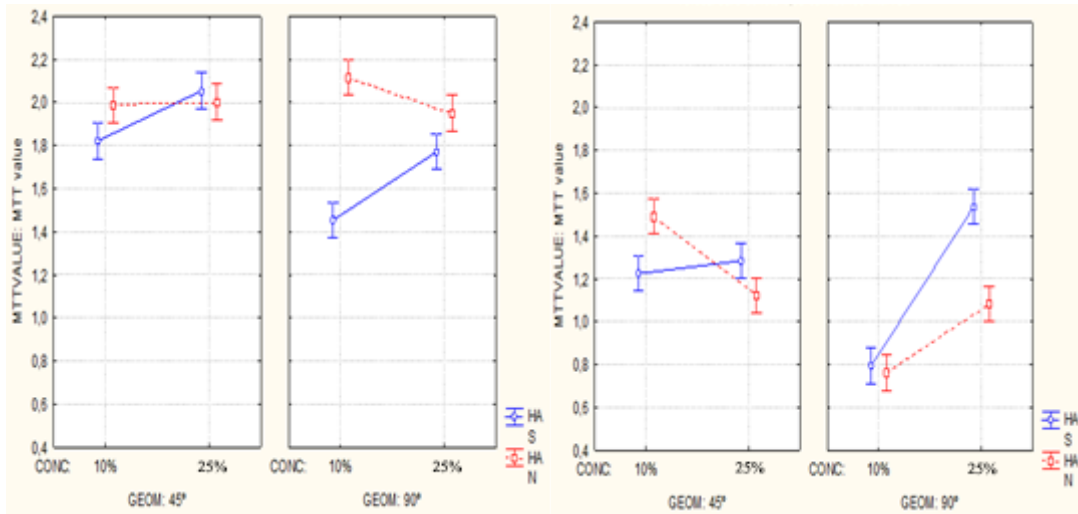


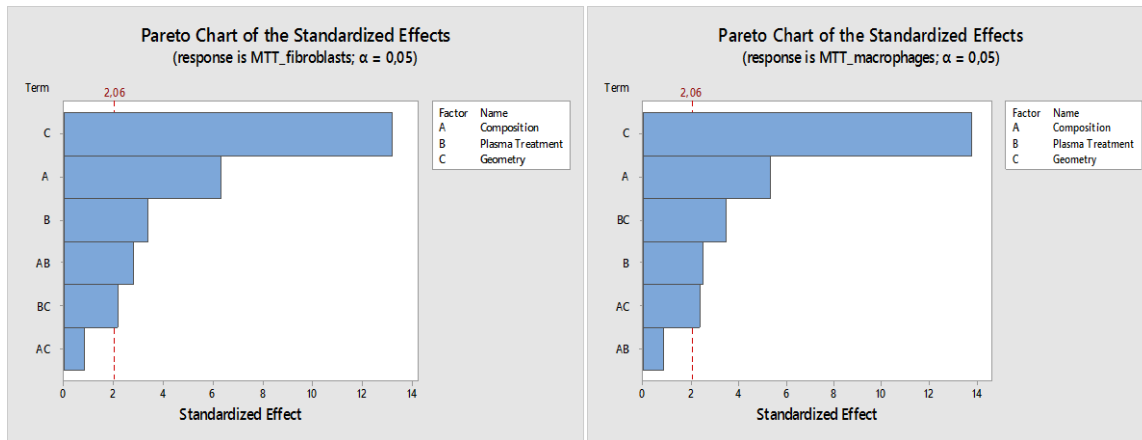
Figure 43 and 44: Influence of the percentage of HA in function of the geometry and type of HA for the pores size of 300 μm and 600 μm , respectively.

Table 6 shows the parameters used in DOE for this analysis. The design layout, generated by the software miniTab is presented in appendix 5.

Table 6: Representation of the factors that were used for the DOE.

Factor	Name	Type	Levels	
			Low (-1)	High (+1)
A	Composition	categorical	PCL	PCL-HA S 10
B	Plasma Treatment	numerical	O	P
C	Geometry	numerical	0/45°	0/90°

Observing Figures 45 to 47, it is possible to conclude that the most significant factor is the geometry, which means that the geometry of the scaffolds has more influence in the metabolic cell activity than the plasma treatment, independently of the cell type that was used. This means that, although the plasma treatment increased the surface hydrophilicity, the total amount of oxygen containing groups and the total surface energy of the scaffolds, a good pore geometry and interconnectivity continues to be essential for the success of the cell-scaffold interaction.



Figures 45 and 46: Pareto Chart for fibroblasts and macrophages, respectively, where A corresponds to the composition of the scaffolds, B to the Plasma treatment and C to the scaffolds geometry.

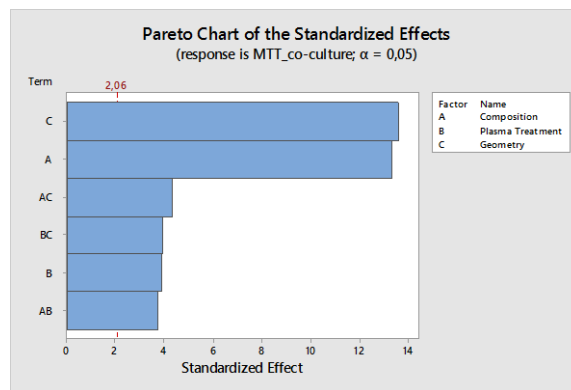


Figure 47: Pareto Chart for the co-culture.

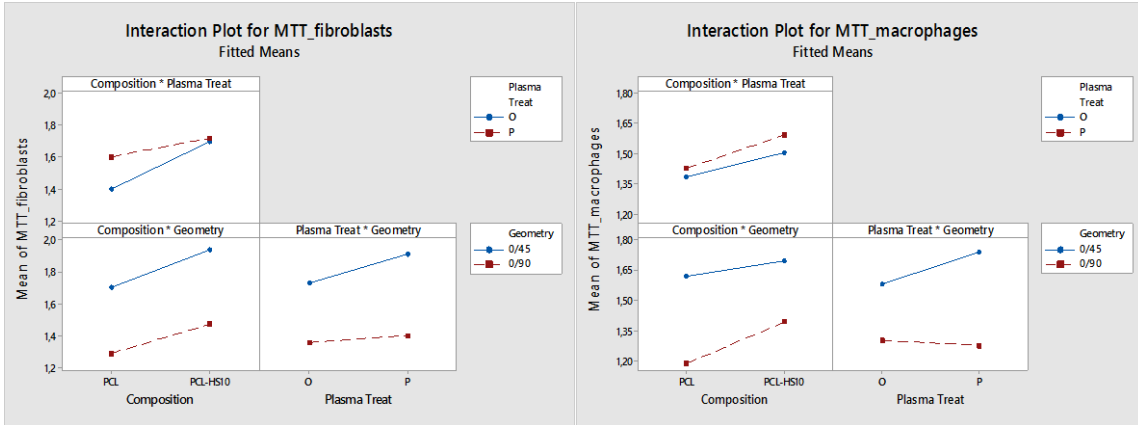
As referred in page 72 a scaffold with interconnected pore structure should improve the attachment and cell proliferation for a complete *in vivo* tissue regeneration.

In these figures (Figures 45 to 47) it can be observed that the scaffolds composition, specifically, the presence or not of HA also has more influence in the results than the plasma treatment. This reflects the high requirement to add HA particles to PCL, in order to increase the bioactivity of the composite scaffolds compared to the scaffolds of pure PCL.

As demonstrated in Figure 47, for the co-culture all the parameters are statistically significant.

In Figures 48 to 50 the interactions between factors after plasma treatment are represented. As it is possible to be seen, the plasma treatment has a major effect to the geometry of 0/45°, since

these pores enable a better air penetration than the pores with a geometry of 0/90°, and there is a higher surface area available for the modification.



Figures 48 and 49: Representation of the interaction between factors with plasma treatment for fibroblasts and macrophages, respectively.

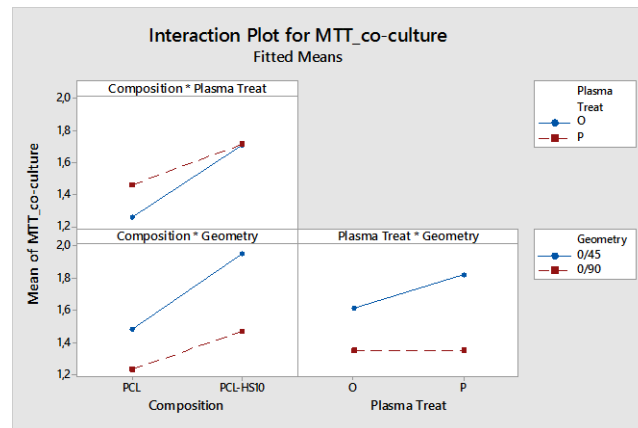


Figure 50: Interactions between factors for co-culture.

In these figures (Figure 48 to 50) it is also possible to see that the plasma treatment has a greater effect for scaffolds of pure PCL, compared to the composite scaffolds of PCL-HA S 10%. This is probably due to the fact that HA, unlike PCL, does not interact with the radicals created by the plasma treatment.

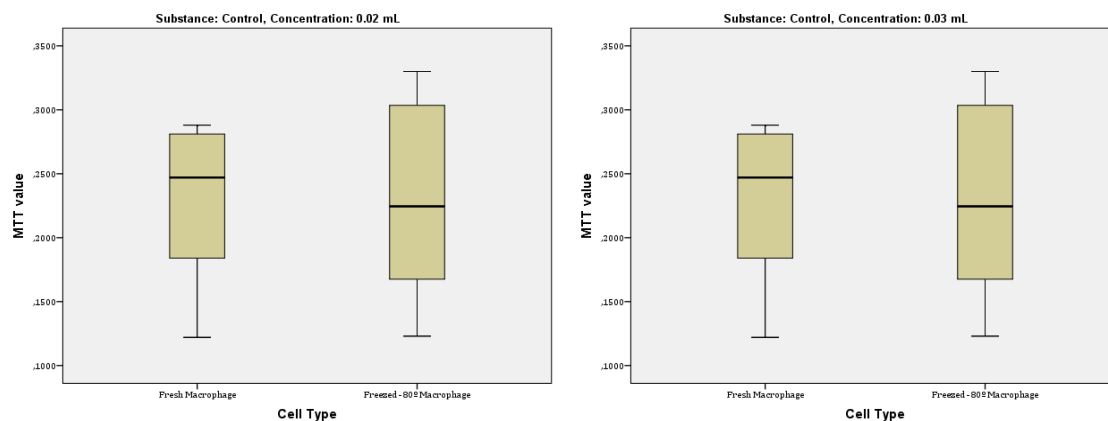
The graphs of the results obtained by the software SPSS are in appendix 6.

5.2 *In vitro* studies with endodontic cements

The macrophages used for this work are peritoneal macrophages, harvested from Wistar rats in IB-IBLI (the same place where the study took place). Using fresh macrophages implies that Wistar rats are available at the time of the experiment. Since macrophages do not divide *in vitro*, their harvest should be done on the eve of the programmed experiment. In this context, prior work has been done in IBILI to test if fresh and frozen³ macrophages would provide reliable and comparable results.

Nevertheless, a comparison between the results obtained with fresh and frozen macrophages was repeated in order to ensure the results and to facilitate the preparation of future assays. Mann-Whitney and Kruskal-Wallis tests were used to calculate ‘*p*’ value among different test groups ($p < 0.001$ indicates a significant difference among different groups).

Thus, for this assay, two different volumes (0.02 and 0.03 mL) of endodontic material were tested. Wells with cells (fresh or frozen macrophages) and culture medium were used as control group. The obtained results are represented in Figures 51-53. As it can be seen in these figures there are no significant differences between fresh and frozen macrophages, independently of the material volume that was used. Thus, the next assays with macrophages could be done using frozen macrophages, since freezing does not alter their properties.



Figures 51 and 52: Representation of the obtained results for fresh and frozen macrophages, with 0.02 mL of material (on the left) and with 0.03 mL of material, on the left.

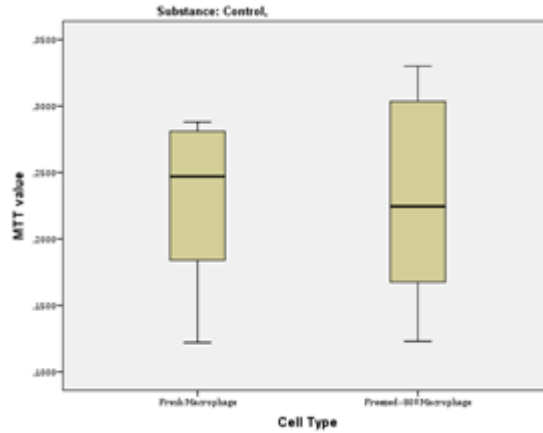


Figure 53: Representation of the obtained results for the control group with fresh and frozen macrophages.

In order to study the influence that different volumes of material might have in the interaction between cells and the endodontic materials, specifically AH Plus JetTM, GuttaFlow[®] 2 and the “improved” GuttaFlow[®], at 72 hours, three different volumes: 0.01, 0.02 and 0.03 mL of each one of the materials, were tested.

From the analysis of the obtained results for each one of the volumes it can be seen that for 0.01 mL, statistically significant differences ($p < 0.05$) have been found between all the materials in study. For the volume of 0.02 mL, statistically significant differences have been found between GuttaFlow[®] 2 and AH Plus JetTM, as well as between GuttaFlow[®] 2 and the “improved” Guttaflow. For tests made with 0.03 mL of the material, statistically significant differences only have been found between GuttaFlow[®] 2 and the “improved” GuttaFlow[®]. However, for each material no statistically significant differences occur between the different used volumes. The obtained “ p ” values are summarized in Table 7.

Table 7: Summary of the obtained “ p ” values for the comparison of the materials for each one of the used volumes. **The significance level is 0.05.**

Sample 1- Sample 2	Volumes of the material (mL)		
	0.01	0.02	0.03
GuttaFlow [®] 2 – AH Plus Jet TM	0.029	0.001	0.051
GuttaFlow [®] 2 – “improved” GuttaFlow [®]	0.000	0.000	0.001
AH Plus Jet TM – “improved” GuttaFlow [®]	0.014	0.191	0.932

Based on the previously referred observations, it can be concluded that the used material has more influence in the results than the chosen volume.

During this work, it was also decided to study a possible temporal influence. To this purpose, tests during 120 hours were also done. Since for 72 hours no significant differences occurred between the different volumes of material that were tested, for 120 hours only two different volumes were tested. The chosen volumes were 0.01 and 0.02 mL, since the previously obtained results for 0.02 and 0.03 mL were very similar. Moreover, the 0.03 mL would be higher than the quantity of the material used in a real endodontic treatment situation.

Comparing the obtained results for 120 hours with the ones obtained for 72 hours, it is possible to conclude that the better results occur for 72 hours, which means that at 120 hours the materials appear to be more toxic to cells. The values decreased with time, and it is also possible to verify that the greatest (negative) variations occur for the highest volume of the material, in this case 0.02 mL (since tests with 0.03 mL were not made at 120 hours). This is supported by the literature, since for longer times, increasing the surface of contact between the root canal sealer and the medium, the amount of leaching molecules within the medium increases and consequently increases the cytotoxicity of the material [133].

For all the assays that were done until now the “improved” GuttaFlow[®] shows better MTT results than AH Plus Jet[™] and GuttaFlow[®] 2, both at 72 and 120 hours.

Since GuttaFlow[®] 2 and the “improved” GuttaFlow[®] have Gutta-percha in a powder form in their composition, and AH Plus Jet[™] *in vivo* is never used without a core obturation material, the behavior of AH Plus Jet[™] combined with small pieces of Gutta-Percha cones was also studied and the results were compared with the ones obtained using only AH Plus Jet[™], GuttaFlow[®] 2 and the “improved” GuttaFlow[®]. The obtained results are represented in Figure 54 for each one of the used cell types. As it is possible to see in this figure, the obtained results for AH Plus Jet[™] are better than the ones obtained for the set AH Plus Jet[™] + small pieces of Gutta-percha. However, between all the tested materials the “improved” GuttaFlow[®] continues to be the less cytotoxic of the tested materials.

AH Plus Jet™ has a complex chemical composition, which is why there are several substances that can be released during the polymerization and thereby cause toxic effects. Thus, a possible explanation for the cytotoxic character of AH Plus Jet™ might be the release of the amine and epoxy resin components of the sealer [74]. Besides this, the present amines also can accelerate the polymerization of the material. Additionally, despite the manufacturer referring this being a “formaldehyde free” material several studies demonstrate that AH Plus Jet™ has a small percentage of this component in its composition [74,134-136]. This endodontic cement has antibacterial effect which can also contribute to the toxic effects [137].

GuttaFlow® 2 appears to be more cytotoxic than AH Plus Jet™ and the “improved” GuttaFlow® in these studies. This could be due to some extra-additives of GuttaFlow® 2. It contains Gutta-percha powder and micro-silver as a preservative. The Gutta-percha powder can have an irritating effect in tissues, and silver according to reported studies has some toxicity [74,137-140].

Tests during 72 hours were also done with fibroblasts and co-culture of fibroblasts and macrophages. In these assays the cytotoxicity of the materials were only tested for two different volumes: 0.01 and 0.02 mL. Thus, observing the obtained results for fibroblast and co-culture no statistically significant differences can be found between the different materials.

It is possible to see in Figure 54 that the behavior of the different materials are similar for all tested cell types, with single exception of GuttaFlow® 2, which provides much better results for the case of co-culture. A hypothesis to explain it could be that GuttaFlow® 2 has properties that stimulate the interaction between the material and connective tissue (e.g: fibroblasts).

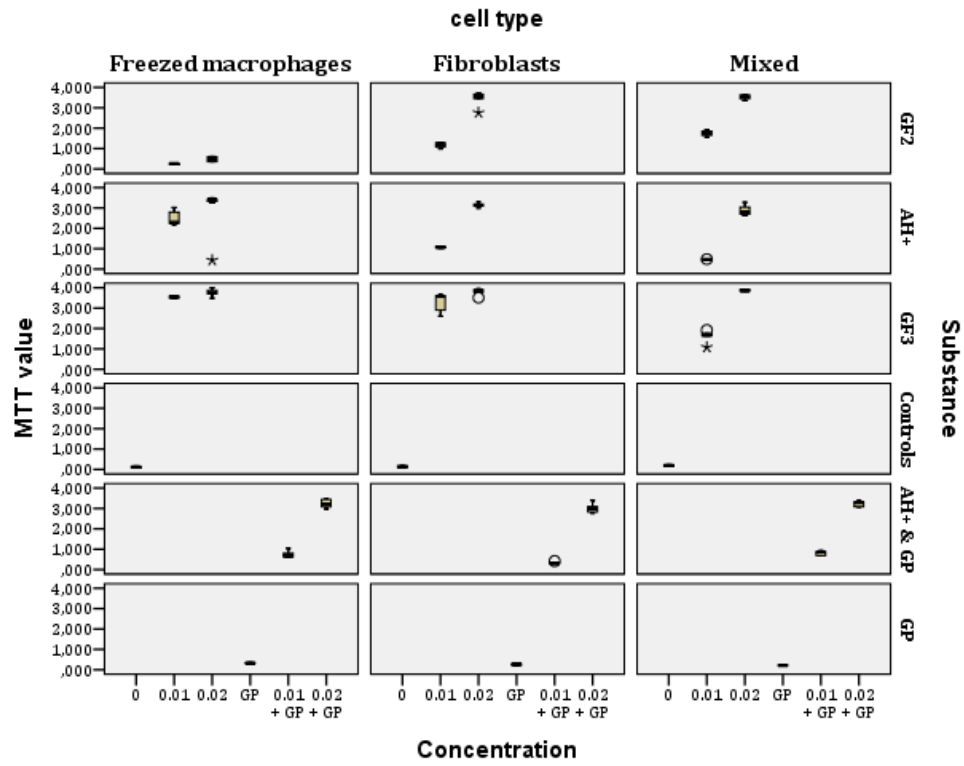


Figure 54: Representation of the behavior of the different materials for all the tested cell types, where GF2 corresponds to GuttaFlow 2, AH+ to AH Plus Jet, GF3 to the “improved” GuttaFlow, AH+&GP, to the set Ah Plus Jet plus small pieces of Gutta-percha cones and finally GP refers to Gutta-percha.

5.3 *In vivo* studies with endodontic cements – Histologic study

As referred in Chapter 4, for the *in vivo* studies, the materials were implanted in the subcutaneous tissue within *abocat* tubes of 8 mm. For this purpose, four different groups have been done. The first group was the control group and consisted in the implantation of empty tubes—in order to study the reaction of the tissue to their presence. The other three groups consisted in the implantation of tubes containing the materials that had been tested: AH Plus Jet™, GuttaFlow® 2 and the “improved” GuttaFlow®. These materials had been implanted in tubes in order to mimic what happens in clinic, as only the tip of the material contained inside the tube can contact with surrounding tissue.

Control

On the 8th day, no formation of fibrous capsule was observed (Figure 55). It was also observed the presence of inflammatory infiltrate. It can thus be concluded that no reaction to the tube has occurred. In Figure 56 an image of the skin without the presence of foreign body reaction can be observed.

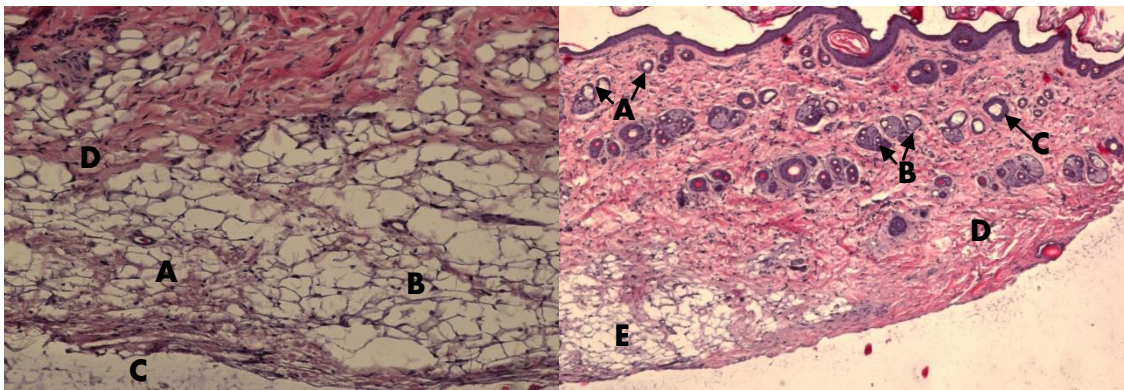


Figure 55: Microscopic image of the site where the control tube has been implanted, being A a blood capillary, B areolar cells, C the subcutaneous tissue where the control tube was implanted and D adipose tissue cells.

Figure 56: Microscopic image of rat skin without tube/material implantation, where A corresponds to hair follicles, B to sebaceous glands, C to the hair erector muscle, D to collagenous fibers and E to the cellular subcutaneous tissue.

AH Plus Jet™

Eight days following the subcutaneous implantation of the tubes containing AH Plus Jet™ the intensity of the inflammatory reaction is milder and the tissue was organized exhibiting the formation of connective fibers (Figures 57-58). The microscopic analysis of the tissue-biomaterial interface showed that AH Plus Jet™ was surrounded by a thin fibrous capsule and was also possible to observe some inflammatory infiltrate (Figure 59).

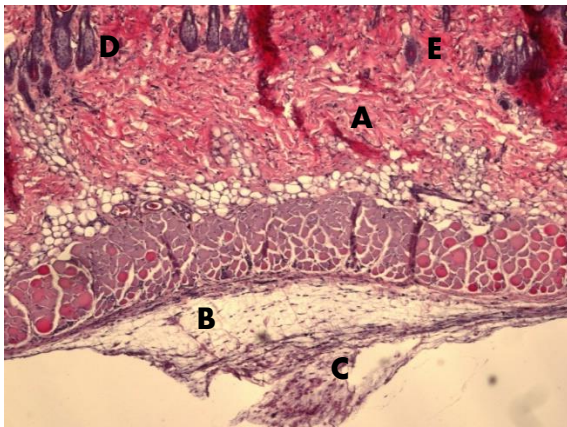


Figure 57: Microscopic image of the site where the tube with AH Plus Jet™ was implanted. In this image it is possible to observe collagen fibers (A), areolar tissue (B), inflammatory infiltrate (C) and also sebaceous glands (D).

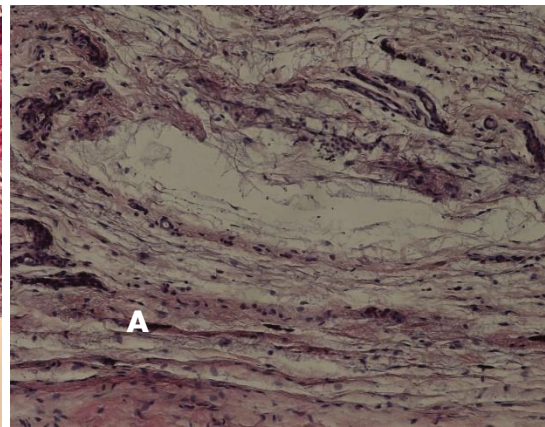


Figure 58: Microscopic image of the site where the tube with AH Plus Jet™ was implanted. In this image it is possible to observe inflammatory infiltrate with medium degree of fibrosis (test during 8 days).

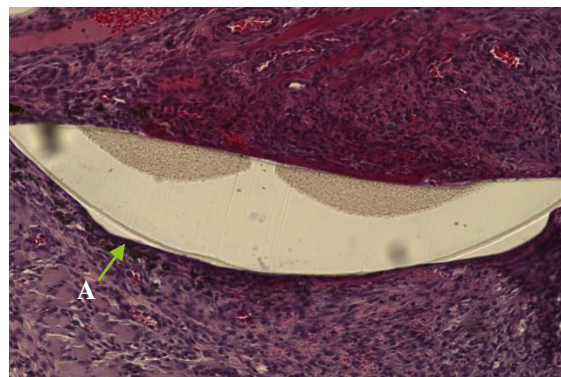


Figure 59: Microscopic image of the site where the tube with AH Plus Jet™ was implanted. In this image it is possible to see a fibrous capsule (A) around the tube with AH Plus Jet™ (test during 30 days).

GuttaFlow® 2

Observing Figure 60 and 61, it can be seen that eight days after the subcutaneous implantation of the tubes containing GuttaFlow 2 an inflammatory reaction is occurring. In these figures, it is also possible to observe a layer of connective tissue with organized collagen fibers.

The microscopic analysis of the tissue-biomaterial interface showed that GuttaFlow® 2 was surrounded by a thin fibrous capsule (Figure 62) more organized than in the case of the tube with AH Plus Jet™. New blood vessels were formed around the implantation site (Figures 60-62).

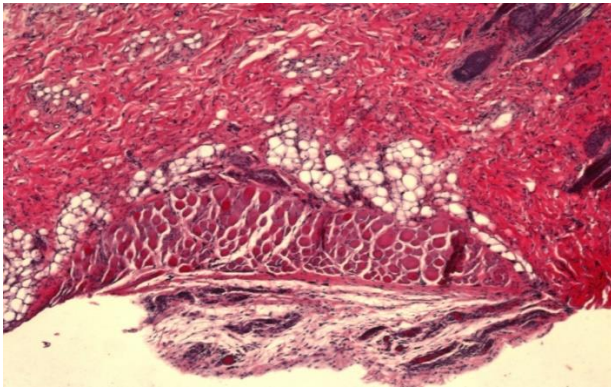


Figure 60: Microscopic image of the site where the tube with GuttaFlow® 2 was implanted. In this image the start of the fibrous organization, as well as some vascularization, can be seen.

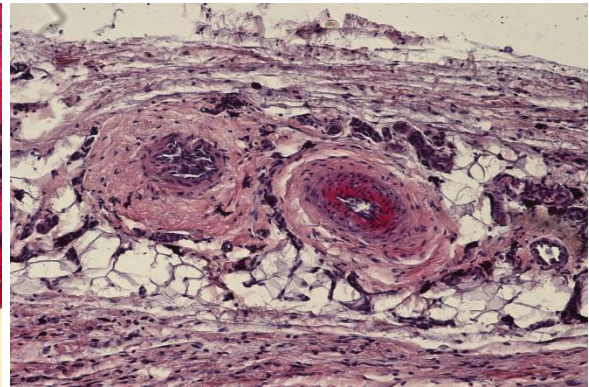


Figure 61: Microscopic image of the site where the tube with GuttaFlow® 2 was implanted. In this image the beginning of an inflammatory reaction can be seen (test during 8 days).

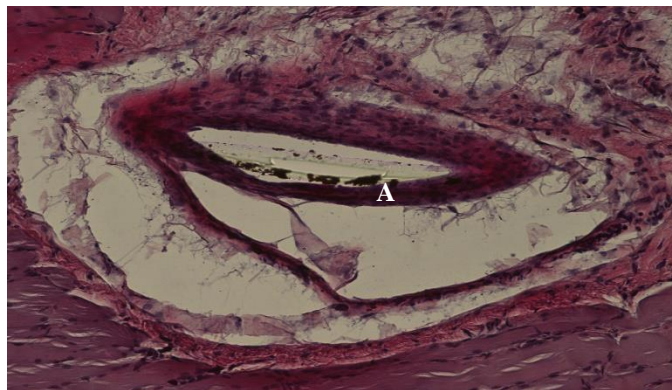


Figure 62: Microscopic image of the site where the tube with GuttaFlow® 2 was implanted. In this image also can be seen a fibrous capsule (A), well defined, around the local where the tube has been implanted (test during 30 days).

“Improved” GuttaFlow

The microscopic analysis of the tissue-“improved” GuttaFlow interface showed some fibrosis, although in the obtained images it is not very evident, as can be seen in Figure 63. Figure 64 represents the place where the tube with the “improved” GuttaFlow is. In this figure some inflammatory infiltrate can be observed, although in a much smaller degree than for the case of the other studied materials.

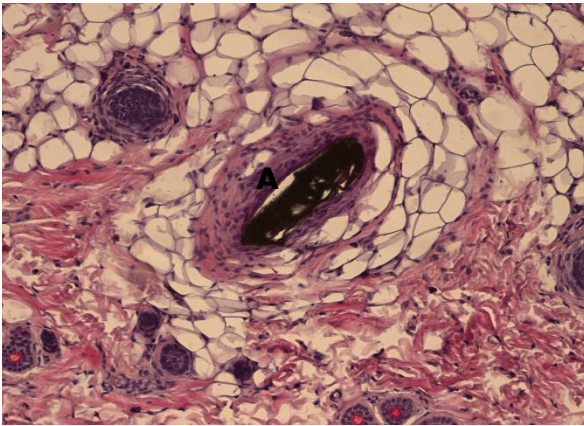


Figure 63: Microscopic image of the site where the tube with “improved” GuttaFlow® was implanted (test during 8 days). In this image, some fibrosis starts to appear, although it is not

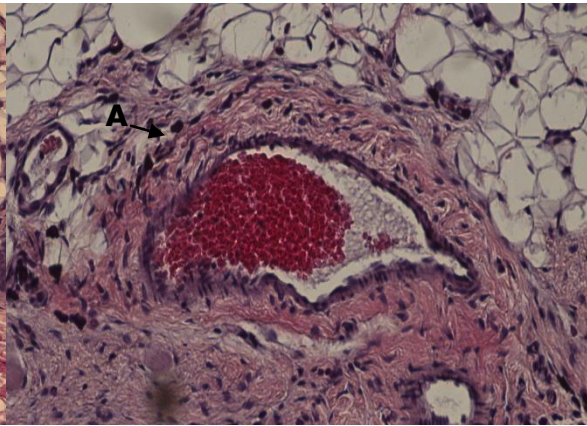


Figure 64: Microscopic image of the site where the tube with “improved” GuttaFlow® was implanted. In this image, some inflammatory infiltrate can be observed (A) (test during 30 days).

Based on the previous results, it can be concluded that no inflammatory reaction occurs due to the presence of the tubes. Thus, the fibrotic capsules that were formed surrounding tubes with GuttaFlow® 2 and AH Plus Jet™ are due to the presence of these materials. Comparing the results obtained for each one of the three tested materials it can be concluded that the highest inflammatory reaction occurs in the presence of AH Plus Jet™, and the less inflammatory reaction occurs in the presence of the “improved” GuttaFlow®.

Chapter 6

Conclusions and future work

In this chapter the main conclusions regarding the obtained results are presented, as well as some perspectives for future work.

6.1 Conclusions

One of the main goals of this work is to determine the effects that the design parameters (pore size and geometry) and materials have on scaffolds' biological properties, specifically in what concerns the cytotoxicity. Furthermore, as previously referred, another main goal of this work is the study of cytotoxic behavior of three endodontic materials with different compositions, in order to determine which of them have better biological properties. The final conclusions of this work are then reported, accord to the goals indicated above and explained in detail in Chapter 3.

6.1.1 Conclusions of the study with scaffolds for TE

The fundamental concept of TE predicts the combination of a scaffold with cells or active biological molecules in order to obtain a bioimplant able to promote tissue reparation and/or regeneration. Thus, the design of scaffolds for TE must obey several mechanical, chemical and biological requirements. However, the quantity and the diversity of these requirements increase the complexity associated with the scaffolds production. To reduce this complexity, additive fabrication technologies, which are able to produce structures with higher geometric precision, have emerged. Therefore, in Chapter 2, a detailed revision of the scaffolds' requirements and of the different additive fabrication technologies was made, namely for those that were specifically developed for TE. Between the different classes of biomaterials used in TE special attention was given to synthetic polymers and ceramic materials, namely to PCL and HA (see Chapter 3). PCL and HA are FDA approved materials, that when combined present better biological and bioactive properties.

In Chapter 4, the description of the performed procedures has been done and in Chapter 5 a detailed analysis of the obtained results was done. Through variation of the pore size and the deposition angle, it was possible to obtain scaffolds with different porosities and pore architectures. The obtained results allow drawing some conclusions:

- from the point of cellular adhesion and differentiation, scaffolds with a pore size of 300 μm and a geometry of 0/45° are those with the best performance;
- the architecture of 300 μm 0/45° correspond to the architecture with the lowest porosity values.

These results show that scaffolds with lower porosity promote a better interaction between cells and scaffolds and consequently, increase the cell adhesion and proliferation.

Since the MTT assay is a qualitative measure of mitochondrial function, it has been used as a measure of cytotoxicity. This assay considers that the number of active living cells is inversely proportional to the cytotoxicity value. Thus, it can be concluded that the higher the number of active cells that adhere and proliferate within the scaffolds, the lower is the cytotoxicity of the scaffold. Therefore, it can be concluded that the scaffold's architecture with a pore size of 300 μm and a geometry of 0/45° is the one with the lowest cytotoxicity behavior.

Beyond the study of the architecture influence, the effect of HA addition to pure PCL scaffolds was also evaluated, as well as the influence of different types and percentages of HA used for the production of PCL-HA composite scaffolds. The mixtures (PCL-HA) were prepared by melt blending (see Chapter 4), which have the advantage of not requiring the use of organic solvents with high toxic potential to the cells. The obtained results for the cytotoxicity studies that were done indicate that the composite scaffolds of PCL-HA have a much higher ability to promote cellular adhesion and survival of macrophages and proliferation of fibroblasts and of their co-culture. Comparing the obtained results with the two different types of HA that were studied (HA N and HA S) it has been verified that the composite scaffolds of PCL-HA N promote a higher cell adhesion and proliferation, which means that these composite scaffolds are less toxic to cells. This probably occurs due to the higher biodegradation rate of HA N, comparatively with the same one of the HA S, which results from the presence of carbonate groups and ions (e.g. magnesium ions) in HA N.

These results lead to the conclusion that the addition of HA increases the bioactivity of scaffolds, independently of the percentage and of the type of HA that was used. It was also possible to conclude that pore size is the factor that most influences the cytotoxicity properties and consequently, cell adhesion and proliferation on scaffolds.

6.1.2 Conclusions of the study with endodontic materials

The second goal of this work, was to evaluate the cytotoxicity of three endodontic cements, respectively AH Plus Jet™, GuttaFlow®2 and the “improved” GuttaFlow®, with different compositions on the presence of cells of the connective tissue (fibroblasts), the immune system (macrophages) and their co-culture. Based on the obtained MTT results it is possible to conclude that the “improved” GuttaFlow® is the material presenting the lowest cytotoxicity, which is expressed by the higher number of cells that adhere and proliferate in contact with this material. The studies with these endodontic sealers also allow verifying that the cytotoxicity of these materials increases with time, namely for higher volumes of material. This occurs since for longer times, as referred in Chapter 5, increasing the surface of contact between the root canal sealer/endodontic cement and the medium, increases the amount of leaching molecules within the medium and consequently increases the cytotoxicity of the endodontic material.

The interpretation of these results is not easy, due the high variation of the effects of each one of the studied materials and each of the used volumes in all the studied parameters. None of the endodontic materials is totally biocompatible, since all of them have some level of cytotoxicity, which is expect attending all the requirements of these materials, namely the bactericidal effect.

In the *in vivo* studies that were performed it was possible to observe an external reaction of the skin to the presence of GuttaFlow® 2. The histological studies allow to conclude that the highest inflammatory reaction occurs in the presence of AH Plus Jet™, and the less inflammatory reaction occurs in the presence of the “improved” GuttaFlow®.

6.2 Future work

Upon the obtained results, tests with dental pulp stem cells, which are multipotent stem cells that have the potential to differentiate into a variety of cell types, including osteoblasts, will be done. For that, an electromagnetic technique using microbeads and specific antibody markers, will be used [12-13].

Studies of tri-culture of fibroblasts, macrophages and osteoblasts could also be done, for both studies with scaffolds and endodontic cements.

The scaffolds observation using SEM technology could also be done in order to clarify if cells migrate to the interior of the scaffolds or if they mainly adhere to the surface.

Results obtained using the scaffolds sterilized with ethylene oxide will be compared with the results obtained with the scaffolds sterilized by gamma radiation.

Based upon the obtained results with fibroblasts, macrophages and their co-culture, and also with osteoblasts and their tri-culture with macrophages and fibroblasts, *in vivo* studies should also be done with scaffolds in order to evaluate the *in vivo* biocompatibility of these materials.

In vivo studies with the endodontic materials should also be done again, but this time they should be implanted in the bone tissue instead of subcutaneously.

References

- [1] Leong, K.F., Chua, C.K., Sudarmadji, N. and Yeong, W.Y. (2008). Engineering functionally graded tissue engineering scaffolds. *Journal of the Mechanical Behaviour of Biomedical Materials*, 1(2), 140-152.
- [2] Sanz-Herrera, J.A., Garcia-Aznar, J.M. and Doblaré, M. (2009). On scaffold designing for bone regeneration: a computational multiscale approach. *Acta Biomaterialia*, 5(1), 219-229
- [3] Bártolo, P. J., Almeida, H., Rezende, R., Laoui, T. and Bidanda, B. (2008). Advanced processes to fabricate scaffolds for tissue engineering. In *Virtual Prototyping & Bio-Manufacturing in Medical Applications*. Springer US. 149-170.
- [4] Bártolo, P. J., Chua, C.K., Almeida, H.A., Chou, S.M. and Lim, A.S.C. (2009). Biomanufacturing for tissue engineering: Present and future trends. *Virtual and Physical Prototyping*, 4(4), 203-216.
- [5] Langer, V., Vacanti, J. P., 1993. Tissue Engineering. *Science*, 260, 921-926.
- [6] Salgado, A. J., Coutinho, O. P. and Reis, R.L. (2004). Bone Tissue Engineering: State of the Art and Future Trends. *Macromolecular Bioscience*, 4(8), 743-765.
- [7] Guariuno, V., Causa, F., Netti, P.A., Ciapetti, G., Pagani, S., Martini, D., Baldini, N., Ambrosio L. (2007). The role of Hydroxyapatite as Solid on Performance of PCL Porous Scaffolds for Bone Tissue Regeneration. *Journal of Biomedical Materials Research Part B: Applied Biomaterials*, 86(2), 548-557.
- [8] Lichte, P., Pape, H.C., Pufe, T., Kobbe, P., Fischer, H. (2011). Scaffolds for bone healing: concepts, materials and evidence. *Injury*, 42(6), 569-573.
- [9] Bose, S., Roy, M., Bandyopadhyay, A. (2012). Recent advances in bone tissue engineering scaffolds. *Trends in Biotechnology*, 30 (10), 546-554.
- [10] Anderson, J.M. (1993). Mechanisms of inflammation and infection with implanted devices. *Cardiovascular Pathology*, 2(3), 33-41.
- [11] Anderson, J.M. (1998). Biocompatibility of tissue-engineered implants. *Frontiers in Tissue Engineering*. Oxford: Elsevier Science, 152-165.
- [12] Nair, L. S., Laurencin, C. T. (2006). Polymers as Biomaterials for Tissue Engineering and Controlled Drug Delivery. In *Tissue Engineering I*. 47-90.
- [13] Thomson, R. C., Wake, M. C., Yaszemski, M. J., Mikos, A. G. (1995). Biodegradable polymer scaffolds to regenerate organs. In *Biopolymers II*. Springer Berlin Heidelberg. 245-274.

- [14] Drobkowski, J., Kolos, R., Kaminski, J., Kowalczyńska, H. M. (1999). Cell adhesion to polymeric surfaces: experimental study and simple theoretical approach. *Journal of biomedical materials research*, 47(2), 234-242.
- [15] Ikada, Y. (1994). Surface modification of polymers for medical applications. *Biomaterials*, 15(10), 725-736.
- [16] y Leon, C. A. L. (1998). New perspectives in mercury porosimetry. *Advances in Colloid and Interface Science*, 76, 341-372.
- [17] Hutmacher, D.W. (2000). Scaffolds in tissue engineering bone and cartilage. *Biomaterials*, 21(24), 2529-2543.
- [18] Chen, G., Ushida, T., Tateishi, T. (2002). Scaffold design for tissue engineering. *Macromolecular Bioscience*, 2(2), 67-77.
- [19] Matassi, F., Nistri, L., Paez, D. C., Innocenti, M. (2011). New biomaterials for bone regeneration. *Clinical Cases in Mineral and Bone Metabolism*, 8(1), 21-24.
- [20] Amoabediny, G., Salehi-Nik, N., Heli, B. (2011). *The role of Biodegradable Engineered Scaffolds in Tissue Engineering*. INTECH Open Access Publisher.
- [21] Middleton, J.C., Tipton, A.J. (2000). Synthetic biodegradable polymers as orthopedic devices. *Biomaterials*, 21(23), 2335-2346.
- [22] Sionkowska, A. (2011). Current research on the blends of natural and synthetic polymers as new materials: Review. *Progress in Polymer Science*, 36(9), 1254-1276.
- [23] Marra, K. G., Szem, J. W., Kumta, P. N., DiMilla, P. A., Weiss, L. E. (1999). In vitro analysis of biodegradable polymer blend/hydroxyapatite composites for bone tissue engineering. *Journal of Biomedical Materials Research*, 47(3), 324-335. 85
- [24] Houchin, M. L., Topp, E. M. (2009). Physical Properties of PLGA Films During Polymer Degradation. *Journal of Applied Polymer Sciences*, 114(5), 2848-2854.
- [25] Reignier, J. and Huneault, M.A. (2006). Preparation of interconnected poly (ϵ -caprolactone) porous scaffolds by a combination of polymer and salt particulate leaching. *Polymer*, 47(13), 4703-4717.
- [26] Whang, K., Thomas, C. H., Healy, K. E., Nuber, G. (1995). A novel method to fabricate bioabsorbable scaffolds. *Polymer*, 36(4), 837-842.
- [27] Peltola, S. M., Melchels, F. P.W., Grijpma, D. K., Kellomäki, M. (2008). A review of rapid prototyping techniques for tissue engineering purposes. *Annals of Medicine*, 40(4), 268-280.
- [28] Woodruff, M. A., Hutmacher, D. W. (2010). The return of a forgotten polymer Polycaprolactone in the 21st century. *Progress in Polymer Science*, 35(10), 1217-1256.

- [29] Lam, C. X. F., Mo, X. M., Teoh, S. H., Hutmacher, D. W. (2002). Scaffold development using 3D printing with a starch-based polymer. *Materials Science and Engineering: C*, 20(1), 49-56.
- [30] Melchels, F. P.W., Domingos, M.A.N., Klein, T.J., Malda, J., Bartolo, P.J. and Hutmacher, D.W. (2012). Additive manufacturing of tissues and organs. *Progress in Polymer Science*, 37(8), 1079-1104.
- [31] Bártolo, P. J. (2011). *Stereolithographic: materials, processes and applications*. Springer Science & Business Media.
- [32] Sachs, E. M., Haggerty, J. S., Cima, M. S., Williams, P. A. (1993). *Three-dimensional printing techniques*. US Patent No 5,204,055.
- [33] Leukers, B., Gülkan, H., Irsen, S. H., Milz, S., Tille, C., Schieker, M., Seitz, H. (2005). Hydroxyapatite scaffolds for bone tissue engineering made by 3D printing. *Journal of Materials Science: Materials in Medicine*, 16(12), 1121-1124.
- [34] Williams, J. M., Adewunmi, A., Schek, R. M., Flanagan, C. L., Krebsbach, P. H., Feinberg, S. E., Hollister, S. J., Das, S. (2005). Bone tissue engineering using polycaprolactone scaffolds fabricated via selective laser sintering. *Biomaterials*, 26(23), 4817-4827.
- [35] Agarwala, M., Bourell, D. Beaman, J., Marcus, H., Barlow, J. (1995). Direct selective laser sintering of metals. *Rapid Prototyping Journal*, 1(1), 26-36.
- [36] Mateus, A. J., Almeida, H. A., Ferreira, N. M., Alves, N. M., Bartolo, P. J., Mota, C. M., Sousa, J. P. (2007). BioExtrusion for Tissue engineering applications. *Virtual and Rapid Manufacturing: Advanced Research in Virtual and Rapid Prototyping*, 171.
- [37] Domingos, M., Chiellini, F., Giglio, E., Grillo-Fernandes, E., Bartolo, P., Chiellini, E. (2010). Evaluation of in vitro degradation of PCL scaffolds fabricated via BioExtrusion. Part 1: Influence of the degradation environment. *Virtual and Physical Prototyping*, 5(2), 65-73.
- [38] Domingos, M., Dinucci, D., Cometa, S., Alderighi, M., Bartolo, P. J., Chiellini, F. (2009). Polycaprolactone Scaffolds Fabricated via Bioextrusion for Tissue Engineering Applications. *International Journal of Biomaterials*, 2009.
- [39] Nelson, S. J., Ash, M. M. (2010). *Wheeler's Dental Anatomy, Physiology and Occlusion*. Elsevier Health Sciences.
- [40] Heymann, H. O., Swift Jr, E. J., Ritter, A. V. (2014). *Sturdevant's art and science of operative dentistry*. Elsevier Health Sciences.
- [41] Black, G. V. (1902). *Descriptive Anatomy of Human Teeth*. SS White Manufacturing Company.
- [42] Cohen, S., Burns, R. C. (2006). *Pathways of the pulp*. Saint Louis, Mo: Elsevier Mosby.
- [43] Metvler, A., Bland, K. (2013). *Dental Anatomy: A review*. Crest® Oral-B® at dentalcare.com

- [44] Judas F, Palma P, Falacho R I, Figueiredo H. (2012). Estrutura e Dinâmica do Tecido Ósseo. Texto de apoio para os alunos do Mestrado Integrado em Medicina. Disciplina de Ortopedia.
- [45] White, T. D., Black M. T., Folkens, P. A. (2011). *Human Osteology*. Academic press.
- [46] <http://www.tpub.com/dental1/26.htm>, consulted in March 2015.
- [47] Nawal, R. R., Parande, M., Sehgal, R., Naik, A., Rao, N. R. (2011). A comparative evaluation of antimicrobial efficacy and flow properties for Epiphany, Guttaflow and AH Plus sealer. *International Endodontic Journal*, 44(4), 307-313.
- [48] <http://www.aae.org/patients/treatments-and-procedures/root-canals/root-canals.aspx>, consulted in June 2015
- [49] Tanomaru-Filho, M., Tanomaru, J. M. G., Barros, D. B., Watanabe, E., Ito, I. Y. (2007). In vitro antibacterial activity of endodontic sealers, MTA-based cements Portland cement. *Journal of Oral Science*, 49 (1), 41-45.
- [50] <http://www.intelligentdental.com/wp-content/uploads/2010/09/new-1-root-cannak-trtmt.gif>, consulted in June 2015.
- [51] Carrotte, P. (2004). Endodontics: Part 8. Filling the root canal system. *British Dental Journal*, 197(11), 667-672.
- [52] Rana, M., Sandhu, G. K., Kaur, T., Arif, M., Galyan, G. (2014). New Self Curing Root Canal Filling Material: Guttaflow 2. *Journal of Advanced Medical and Dental Sciences Research*, 2 (4), 15-20.
- [53] Asgary, S., Shahabi, S., Jafarzadeh, T., Amini, S., Kheirieh, S. (2008). The properties of a new endodontic material. *Journal of endodontic*, 34(8), 990-993.
- [54] Asgary, S., Eghbal, M. J., Parirokh, M. (2008). Sealing ability of a novel endodontic cement as a root-end filling material. *Journal of Biomedical Materials Research Part A*, 87(3), 706-709.
- [55] Orstavik, D. (2005). Materials used for root canal obturation: technical, biological and clinical testing. *Endodontic Topics*, 12(1), 25-38.
- [56] Carrotte, P. (2004). Endodontics: Part 5. Basic instruments and materials for root canal treatment. *British Dental Journal*. 197(8), 455-464.
- [57] Pascon, E. A., Spangberg, L. S. (1990). In Vitro Cytotoxicity of Root Canal Filling Materials: 1.Gutta-percha. *Journal of endodontics*, 16 (9), 429-433.
- [58] Friedman, C. E., Sandrick, J. L., Heuer, M. A., Rapp, G. W. (1977). Composition and physical properties of gutta-percha endodontic filling materials. *Journal of endodontics*, 2(8), 304-308.
- [59] Hashieh, I. A., Pommel, L., Camps, J. (1999). Concentration of Eugenol Apically Released from Zinc Oxide-Eugenol-Based Sealers. *Journal of endodontics*, 25(11), 713-715.

- [60] De-Deus, G., Brandão, M. C., Fidel, R. A. S., Fidel, S. R. (2007). The sealing ability of GuttaFlow™ in oval-shaped canals: an ex vivo study using polymicrobial leakage model. *International Endodontic Journal*, 40(10), 794-799.
- [61] Bouillaguet, S., Wataha, J. C., Tay, F. R., Brackett, M. G., Lockwood, P. E. (2006). Initial In Vitro Biological Response to Contemporary Endodontic Sealers. *Journal of Endodontics*, 32(10), 989-992.
- [62] Lee, K., Williams, M. C., Camps, J. J., Pashley, D. H. (2002). Adhesion of Endodontic Sealers to Dentin and Gutta-Percha. *Journal of Endodontics*, 28(10), 684-688.
- [63] Flores, D. S. H., Rached-Júnior, F. J. A., Versiani, M. A., Guedes, D. F. C., Sousa-Neto, M. D., Pécora, J. D. (2010). Evaluation of physicochemical properties of four root canal sealers. *International Endodontic Journal*, 44(2), 126-135.
- [64] Markowitz, K., Moynihan, M., Liu, M., Kim, S. (1992). Biologic properties of eugenol and zinc oxide-eugenol. A clinically oriented review. *Oral Surgery Oral Medicine Oral Pathology*, 73(6), 729-737.
- [65] Chandrasekhar, V., Morishetty, P. K., Metla, S. L., Raju, C. (2011). Expansion of Gutta-Percha in Contact with Various Concentrations of Zinc Oxide-Eugenol Sealer: A Three-dimensional Volumetric Study. *Journal of Endodontics*, 37(5), 697-700.
- [66] Desai, S., Chandler, N. (2009). Calcium Hydroxide-Based Root Canal Sealers: A Review. *Journal of Endodontics*, 35(4), 475-480.
- [67] Tronstad, L., Barnett, F., Flax, M. (1988). Solubility and biocompatibility of calcium hydroxide-containing root canal sealers. *Dental Traumatology Journal*, 4(4), 152-159.
- [68] <http://www.dl.begellhouse.com/scihub.org/journals/1bef42082d7a0fdf,56437700108bb47c,795c,cf0e387142f6.html>
- [69] Friedman, S., Lost, C., Zarrabian, M., Trope, M. (1995). Evaluation of Success and Failure after Endodontic Therapy Using a Glass Ionomer Cement Sealer. *Journal of Endodontics*, 21(7), 384-390.
- [70] Lee, S., Chung, J., Na, H., Park, E., Jeon, H., Kim, H. (2013). Characteristics of novel root-end filling materials using epoxy resin and Portland cement. *Clinical Oral Investigations*, 17(3), 1009-1015.
- [71] Huumonen, S., Lenander-Lumikari, M., Sigurdsson, A., Orstavik, D. (2003). Healing of apical periodontitis after endodontic treatment: a comparison between a silicone-based and zinc oxide-eugenol-based sealer. *International Endodontic Journal*, 36(4), 296-301.
- [72] Eldeniz, A. U., Mustafa, K., Orstavik, D., Dahl, J. E. (2007). Cytotoxicity of new resin-, calcium hydroxide- and silicone-based root canal sealers on fibroblasts derived from human gingiva and L929 cell lines. *International endodontic journal*, 40(5), 329-337.

- [73] Tyagi, S., Mishra, P., Tyagi, P. (2013). Evaluation of root canal sealers: An insight story. *European Journal of General Dentistry*, 2(3), 99-218.
- [74] Causa, F., Netti P. A., Ambrosio, L., Ciapetti, G., Baldini, N., Pagani, S., Martini, D., Giunti, A. (2005). Poly ϵ -caprolactone/hydroxyapatite composites for bone regeneration: in vitro characterization and human osteoblast response. *Journal of Biomaterials Research Part A*, 76(1), 151-162
- [75] Mezahi, F. Z., Oudadesse, H., Harabi, A., Le, G. Y., & Cathelineau, G. (2011). Sintering effects on physicochemical properties of bioactivity of natural and synthetic hydroxyapatite. *Journal of the Australasian Ceramic Society*, 47(1), 23-27.
- [76] Assis, C. M., Vercik, L. C. O., Santos, M. L., Fook, M. V. L. F., Guastaldi, A. C. (2005). Comparison of Crystallinity between Natural Hydroxyapatite and Synthetic cp-Ti/HA Coatings. *Materials Research*, 8(2), 207-211.
- [77] Chuenjitkuntaworn, B., Inrung, W., Damrongsri, D., Mekaapiruk, K., Supaphol, P., Pavasant, P. (2009). Polycaprolactone/Hydroxyapatite composite scaffolds: Preparation, characterization, and *in vitro* and *in vivo* biological responses of human primary bone cells. *Journal of Biomaterials Research Part A*, 94(1), 241-251.
- [78] Calandrelli, L., Immirzi, B., Malinconico, M. (2004). Natural and Synthetic Hydroxyapatite Filled PCL: Mechanical Properties and Biocompatibility Analysis. *Journal of Bioactive and Compatible Polymers*, 19(4), 301-313.
- [79] Heo, S., Kim, S., Wei, J., Hyun, Y., Yun, H., Kim, D., Shin, J. W. (2009). Fabrication and characterization of novel nano- and micro- HA/PCL composite scaffolds using a modified rapid prototyping process. *Journal of Biomaterials Research Part A*, 89(1), 108-116.
- [80] Sobczak, A., Kowalski, Z., & Wzorek, Z. (2009). *Acta of Bioengineering and Biomechanics. Acta of Bioengineering and Biomechanics*, 11(4), 31-36.
- [81] Suchanek, W., Yoshimura, M. (1998). Processing and properties of hydroxyapatite-based biomaterials for use as hard tissue replacement implants. *Journal of Materials Research*, 13(01), 94-117.
- [82] Gao, Y., Cao, W., Wang, X., Gong, Y., Tian, J., Zhao, N., Zhang, X. (2006). Characterization and osteoblast-like cell compatibility of porous scaffolds: bovine hydroxyapatite and novel hydroxyapatite artificial bone. *Journal of Material Science: Materials in Medicine*, 17(9), 815-823.
- [83] Komlev, V. S., Mastrogiacomo, M., Pereira, R. C., Peyrin, F., Rustichelli, F., Cancedda, R. (2010). Biodegradation of porous calcium phosphate scaffolds in an ectopic bone formation model studied by X-ray computed microtomograph. *European Cells & Materials*, 19(136), e46
- [84] Moore, W. R., Graves, S. E, Bain, G. I. (2001). Synthetic bone graft substitutes. *ANZ journal of surgery*, 71(6), 354-361.

- [85] Joschek, S., Nies, B., Krotz, R., Gopferich, A. (2000). Chemical and physicochemical characterization of porous hydroxyapatite ceramics made of natural bone. *Biomaterials*, 21(16), 16445-1658.
- [86] Roeder, R. K., Converse, G. L., Kane, R. J., & Yue, W. (2008). Hydroxyapatite-reinforced polymer biocomposites for synthetic bone substitutes. *Jom*, 60(3), 38-45.
- [87] Figueiredo, M., Fernando, A., Martins, G., Freitas, J., Judas, F., & Figueiredo, H. (2010). Effect of the calcination temperature on the composition and microstructure of hydroxyapatite derived from human and animal bone. *Ceramics International*, 36(8), 2383-2393.
- [88] Flynn, J. H., Wall, L. A. (1966). General Treatment of the thermogravimetry of polymers. *Journal of Research of the national Bureau of Standarts*, 70(6), 487-523.
- [89] Coats, A. W., Redfern, J. P. (1963). Thermogravimetric analysis. A review. *Analyst*, 88(1053), 906-924.
- [90] Monteiro, S. N., Calado, V., Margem, F. M., Rodriguez, R. J. S. (2012). Thermogravimetric Stability Behaviour of Less Common Lignocellulosic Fibers- a Review. *Journal of materials research and technology*, 1(3), 189-199.
- [91] <http://www.intertek.com/analysis/thermogravimetric/>, consulted in 23/04/2015.
- [92] Shea, J. E. (1954). Apparatus for Measuring Volumes of Solid Materials. US Patent No 2, 667,782.
- [93] Rude, T. J., Strait, L. H., Ruhala, L. A. (2000). Measurement of Fiber Density by Helium Pycnometry. *Journal of Composite Materials*, 34(22), 1948-1958.
- [94] Grant, P. V., Vaz, C. M., Tomlins, P. E., Mikhalovska, L., Mikhalovsky, S., James, S., Vadgama, P. (2006). Physical Characterisation of a polycaprolactone tissue scaffold. *Surface Chemistry in Biomedical and Environmental Science*. 215-228.
- [95] European Pharmacopeia 5.0. Pycnometric Density.
- [96] <http://www.mddionline.com/article/surface-modification-using-low-pressure-plasmatechnology> consulted in August 2015.
- [97] Getty, J. (2002). How plasma-enhanced surface modification improves the production of microelectronics and optoelectronics. *Chip scale review*, (01/02), 72-75.
- [98] http://ieeexplore.ieee.org.xpls/abs_all.jsp?arnumber=904189, consulted in June 2015.
- [99] Freytes, D. O., Badylak, S. F. (2006). Sterilization of biologic scaffold materials. *Encyclopedia of Medical Devices and Instrumentation*.
- [100] <http://www.eurotherm.com/industries/life-sciences/applications/eto-sterilization/>, consulted in July 2015.

- [101] Mendes, G. C., Brandao, T. R., Silva, C. L. (2007). Ethylene oxide sterilization of medical devices: a review. *American journal of infection control*, 35(9), 574-581.
- [102] Sykes, G. (1958). Disinfection and sterilization. *Disinfection and sterilization*.
- [103] <http://apps.who.int/phint/en/p/docf/>, consulted in July 2015.
- [104] Nunes, V. H., Silva, R. G., Alfredo, E., Sousa-Neto, M. D., Silva-Sousa, Y. T. C. (2008). Adhesion of Epiphany and AH Plus Sealers to Human Root Dentin Treated with Different Solutions. *Brazilian Dental Journal*, 19(1), 46-50.
- [105] Bouillaguet, S., Shaw, L., Barthelemy, J., Krejci, I., Wataha, J. C. (2008). Long-term sealing ability of Pulp Canal Sealer, AH-Plus, GuttaFlow and Epiphany. *International Endodontic Journal*, 41(3), 219-226.
- [106] Mandal, P., Zhao, J., Sab, S. K., Huang, Y., Liu, J. (2014). In vitro Cytotoxicity of GuttaFlow 2 on Human Gingival Fibroblasts. *Journal of Endodontics*, 40(8), 1156-1159.
- [107] Accardo, C., Himel, V. T., Lallier, E. (2014). A Novel GuttaFlow Sealer Supports Cell Survival and Attachment. *Journal of Endodontics*, 40(2), 231-234.
- [108] Michalany, J. (1998). Técnica histológica em anatomia patológica: com instruções para o cirurgião, enfermeira e citotécnico. In *Técnica histológica em anatomia patológica: com instruções para o cirurgião, enfermeira e citotécnico*. Michalany.
- [109] Bancroft, J. D., & Gamble, M. (2008). *Theory and practice of histological techniques*. Elsevier Health Sciences.
- [110] Gartner, L. P., & Hiatt, J. L. (2001). *Colour textbook of histology*. London: WB Saunders.
- [111] http://histologylab.ccnmtl.columbia.edu/histological_techniques/fixation.html, consulted in August 2015.
- [112] <http://protocolsonline.com>, consulted in August 2015.
- [113] <http://www.marietta.edu/~spilatr/biol309/labexercises/Histology.pdf>, consulted in August 2015.
- [114] Hill, P. A., B. D. S., F.D.S., M. ORTH., B. SC., PH. D. (1998). Bone remodelling. *British Journal of Orthodontics*, 25, 101-107.
- [115] Gamblin, A. L., Brennan, M. A., Renaud, A., Yagita, H., Lézot, F., Heymann, D., Layrolle, P. (2014). Bone tissue formation with human mesenchymal stem cells and biphasic calcium phosphate ceramics: the local implication of osteoclasts and macrophages. *Biomaterials*, 35(36), 9660-9667.
- [116] Amaral, C. E. R., Bueno, D. F., Almeida, A. B., Jorgetti V., Costa, C. C., Gouveia C. H., Vulcano, L. C., Fanganiello R. D., Bueno, M. R. P., Alonso, N. (2014). Is bone transplantation the gold

standard for repair of alveolar bone defects?. *Journal of Tissue Engineering*, 5, 2041731413519352.

- [117] Aghaloo, T. L., & Moy, P. K. (2006). Which hard tissue augmentation techniques are the most successful in furnishing bony support for implant placement?. *The International Journal of Oral & Maxillofacial Implants*, 22, 49-70.
- [118] <http://www.animaethics.org.au/three-rs>, consulted in July 2015.
- [119] <http://ec.europa.eu/health/opinions/en/non-human-primates/glossary/tuv/three-rs-principle.htm>, consulted in July 2015.
- [120] <http://www.siumed.edu/~dking2/intro/ct.htm#ordinspecial>, consulted in May 2015.
- [121] <http://iws.collin.edu/cdoumen/HistoCCCCD/LabSlides/Connective.html>, consulted in May 2015.
- [122] http://medcell.med.yale.edu/histology/connective_tissue_lab.php, consulted in June 2015
- [123] <http://www.nature.com/subjects/macrophages>, consulted in July 2015.
- [124] Vendramini, A. P., Melo, R. F., Marcantonio, R. A. C., Carlos, I. Z. (2006). Biocompatibility of a cellular dermal matrix graft evaluated in culture of murine macrophages. *Journal of Applied Oral Science*, 14(2), 67-70.
- [125] http://faculty.ucc.edu/biology-potter/connective_tissues.htm, consulted in May 2015.
- [126] Santos, A. C. (2002). *Água trocável do pulmão – contribuição para o desenvolvimento de uma metodologia para a sua avaliação*. Tese de Doutoramento, Universidade de Coimbra.
- [127] Burg, K. J. L., Porter, S., Kellam, J. F. (2000). Biomaterial developments for bone tissue engineering. *Biomaterials*, 21(23), 2347-2359.
- [128] Shin, S. Y., Rios, H. F., Giannobile, W. V., Oh, T., Periodontal regeneration: Current Therapies. *In Stem Cell Biology and Tissue Engineering in Dental Sciences*. Chapter 36.
- [129] Kneser, U., Schaefer, D. J., Munder, B., Klemm, C., Andree, C., Stark, G. B. (2002). Tissue engineering of bone. *Minimally Invasive & Allied Technologies*, 11(3). 107-116.
- [130] Dumitrescu, A. L. (2011). Bone Grafts and Bone Graft Substitutes in Periodontal Therapy. *Chemicals in Surgical Periodontal Therapy*, 73-144.
- [131] Borges, F. J.V. (2009). Isolamento e cultura primária de macrófagos peritoneais de rato . estudo de protocolo alternativo de criopreservação. Licenciatura Biotápica em Análises Clínicas e de Saúde Pública, Campus Académico de Macedo de Cavaleiros.
- [132] Matos, C. M. (2012). *GUVs - Estudos de citotoxicidade num modelo de edema pulmonar agudo & Criação de criobanco de macrófagos e fibroblastos de rato e ratinho*. Mestrado em Bioquímica, Universidade de Coimbra.

- [133] Camps, J. (2003). Cytotoxicity Testing of Endodontic Sealers: A New Method. *Journal of Endodontics*, 29(9), 583-586.
- [134] Cohen, B. I., Pagnillo, M. K., Musikant, B. L., Deutsch, A. S. (2000). An in vitro study of the cytotoxicity of two root canal sealers. *Journal of Endodontics*, 26(4), 228-229.
- [135] Merdad, K., Pascon, A., E., Kulkarni, G., Santerre, P., Friedman, S. (2007). Short-term cytotoxicity assessment of components of the Epiphany resin-percha obturation system by indirect and direct contact millipore filter assay. *Journal of Endodontics*, 33(1), 24- 27.
- [136] Leonardo, M. R., da Silva, L. A. B., Tanomaru Filho, M., da Silva, R. S. (1999). Release of formaldehyde by 4 endodontic sealers. *Oral Surgery Oral Medicine Oral Pathology*, 88(2), 221-225.
- [137] Kayaoglu, G., Erten, H., Alacam, T., Orstavik, D. (2005). Short-term antibacterial activity of root canal sealers towards *Enterococcus faecalis*. *International Endodontic Journal*, 38(7), 483-488.
- [138] Sjögren U., Sundqvist, G., Nair, P. M. (1955). Tissue reaction to gutta-percha particles of various sizes when implanted subcutaneously in guinea pigs. *European Journal of oral Sciences*, 103(5) 313–321.
- [139] Zhang, F.Q., She, W.J., Fu, Y. F. (2005). Comparison of the cytotoxicity in vitro among six types of nano-silver base inorganic antibacterial agents. *Zhonghua kou qiang yi xue za zhi= Zhonghua kouqiang yixue zazhi= Chinese journal of stomatology*, 40(6), 504–507.
- [140] Baker, C., Pradhan, A., Pakstis, L., Pochan, D. J., & Shah, S. I. (2005). Synthesis and antibacterial properties of silver nanoparticles. *Journal of Nanoscience and Nanotechnology*, 5(2), 244-249.

Appendix 1 – Full factorial design

Factors: 4 Base Design: 4; 16
 Runs: 64 Replicates: 4
 Blocks: 1 Center pts (total): 0

All terms are free from aliasing.

StdOrder	HA Type	HA (%)	Pore size(μm)	Geometry	MTT_fibroblast	MTT_macrophage	MTT_co-culture
1	S	10	300	0/45	1,827	1,762	1,794
2	N	10	300	0/45	1,934	1,937	2,124
3	S	25	300	0/45	2,166	1,957	2,0444
4	N	25	300	0/45	2,187	1,899	1,988
5	S	10	600	0/45	1,027	1,126	1,382
6	N	10	600	0/45	1,816	1,458	1,253
7	S	25	600	0/45	1,308	1,395	1,034
8	N	25	600	0/45	1,062	1,160	1,022
9	S	10	300	0/90	1,434	1,266	1,383
10	N	10	300	0/90	2,150	2,125	2,089
11	S	25	300	0/90	1,744	1,886	1,676
12	N	25	300	0/90	2,055	1,878	1,985
13	S	10	600	0/90	0,789	0,815	0,797
14	N	10	600	0/90	0,926	0,741	0,827
15	S	25	600	0/90	1,572	1,710	1,252
16	N	25	600	0/90	1,085	0,852	1,578
17	S	10	300	0/45	2,041	1,507	2,003
18	N	10	300	0/45	1,984	1,970	1,896
19	S	25	300	0/45	2,144	2,004	2,001
20	N	25	300	0/45	2,118	1,987	1,869
21	S	10	600	0/45	1,154	1,170	1,4411
22	N	10	600	0/45	1,802	1,459	1,257
23	S	25	600	0/45	1,098	1,627	1,269
24	N	25	600	0/45	1,087	1,258	1,114
25	S	10	300	0/90	1,469	1,490	1,686
26	N	10	300	0/90	1,143	2,101	2,091
27	S	25	300	0/90	1,610	1,807	1,850
28	N	25	300	0/90	1,994	1,867	2,013
29	S	10	600	0/90	0,800	0,800	0,755
30	N	10	600	0/90	0,756	0,638	0,646
31	S	25	600	0/90	1,845	1,441	1,243
32	N	25	600	0/90	0,956	0,866	1,389
33	S	10	300	0/45	1,967	1.645	1,867

34	N	10	300	0/45	1,956	1,956	1,967
35	S	25	300	0/45	2,156	1,978	2,034
36	N	25	300	0/45	2,123	1,900	1,899
37	S	10	600	0/45	1,099	1,189	1,390
38	N	10	600	0/45	1,835	1,458	1,187
39	S	25	600	0/45	1,178	1,478	1,099
40	N	25	600	0/45	1,137	1,22	1,045
41	S	10	300	0/90	1,454	1,367	1,549
42	N	10	300	0/90	2,148	2,117	2,087
43	S	25	300	0/90	1,754	1,834	1,744
44	N	25	300	0/90	1,999	1,875	1,856
45	S	10	600	0/90	0,798	0,809	0,764
46	N	10	600	0/90	0,845	0,689	0,699
47	S	25	600	0/90	1,689	1,556	1,247
48	N	25	600	0/90	0,845	0,863	1,450
49	S	10	300	0/45	1,935	1,554	1,954
50	N	10	300	0/45	1,961	1,963	2,189
51	S	25	300	0/45	2,148	2,001	2,010
52	N	25	300	0/45	2,156	1,956	1,945
53	S	10	600	0/45	1,123	1,223	1,405
54	N	10	600	0/45	1,797	1,460	1,223
55	S	25	600	0/45	1,256	1,534	1,145
56	N	25	600	0/45	1,106	1,187	1,078
57	S	10	300	0/90	1,447	1,434	1,456
58	N	10	300	0/90	2,150	2,090	2,090
59	S	25	300	0/90	1,678	1,857	1,809
60	N	25	300	0/90	2,023	1,869	1,987
61	S	10	600	0/90	0,795	0,813	0,789
62	N	10	600	0/90	0,899	0,723	0,742
63	S	25	600	0/90	1,723	1,678	1,500
64	N	25	600	0/90	0,970	0,857	1,289

Appendix 2

2.1) Factorial Regression: MTT_fibroblasts vs HA type; HA (%); Pore size (µm); Geometry

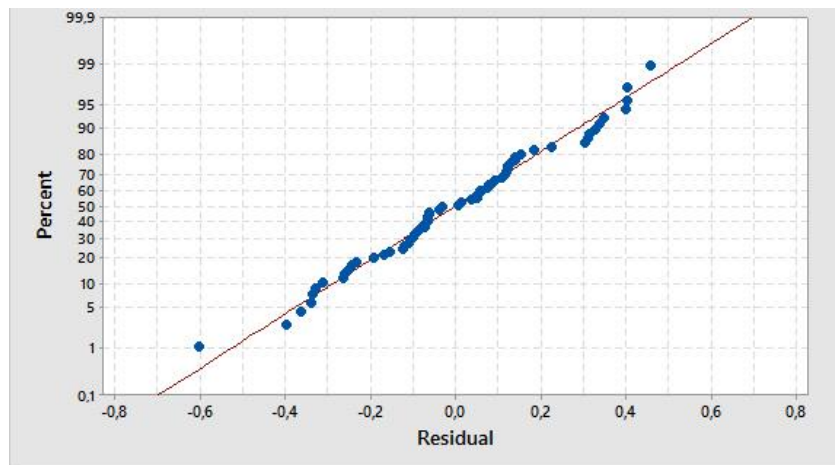
Analysis of Variance

Source	DF	Adj SS	Adj MS	F-Value	P-Value
Model	10	11,3935	1,13935	18,81	0,000
Linear	4	9,6761	2,41903	39,93	0,000
tipo HA	1	0,1213	0,12128	2,00	0,163
HA (%)	1	0,3455	0,34545	5,70	0,021
poro (um)	1	8,1710	8,17102	134,88	0,000
geometria	1	1,0384	1,03836	17,14	0,000
2-Way Interactions	6	1,7174	0,28623	4,72	0,001
tipo HA*HA (%)	1	0,7877	0,78766	13,00	0,001
tipo HA*poro (um)	1	0,1855	0,18555	3,06	0,086
tipo HA*geometria	1	0,0677	0,06773	1,12	0,295
HA (%)*poro (um)	1	0,0302	0,03019	0,50	0,483
HA (%)*geometria	1	0,6316	0,63163	10,43	0,002
poro (um)*geometria	1	0,0146	0,01464	0,24	0,625
Error	53	3,2108	0,06058		
Lack-of-Fit	5	2,2859	0,45719	23,73	0,000
Pure Error	48	0,9249	0,01927		
Total	63	14,6043			

Model Summary

S	R-sq	R-sq(adj)	R-sq (pred)
0,246133	78,01%	73,87%	67,94%

2.2) Normal Probability Plot (response is MTT_fibroblasts)



Appendix 3

3.1) Factorial Regression: MTT_macrophages vs HA type; HA (%); Pore size (µm); Geometry

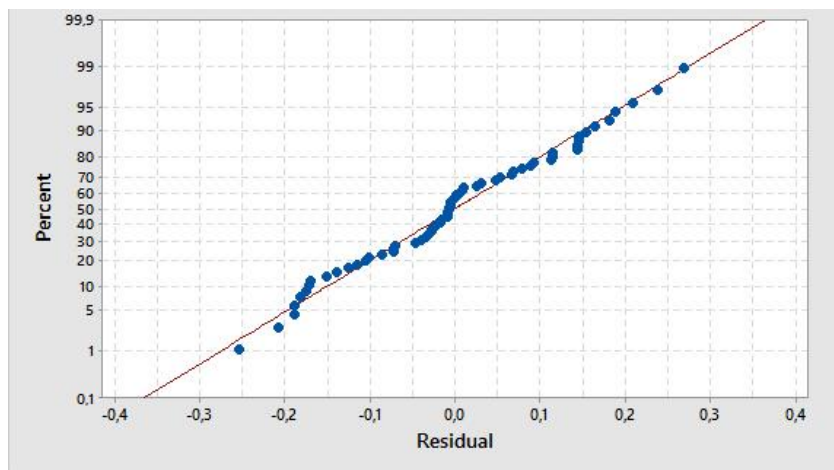
Analysis of Variance

Source	DF	Adj SS	Adj MS	F-Value	P-Value
Model	10	11,3679	1,13679	68,55	0,000
Linear	4	8,6170	2,15426	129,90	0,000
tipo HA	1	0,0070	0,00699	0,42	0,519
HA (%)	1	0,6370	0,63700	38,41	0,000
poro (um)	1	7,2785	7,27853	438,89	0,000
geometria	1	0,6945	0,69451	41,88	0,000
2-Way Interactions	6	2,7509	0,45848	27,65	0,000
tipo HA*HA (%)	1	1,3113	1,31131	79,07	0,000
tipo HA*poro (um)	1	0,9056	0,90559	54,61	0,000
tipo HA*geometria	1	0,0348	0,03483	2,10	0,153
HA (%)*poro (um)	1	0,0531	0,05307	3,20	0,079
HA (%)*geometria	1	0,1379	0,13792	8,32	0,006
poro (um)*geometria	1	0,3082	0,30816	18,58	0,000
Error	53	0,8789	0,01658		
Lack-of-Fit	5	0,7107	0,14213	40,54	0,000
Pure Error	48	0,1683	0,00351		
Total	63	12,2469			

Model Summary

S	R-sq	R-sq(adj)	R-sq (pred)
0,128778	92,82%	91,47%	89,53%

2.2) Normal Probability Plot (response is MTT_macrophages)



Appendix 4

4.1) Factorial Regression: MTT_co-culture vs HA type; HA (%); Pore size (µm); Geometry

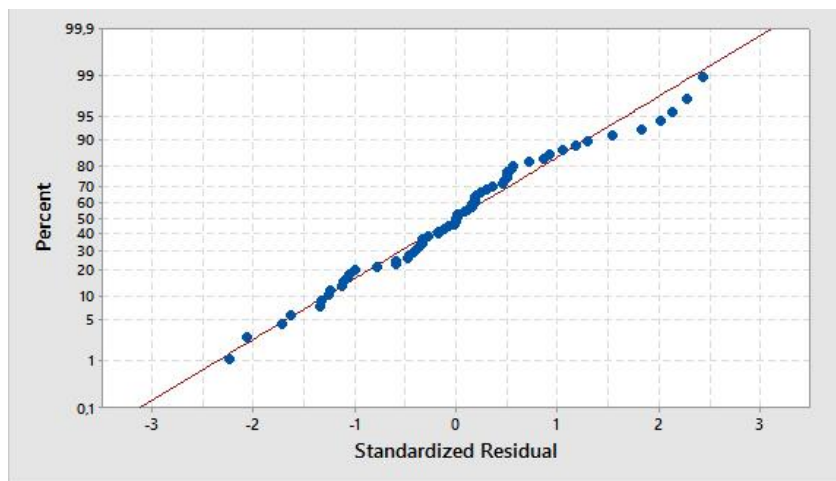
Analysis of Variance

Source	DF	Adj SS	Adj MS	F-Value	P-Value
Model	10	11,5837	1,15837	53,02	0,000
Linear	4	10,1404	2,53510	116,03	0,000
tipo HA	1	0,1002	0,10017	4,58	0,037
HA (%)	1	0,2153	0,21530	9,85	0,003
poro (um)	1	9,4972	9,49718	434,69	0,000
geometria	1	0,3278	0,32776	15,00	0,000
2-Way Interactions	6	1,4433	0,24055	11,01	0,000
tipo HA*HA (%)	1	0,0320	0,03204	1,47	0,231
tipo HA*poro (um)	1	0,2374	0,23741	10,87	0,002
tipo HA*geometria	1	0,2632	0,26317	12,05	0,001
HA (%)*poro (um)	1	0,1175	0,11748	5,38	0,024
HA (%)*geometria	1	0,7930	0,79299	36,30	0,000
poro (um)*geometria	1	0,0002	0,00020	0,01	0,924
Error	53	1,1580	0,02185		
Lack-of-Fit	5	0,8353	0,16707	24,85	0,000
Pure Error	48	0,3226	0,00672		
Total	63	12,7417			

Model Summary

S	R-sq	R-sq(adj)	R-sq (pred)
0,147812	90,91%	89,20%	86,75%

2.2) Normal Probability Plot (response is MTT_co-culture)



Appendix 5 – Full factorial design

Factors: 3 Base Design: 3; 8
Runs: 32 Replicates: 4
Blocks: 1 Center pts (total): 0

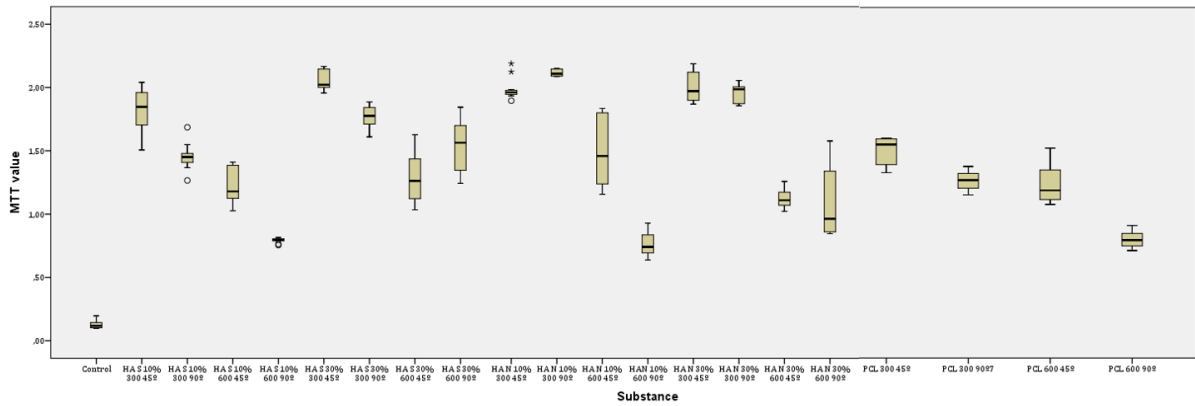
All terms are free from aliasing.

Coded Coefficients

Term	Effect	Coef	SE Coef	T-Value	P-Value	VIF
Constant		1,6017	0,0166	96,63	0,000	
Compositon	0,2093	0,1047	0,0166	6,31	0,000	1,00
Plasma Treatment	0,1113	0,0557	0,0166	3,36	0,003	1,00
Geometry	-0,4374	-0,2187	0,0166	-13,20	0,000	1,00
Composition*Plasma Treat	-0,0922	-0,0461	0,0166	-2,78	0,010	1,00
Composition*Geometry	-0,0274	-0,0137	0,0166	-0,83	0,416	1,00
Plasma Treat.*Geometry	-0,0704	-0,0352	0,0166	-2,12	0,044	1,00

Appendix 6 – Results obtained for the *in vitro* studies with scaffolds using SPSS

6.1) Studies with scaffolds before low-pressure plasma surface modification



6.2) Studies with scaffolds after low-pressure plasma surface modification

